

POLITECNICO DI TORINO

Corso di Laurea Magistrale in Ingegneria Energetica e Nucleare
Progettazione e Gestione di Impianti Energetici

Tesi di Laurea Magistrale

Analysis of the state of the art of vulnerability and
impairment thresholds associated to physical effects of a
CO₂ release.

Application to the Allam cycle case study.



Relatore:

Prof. Andrea Carpignano

Co-relatrici:

Prof.ssa Raffaella Gerboni

Dott.ssa Anna Chiara Ugenti

Candidato:

Alma Gallo

Anno Accademico 2020/2021

Abstract

Carbon Capture Utilization and Storage (CCUS) technology is considered a mitigation measure to control the increasing CO₂ emissions in atmosphere during energy transition. Even if CO₂ infrastructures already exist in remote areas of USA and Europe, the CCUS facilities have to be deeply analyzed as safer systems, considering new issues strictly connected to their presence in more densely populated areas. As part of the Quantitative Risk Assessment, the critical transportation conditions and the released stream characteristics have been analyzed to assess the effects of an unexpected CO₂ release event.

The aim of this thesis is to fill the gaps of knowledge in the Quantitative Risk Assessment for dense phase CO₂, for which consolidated and shared methods do not exist, due to limited use of this stream in traditional plants. The evaluation of vulnerability of people and facilities has been done, collecting information about effects of dangerous doses of inhaled CO₂ and consequences of exposure to critical release conditions. Additional considerations for the Escape, Evacuation and Rescue Analysis have been done, collecting data about impairment caused by lack of visibility, low temperatures, physical blast and inhalation of toxic substances. Additional engineering hazards have been analyzed in order to identify the prevalent phenomena able to affect the structures integrity within a reduced exposure time.

The vulnerability analysis results in definition of threshold values for each dangerous effect of a CO₂ release. Analyzing the state of the art about CCUS plant risk assessment, existing mortality predictive models have been considered. For those aspects of the analysis not yet discussed in literature, some assumptions have been done to associate to some physical effects the expected consequences on exposed individuals and materials.

Dose-based criteria have been analyzed to consider the toxicity of CO₂. Also the released plume cryogenic effects have been investigated. Due to absence of references about lethality of low temperatures, correlations between ambient temperature, duration of exposure and probability of death have been extracted from medical papers. In conclusion, overpressure values able to cause 0% and 100% mortality for outdoor or indoor populations have been obtained from Energy Institute's evaluations about CO₂ releases from pipelines. Vulnerability of facilities exposed to the CO₂ cold plume may be referred to conducted tests on different types of metallic and non-metallic materials, considering their embrittlement and hardening points and their thermo-dynamic interaction with CO₂. In addition, some limit operating temperatures for emergency equipment have been collected for QRA and EERA evaluations.

The obtained vulnerability results have been applied to the Allam cycle case study. Through the DNV software Phast 8.23, the analysis of consequences of liquid, vapour and supercritical CO₂ releases has been conducted, starting from process data extracted from Eni previous works. Following a sensitivity analysis, all required parameters have been set to obtain downwind concentration and temperature values. Collecting distance results, the 1% and the 50% fatality regions have been determined, adopting models chosen in the first part of the analysis. Finally, safety distances from CO₂ releases have been compared with that defined to consider a CH₄ discharge from equipment of the same Allam cycle plant.

Table of Contents

| | |
|---|----|
| Abstract | 3 |
| List of Figures..... | 6 |
| List of Tables..... | 8 |
| Acronyms | 9 |
| 1. Introduction | 10 |
| 2. Methodology used to identify vulnerability and impairment thresholds..... | 12 |
| 3. CO ₂ properties and behavior..... | 12 |
| 4. Health effects of CO ₂ inhalation | 14 |
| 4.1. Definition of dangerous CO ₂ volumetric thresholds..... | 14 |
| 4.1.1. Occupational exposure limits | 16 |
| 4.2. Asphyxiation due to oxygen depletion | 17 |
| 4.2.1. Summary of combined effect of O ₂ depletion and CO ₂ inhalation..... | 20 |
| 5. Statistical probability of death due to CO ₂ exposure | 23 |
| 5.1. SLOT and SLOD Dangerous Toxic Loads..... | 23 |
| 5.1.1. The effect of concentration fluctuations on toxic load | 24 |
| 5.1.2. Application of concentration limits or DTL curves for QRA..... | 26 |
| 5.2. The probit method | 28 |
| 5.2.1. The UK HSE probit correlation..... | 28 |
| 5.2.2. The Tebodin probit correlation..... | 29 |
| 5.2.2.1. Sub-lethal effects | 30 |
| 5.2.3. Comparisons between different probit functions..... | 30 |
| 6. Cryogenic effects of a CO ₂ release..... | 33 |
| 6.1. Cryogenic effects on human health | 34 |
| 6.1.1. Correlations between temperature values and health effects..... | 35 |
| 6.1.2. Mortality thresholds for low temperatures exposure | 38 |
| 6.1.3. Effects of impact with solid CO ₂ particles | 39 |
| 6.1.4. Low temperatures and high CO ₂ concentration..... | 40 |
| 6.2. Cryogenic effects on equipment | 44 |
| 6.2.1. From the leak to the break of the pipeline due to embrittlement..... | 44 |
| 6.2.2. The embrittlement of metals and sealants | 45 |
| 7. Visibility issues | 48 |
| 8. Health effects of generated physical blast | 50 |
| 8.1. Direct effects of blast..... | 51 |
| 8.2. Indirect effects of blast | 53 |
| 8.3. Blast effects compared with toxic effects of CO ₂ | 54 |

| | | |
|-----------|--|-----|
| 9. | Effects of impurities on human health..... | 56 |
| 9.1. | Health effects of high concentration of H ₂ S | 59 |
| 9.1.1. | The Mattoon Site project evaluations..... | 60 |
| 9.2. | Acceptable concentrations of impurities | 62 |
| 10. | Secondary engineering hazards | 65 |
| 11. | Summary of proposed vulnerability thresholds..... | 67 |
| 12. | Application to the case study..... | 69 |
| 12.1. | Allam cycle description..... | 70 |
| 12.2. | Methodology..... | 72 |
| 12.2.1. | Modelling with Phast 8.23..... | 72 |
| 12.2.1.1. | DISC, ATEX and UDM models validated on CO ₂ releases..... | 75 |
| 12.2.2. | System modelling..... | 75 |
| 12.2.2.1. | Variable parameters of the simulation..... | 80 |
| 12.2.3. | Vulnerability criteria applied to Phast results..... | 81 |
| 12.3. | Results | 83 |
| 12.3.1. | Definition of the damage areas..... | 87 |
| 12.3.2. | Comparison between CO ₂ and CH ₄ release consequences..... | 90 |
| 13. | Conclusions | 92 |
| | Appendix A | 94 |
| | Appendix B..... | 95 |
| | Appendix C..... | 96 |
| | Appendix D | 100 |
| 14. | References | 101 |
| | Ringraziamenti | 107 |

List of Figures

| | |
|--|----|
| Figure 1 CO ₂ phase diagram. (Holt, 2020)..... | 13 |
| Figure 2 Health effects of inhalation of CO ₂ . (Holt, 2020)..... | 15 |
| Figure 3 Occupational Exposure Limits for CO ₂ (DNV-RP-J202, April 2010)..... | 16 |
| Figure 4 Unconsciousness due to carbon dioxide exposure. (IOGP Risk Assessment Data Directory, March 2010)..... | 17 |
| Figure 5 Effects of oxygen depletion. (OSD3.2, January 2006) | 18 |
| Figure 6 The four stages of asphyxiation. (OSD3.2, January 2006) | 18 |
| Figure 7 Time to unconsciousness for humans exposed to CO ₂ in a low and in a high O ₂ environment. (Rice, 2004)..... | 19 |
| Figure 8 Relationship between CO ₂ and O ₂ in air. (Holt, 2020) | 20 |
| Figure 9 SLOT DTL and SLOD DTL curves. (Holt, 2020)..... | 24 |
| Figure 10 Prediction of mean concentration in a CO ₂ jet. The three pairs of curves show the locations of the SLOD and SLOT calculated using different load models. (Gant & Kelsey, 2011)..... | 25 |
| Figure 11 Change in mean CO ₂ concentration with time and distance from the release point. (Lyons, Race, Hopkins, & Cleaver, 2015)..... | 26 |
| Figure 12 Change in equivalent CO ₂ concentration with time and distance from the release point. (Lyons, Race, Hopkins, & Cleaver, 2015)..... | 26 |
| Figure 13 Probability of fatality for CO ₂ based on SLOT and SLOD (UK HSE) data. (Energy Institute, 2010)..... | 28 |
| Figure 14 CO ₂ dose-fatality correlation based on SLOD and SLOT (UK HSE) data. (Energy Institute, 2010) | 29 |
| Figure 15 Lethality levels UK HSE 2008. (W ter Burg, 2021) | 29 |
| Figure 16 Probit relations to calculate sub-lethal effect areas. The ‘k1’ values of all these functions are obtained considering an exposure duration of 30 minutes. (Geldereren, 2013) | 30 |
| Figure 17 Lethality chance of CO ₂ for different probit relations. (*) Values obtained from the too optimistic OCAP correlation are not representative because higher than the 100%.Data based on (Geldereren, 2013). ... | 31 |
| Figure 18 Comparisons between Tebodin, HSE, TNO and Lievensse probit functions for exposure of 1 min and 60 min. (M. M.j. Knoope, 1 January 2014) | 32 |
| Figure 19 Comparisons between TNO and Lievensse probit functions for exposure of 1 min, 5min, 60 min, 240 min. (Joris Koornneef, 2009)..... | 32 |
| Figure 20 Surface temperature as function of time for frostnip (skin at 0°C). (Juhani Hassi, December 1999 - May 2001) | 36 |
| Figure 21 Surface temperature as function of time for numbness condition (skin at 7°C). (Juhani Hassi, December 1999 - May 2001)..... | 36 |
| Figure 22 Surface temperature as function of time for pain condition (skin at 15°C). (Juhani Hassi, December 1999 - May 2001) | 36 |
| Figure 23 Surface temperature as function of time for pain condition during gripping conditions (skin at 15°C). (Juhani Hassi, December 1999 - May 2001)..... | 37 |
| Figure 24 Drop in finger temperature with time, at low activity. Hand protection of 2 clo. (Juhani Hassi, December 1999 - May 2001)..... | 37 |
| Figure 25 Drop in finger temperature with time, at high activity. Hand protection of 1.4 clo. (Juhani Hassi, December 1999 - May 2001)..... | 38 |
| Figure 26 Pressurized CO ₂ release and sublimating bank dynamics with reference to a general time scale. (Mocellin, Vianello, & Maschio, 2016) | 40 |
| Figure 27 Environmental and experimental conditions of the three different release tests. (Guo, et al., 2016) | 41 |
| Figure 28 CO ₂ concentration evolution along the axial line. (Guo, et al., 2016) | 42 |
| Figure 29 Temperature evolution along the axial line. (Guo, et al., 2016)..... | 42 |
| Figure 30 Change in internal temperature with time and distance from the release point. (Lyons, Race, Hopkins, & Cleaver, 2015)..... | 43 |

| | |
|---|-----|
| Figure 31 Fracture toughness of various metals at low temperatures. At low temperatures, nickel steels (b.c.c.) decrease in toughness and become brittle, whereas austenitic stainless steels (f.c.c.) such as AISI 310 and AISI 316 remain tough reducing temperature. Ti-6% and Al-4% (h.c.p.) toughness drops more moderately. (Data compiled from Tobler and McHenry 1983, Mann 1978, and Fowlkes and Tobler 1976.) | 46 |
| Figure 32 Materials resistant to extremely low temperatures. (Gasperini, 2019) | 46 |
| Figure 33 EI effect criteria for outdoor populations. (Energy Institute, 2010) | 51 |
| Figure 34 EI effect criteria for indoor population. (Energy Institute, 2010) | 51 |
| Figure 35 Pressure-impulse graph for lung damage according to TNO Green Book. The red line is the highest scaled overpressure value proposed by EI, associated with 689 mbar. (Roos, December 1989) | 52 |
| Figure 36 117 mm pipeline release outdoor fatality footprint (red=100%; yellow=10%; green=1%). (Energy Institute, 2010) | 55 |
| Figure 37 Blast-distance relationship for 117 mm line rupture. (Energy Institute, 2010) | 55 |
| Figure 38 Indicative composition of dried CO ₂ streams (IEA GHG). Unit % volume. (DNV-RP-J202, April 2010) | 57 |
| Figure 39 Compounds from different power production methods with CO ₂ capture. Indicative maximum values. (Oosterkamp & Ramsen, 2008) | 57 |
| Figure 40 Effects of exposure to hydrogen sulfide. (OSD3.2, January 2006) | 59 |
| Figure 41 Exceedance of occupational health criteria for workers. (U.S. Department of Energy - National Energy Technology Laboratory, November 2007) | 61 |
| Figure 42 Type of effects and hazard endpoints for receptors. (U.S. Department of Energy - National Energy Technology Laboratory, November 2007) | 62 |
| Figure 43 Proposed limits of impurities concentrations. (Johnsen, Holt, Helle, & Sollie, 2009) | 63 |
| Figure 44 CO ₂ stream compositions recommended limits. (Herrom & Myles, 2013) | 64 |
| Figure 45 CO ₂ hydrate phase diagram. Abbreviations: L - liquid, V - vapor, S - solid, I - water ice, H - hydrate. (Mike Bilio, 2009) | 66 |
| Figure 46 Simplified PFD of Allam Cycle | 70 |
| Figure 47 Radar chart obtained from pure CO ₂ release outputs. Values for different orifice diameters (7, 22, 70, 150 mm), stability class (2F, 5D) and for releases with (Y) or without (N) impingement | 84 |
| Figure 48 IDLH maximum distances obtained from different stagnation data. | 88 |
| Figure 49 Typical pre-AWD temperature profiles for 22 mm leak | 89 |
| Figure 50 Maximum concentration and probit Footprints for scenario CO ₂ _recpump_out, weather 2F, orifice diameter 22mm and impinging release. 8% CO ₂ and probit 2.67 (blue curve); 11% CO ₂ and probit 5.0 (green curve) | 97 |
| Figure 51 Maximum distances for 1% or 50% fatality due to low temperatures and high CO ₂ concentrations. For solid fraction of 28%, releases of both supercritical (s) and liquid (l) CO ₂ are represented. | 98 |
| Figure 52 Minimum distances from release points to install valves and lighting (red curves) or circuit breakers (blue curves) | 98 |
| Figure 53 Effect Zones for 8% CO ₂ (outer Footprint) and 11% CO ₂ (inner Footprint). Grid squares of 10 meters. | 100 |
| Figure 54 Effect Zones for probit value of 2.67 (outer Footprint) and of 5.0 (inner Footprint). Grid squares of 10 meters. | 100 |

List of Tables

| | |
|--|----|
| Table 1 Health effects of CO ₂ when O ₂ concentration is high enough to not cause asphyxia | 20 |
| Table 2 Health effects of CO ₂ when depletion of O ₂ starts to be perceived | 21 |
| Table 3 Health effects of CO ₂ when asphyxia due to oxygen depletion stars to occur | 21 |
| Table 4 Health effects of oxygen depletion..... | 22 |
| Table 5 Tebodin probit relations | 30 |
| Table 6 Suggested fatality criteria for exposure to cryogenic conditions. Data based on (Rettner, 2019)..... | 38 |
| Table 7 Overpressure effects. (HSE UK) | 52 |
| Table 8 Injuries from fragments. (HSE UK) | 53 |
| Table 9 Lethal levels of CO exposure by UK HSE and TNO | 58 |
| Table 10 Lethal levels of SO ₂ exposure by UK HSE and TNO | 58 |
| Table 11 Lethal levels of NO ₂ exposure by UK HSE and TNO..... | 59 |
| Table 12 Lethal levels of H ₂ S exposure by UK HSE and TNO | 59 |
| Table 13 Proposed fatality criteria..... | 68 |
| Table 14 Some vulnerability thresholds for safety system materials. Temperatures in breakers refer to advanced technologies for cryogenic applications. | 69 |
| Table 15 Thermo-physical characterization of modelled points of the Allam cycle..... | 78 |
| Table 16 Leak frequencies for plant components (IOGP, 2021)..... | 79 |
| Table 17 Fatality threshold for temperature and concentration..... | 81 |
| Table 18 CO ₂ toxic contours | 82 |
| Table 19 Suggested fatality criteria for thermal radiation. (OSD3.2, January 2006) | 82 |
| Table 20 Solid percentage at the equilibrium plane | 85 |
| Table 21 Minimum distances from the release to install typical plant equipment | 90 |
| Table 22 Comparison between 50% and 1% fatality distances generated by a CH ₄ or a CO ₂ release..... | 91 |
| Table 23 Phast generated cloud Side Views at the end of horizontal releases with impingement, for weather condition 2F and CO ₂ concentration of 15000 ppm (STEL). | 96 |
| Table 24 Limit distances and leak frequencies for different release scenarios..... | 96 |
| Table 25 Phast generated Effect Zones for CH ₄ and CO ₂ different hazards..... | 99 |

Acronyms

| | | | |
|--------------------------------|--|-----------------|--|
| ACGIH | American Conference of Governmental Industrial Hygienists | IDLH | Immediate Dangerous to Life and Health |
| Ar | Argon | LD | Lethal Dose |
| ASU | Air Separation Unit | IGCC | Integrated Gasification Combined Cycle |
| ATEX | Atmospheric Expansion model | IOGP | International Oil&Gas Producers |
| BDV | Blow Down Valve | MEL | Maximum Exposure Limit |
| CATO | CO ₂ Capture, Transport and Storage | N ₂ | Nitrogen |
| CCUS | Carbon Capture Utilization and Storage | NIOSH | National Institute for Occupational Safety and Health |
| clo | Clothes thermal insulation (1 [clo] = 0.155 [m ² K/W]) | NO _x | Nitrogen Oxides |
| CLP | Classification, Labelling and Packaging | NOAEL | No Observed Adverse Effect Level |
| CO | Carbon Monoxide | O ₂ | Oxygen |
| CO ₂ | Carbon Dioxide | OEL | Occupational Exposure Limit |
| CPU | CO ₂ Purification Unit | OSHA | Occupational Safety and Health Administration |
| DISC | Discharge model | PEL | Permissible Exposure Limit |
| DOE | Department of Energy | PFD | Process Flow Diagram |
| DTL | Dangerous Toxic Load | ppm | Parts per Million |
| ECHA | European Chemical Agency | ppmv | Parts Per Million Volume |
| EERA | Escape, Evacuation and Rescue Analysis | QRA | Quantitative Risk Assessment |
| EHR | Enhanced Hydrocarbon Recovery | REL | Recommended Exposure Limit |
| ERDF | European Regional Development Fund | SDV | Shutdown Valve |
| FBR | Full Bore Rupture | SLOD | Significant Likelihood Of Death |
| FeCO ₃ | Iron Carbonate | SLOT | Specified Level Of Toxicity |
| FeS | Iron Sulfide | SO _x | Sulfur Oxides |
| GHS | Global Harmonized System | STEL | Short Term Exposure Limit |
| H ⁺ | Hydrogen ion | TEEL | Temporary Emergency Limits |
| H ₂ | Hydrogen | TNT | Trinitrotoluene |
| H ₂ CO ₃ | Carbonic Acid | TWA | Time Weighted Average |
| H ₂ S | Hydrogen Sulfide | UDM | Unified Dispersion Model |
| HSE | Health and Safety Executive | USEPA | US Environmental Protection Agency |

1. Introduction

Climate changes and the increasing of greenhouse gases level are well known problems of the last decades. Among these gases, the presence of CO₂ in atmosphere needs to be taken under control in order to reach the net-zero emissions in 2050 (International Energy Agency, 2021). Among all possible technological strategies proposed to reach the goal, the Carbon Capture Utilization and Storage (CCUS) process can assume an important role, providing to the 55% of the needed mitigation efforts (Vitali, et al., 2021). This technology may be able to reduce the amount of CO₂ globally present in the atmosphere by capturing the 20% of that. In this way, the carbon dioxide coming from different industrial processes, chemical plants, oil and gas facilities and power plants may be captured, transported and stored or reused, exploiting a circular business.

Especially for coal fired processes, the CCUS retrofitting of operating plants, which current total capacity is of about 2000 GW, can improve their environmental impact (Vitali, et al., 2021). Also the “blue hydrogen” production from coal and gas plants can be a field of application of CCUS during the energy transition. New solutions also investigate the possibility of exploiting existing hydrocarbons pipelines and facilities for CCUS, in order to give them a new life in safe conditions.

The captured CO₂ can be stored in depleted reservoirs or reused, so it is usually transported by pipelines from one site to the other one, in a techno-economically convenient way. The transportation of CO₂ by onshore pipelines is a common practice in USA, where 8000 km of pipework are nowadays used especially for Enhanced Oil Recovery (EOR) activities. The technologies associated with capture, transportation and storage of CO₂ for EOR field of application are mature and the linked hazards are well understood and regulated by standard and practical guidance. However, the extrapolation of this knowledge for dense-phase CO₂ projects, has to be carefully managed (Jensen, Schlasner, Sorensen, & Hamling, 2014) . In addition, there is a lack of operational experience in managing large-scale CO₂ infrastructures, such as pipelines analyzed for new CCUS projects, which are longer than that already used in USA and able to transport a larger amount of CO₂ (thousands of tons of compressed carbon dioxide). Transportation in Europe and in other countries different from USA will cross more densely populated areas. This aspect provides more probability of damage of pipelines by third parties and more people and infrastructures that could be affected by an unexpected CO₂ release.

The CCUS facilities usually transport compressed CO₂ able to reach supercritical and liquid conditions (defined as ‘dense phase’). Even if carbon dioxide cannot be classified as a toxic, flammable or explosive gas due to the fact that it is fully oxidized, because of the high concentrations reached during a leak and critical transportation conditions, the CO₂ behavior has to be analyzed in order to establish how to manage the connected risks. A significant leak from an inventory can generate a very low temperature cloud of two-phase carbon dioxide, densely distributed to the ground level, and an uncontrollable release of energy. All the related consequences would have the potential to be life-threatening to people, being also able to generate a major accident event. In fact, people near CCUS infrastructures can be exposed at serious injuries, so the safety distance needs to be evaluated.

The objective of this thesis is to investigate all the potential consequences; associated with a CCUS hazardous event, and corresponding vulnerability thresholds for individuals and equipment. The resulting vulnerability analysis will be applied to a case study, in order to investigate the potential of a supercritical CO₂ release. Comparisons with accidental release of flammable methane will also be done, to evaluate the applicability of typical QRA methodologies to CO₂ and its impact on plants risk assessment.

First of all, the effects caused by inhalation of carbon dioxide on human health will be explored, defining some values of volumetric concentration of CO₂ and duration of exposure able to cause sever damages, on human health. Also the asphyxiating effect of CO₂ will be analyzed. The second aspect taken into account is the impact of the very low temperatures reached during the release, as a consequence of the Joule-Thomson effect. The inhalation of cold air and the possible cold burns caused by the impact with cold jets, solid CO₂ particles and cooled surfaces, will be studied.

In addition, the cryogenic consequences on materials such as metals or sealants, impinged by the cold plume, will be considered by describing the loss of structural integrity linked with low temperatures and enhanced by the presence of some impurities in the released flow. Also the lack of visibility inside the cloud will be analyzed, finding correlation between the level of CO₂ in the cloud and the formed fog able to reduce the ability of people to escape. In addition, the vulnerability of people exposed to the shock wave, generated by the rapid expansion of the stream during the release, will be evaluated.

Apart from these physical effects of a CO₂ release, other secondary effects will be assessed. Firstly, the presence of impurities within CO₂ streams will be discussed. Through literature analysis, some limit concentrations of impurities inside the stream will be proposed, also considering their ability to reduce the integrity of structures after their release. For each considered hazard, starting from literature review, vulnerability criteria will be defined. This first part of the analysis will be presented with the following structure:

- In Chapter 2, the methodology used to identify vulnerability thresholds will be described.
- In Chapter 3, CO₂ main properties will be analyzed, also considering CO₂ behavior during discharge and dispersion phases.
- In Chapter 4, the asphyxiating and toxic properties of CO₂ will be discussed.
- In Chapter 5, some probit or dose-based models will be compared, also investigating literature examples about definition of lethality areas for inhalation.
- In Chapter 6, the cryogenic effects of rapid depressurization on people and materials will be considered. The phenomenon entity will be investigated through literature examples about the definition of discharged plume behavior. Limit temperatures for emergency equipment will be proposed.
- In Chapter 7, a possible correlation between lack of visibility and CO₂ plume concentration will be studied.
- In Chapter 8, the direct and indirect effects of a blast on human health will be discussed, comparing shared vulnerability thresholds available in literature with Energy Institute's results. Literature experiments and simulations about near-field consequences will be reported.
- In Chapter 9, the impact of potentially released impurities will be analyzed, comparing the toxicity of CO₂ to that of other stream components.
- In Chapter 10, the action of some secondary engineering hazards will be discussed.
- In Chapter 11, a summary of suggested vulnerability criteria will be reported.

In the second part of this thesis, these results will be applied to a case study: The 'Allam cycle' plant. This oxy-fuel gas fired power plant will be described, referring to Eni's previous works. As part of the plant QRA, the analysis of consequences will be done using the DNV GL software Phast 8.23. The aim of this section is the identification of damage areas, by associating the proposed vulnerability thresholds with the characteristics of the dispersed CO₂ plume calculated by the software. The applicability of Phast to the supercritical CO₂ release modelling and its limitations will be discussed. The analysis of the case study will be divided in the following parts:

- In Chapter 12.1, the case study will be presented, describing the Allam cycle plant and the secondary CO₂ and oxidant purification units.
- In Chapter 12.2, the methodology used for the identification of damage areas will be explained, focusing on the post-processing of outputs of the simulation conducted with software Phast 8.23. The proposed vulnerability thresholds for people and equipment will be described.
- In Chapter 12.3, the results will be presented, identifying the most critical simulated scenario by showing the obtained damage areas.

In Chapter 13, the drawn conclusions will be discussed, highlighting uncertainties faced during the analysis and proposed future works needed to fill the gaps in knowledge about modelling supercritical CO₂ release and consequences on people and equipment.

This work is the result of a collaboration with Eni SpA, thanks to which it was possible to gain access to specific information about Eni's previous activities on CCUS projects.

2. Methodology used to identify vulnerability and impairment thresholds

In order to identify vulnerability and impairment thresholds associated to a CO₂ release, all physical effects have been investigated by collecting information about their ability to cause damages on human health and equipment. When vulnerability models are found in literature, their applicability to supercritical CO₂ releases has been verified. When, on the contrary, a physical effect has never been considered before in QRA for CCUS applications, new approaches have been proposed in this first section of the analysis, in order to identify vulnerability and impairment thresholds.

First of all, the CO₂ toxicity and its asphyxiating effects have been analyzed, considering that consequences of CO₂ inhalation are well known thanks to military experience and laboratory tests conducted for decades, not strictly related to CCUS applications. Once that common correlations between concentration of inhaled CO₂ and lethal effects on people have been determined, literature statistical approaches have been investigated in order to find a methodology able to match these lethal limits. Among all probit functions found in literature, the most appropriate one has been identified.

Considering low temperatures generated during a CO₂ release, because of the absence of shared methods and statistical approaches able to associate lethality to exposure to cryogenic conditions, a correlation between medical parameters and mortality has been proposed. By applying thresholds methodology, the 1% lethal limit has been associated to physiological states able to cause death of highly susceptible people, while the 50% limit has been correlated to medical conditions able to determine 50% probability of death of all exposed people. The impairment of equipment exposed to cold jet and generated solid particles of CO₂ has been evaluated. The cryogenic embrittlement of metals has been discussed, defining some design rules needed to avoid materials degradation. Also functionality of emergency and safety systems has been considered, proposing some limit temperatures according to which their proper installation has to be done.

Referring to DNV GL guidance on CCS risk management (Holt, 2020), also lack of visibility, huge release of energy and dispersion of dangerous stream impurities have been identified as effects of a CO₂ release. Comparing experimental results found in literature, a correlation between reduced visibility and corresponding CO₂ concentration in the plume has been looked for. Concerning the overpressure generated by the rapid release of energy during the discharge, vulnerability models found in literature for CCS risk assessment have been compared with common standard models about blast effects on human health. The release of toxic impurities transported with CO₂ has been analyzed. Some existing limitations about their volumetric percentage in captured and stored stream have been collected and compared with data about conducted experiments found in literature.

Finally, also secondary engineering hazards, that need to be better understood, modeled and quantified, have been analyzed, in order to verify if their impact on equipment has to be considered for a comprehensive QRA.

The results of this first part of the analysis are vulnerability and impairment thresholds applied to outputs of the Allam cycle case study's simulation.

3. CO₂ properties and behavior

Carbon dioxide is part of atmospheric mixture and of the life cycle of animals and plants. Humans and animals produce energy from oxygen, releasing CO₂ in the environment that is absorbed by plants during the photosynthesis process. An amount 50 times higher than that of CO₂ in atmosphere is dissolved in oceans and

lakes. The obtained balance between plant and animals' life cycles and content in water results in the presence of 0.038% of carbon dioxide in atmosphere.

At normal atmospheric conditions CO₂ is a colorless and odorless gas. At standard conditions the carbon dioxide shows a density 1.5 times that of air (1.98 kg/m³), while in its supercritical phase, above the critical point (pressure of 73.9 bar and temperature of 31.1 °C), it exhibits a viscosity similar to a gas and a density similar to a liquid. The following diagram shows the conditions for which CO₂ can exist in its gas, liquid, solid or supercritical phase and the typical pressure and temperature values of transportation and storage. In particular, the sublimation line, for temperature and pressure values below the CO₂ triple point (-56.7°C and 5.18 bar), defines the conditions for which the transformation from solid to gas and back is possible without the formation of the intermediate liquid phase. During supercritical CO₂ releases, this curve is followed until expansion to the ambient pressure, underlining the generation of a solid-vapour two-phase cloud.

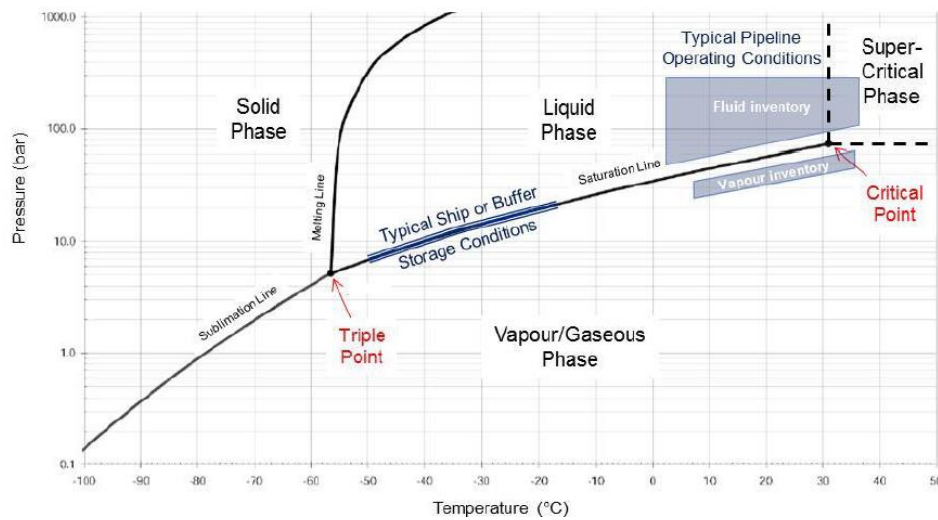


Figure 1 CO₂ phase diagram. (Holt, 2020)

The release of CO₂ in CCUS plants may be controlled or accidental. In the first case, the depressurization is related to pipeline venting or equipment blow down. On the other hand, an uncontrolled release from vessel or pipeline is the consequence of a rupture or a leakage.

When a leak of dense CO₂ occurs, the P-H diagram can be used to evaluate the phase changes and the energy transferred during the obtained depressurization. In this way, the flow characteristics at the pipe or vessel exit, starting from the stagnation conditions, may be determined. After the discharge, an isenthalpic expansion takes place, during which the jet internal energy is preserved. This second part of the process description is useful to determine the jet properties at ambient pressure, considering that the temperature of the real gas may change even if no heat is absorbed or released. This phenomenon, called Joule-Thomson effect, is characterized by a transition temperature below which the expansion at constant enthalpy causes cooling effects. The Joule-Thomson transition temperature for CO₂ at ambient pressure is of about 1500 K. During expansion, a vapour-solid jet is obtained. In case of horizontal releases, part of the formed solid particles may deposit on the ground, while the remainder may sublime within the expanding jet. The generated dry-ice bank sublimates thanks to external heat, forming an additional delayed source of CO₂.

The expanded flow properties are the initial conditions for the third part of the event, the dispersion of the cloud, during which the losing of momentum occurs. The obtained 'Gaussian' CO₂ plume, mixed with air, will travel for a certain distance, changing its characteristics that need to be modeled and predicted (Liu, Godbole, Lu, Michal, & Venton, 2015). The mixing with air and the wind action gradually reduce the CO₂ concentration in the cloud and the plume temperatures.

4. Health effects of CO₂ inhalation

The carbon dioxide is a gas normally present in human blood, but a huge concentration of it can cause adverse effects, not only due to oxygen depletion and asphyxiation, but also because it can increase acidity of blood. Even if CO₂ is not classified as a toxic gas, for CCUS risk evaluations, where a very large quantity of CO₂ can be released, depending on concentration and exposure duration it can cause headache, dizziness, muscle twitching and unconsciousness, making people unable to escape, until death. In addition, high concentration of CO₂ may increase respiratory rate, enhancing inhalation of other toxic substances potentially released in the area.

An acute exposure to CO₂ may be followed by acute or long-term effects. The acute effects are linked with the CO₂ capability to attack the respiratory regulation system and the oxygen supply (W ter Burg, 2021). The high exposure symptoms are hypercapnia, hypoxia, metabolic acidosis, unconsciousness and lethal respiratory arrest. The long-term effects of an exposure are due to lack of oxygen supply to sensitive tissues like brain. There are uncertainties on long-term effects correlated with hypercapnia, as it is not clear if damages to lungs and brain tissues are caused by CO₂ toxicity or by fatigue due to generated hyperventilation.

Normally in human lungs there is about 5% of CO₂ and 14% of O₂ in volume. During breathing action oxygen is transferred to the blood and carbon dioxide is expelled from blood to the outside. The 5% of CO₂ generated in the body is dissolved in serum and cytoplasm, while the 90% can reach the red blood cells where it reacts with water to form carbonic acid, ionized to bicarbonate, that limits the acidity of blood. The last 5% of CO₂ reacts with amino groups in hemoglobin, forming carbamino (Holt, 2020).

CO₂ is present in atmosphere at a volumetric concentration of 0.038% and human body is very sensitive to a variation of this value. The respiratory rate depends on the need of cells for oxygen and the need of cell to eliminate CO₂, so gases concentrations can stimulate the respiratory center of brain. When the concentration of CO₂ in blood is too high, the respiratory center reacts to the increase of acidity and to the reduction of H⁺ ions, by increasing the breathing rate. At the end of the exposure, the resulting hyperventilation can restore the normal pH value of blood, but if CO₂ concentration increases, the more intensive cardiac and respiratory rates cannot compensate the CO₂ excess, so the carbon dioxide will accumulate in the blood and tissues. Acidosis may occur in humans after one-hour-exposure to 2.8% of CO₂, while, at higher concentrations (10%), the decreasing of pH is observed after 10 minutes.

The effects of CO₂ inhalation on human body depends not only on concentration and duration of the exposure, but also on age, health, physiological make-up, occupation and lifestyle of affected people. For this reason, all military studies about inhalation of high CO₂ concentration can be considered too optimistic.

For example, prolonged exposure to low CO₂ concentration has seemingly benign effects on healthy and young adults. They suffer the decreasing of 20% of blood pressure only after 5 days exposed to 1.2% of CO₂ and a significant performance decrement after 8 days exposed to 3% of CO₂. Same studies have been conducted on sensitive populations to evaluate the prolonged low-level CO₂ exposure consequences. In particular, the induced increasing in lung dead space volume can be not reversible in patients with pulmonary diseases. In addition, elevated pulmonary blood pressure is not well tolerated by people suffering hypertension, and the decreasing of bone formation can be a problem for people with bone diseases and osteoporosis (Rice, 2004).

4.1. Definition of dangerous CO₂ volumetric thresholds

The evaluation of consequences of CO₂ inhalation is based on the definition of volumetric thresholds of CO₂ concentration, that can be considered representative of some effects on human health, changing the duration of the exposure. For example, inhalation of 3% of CO₂ can cause headache, after one hour, changing ventilation rate, while a concentration of 2% can have the same effects after several hours. Available data indicate that dyspnea occurs when exposed to a CO₂ concentration higher than 3%, even at rest, while headache, is proved to be severe, in particular during exercise, after 30 minutes exposed to the same CO₂ percentage. If this

disease disappears soon after an acute exposure, it means that this condition has been caused by CO₂ induced acidosis. In case of prolonged effects, the headache can be linked with the dilatation of cerebral blood vessels.

For IOGP (International Oil&Gas Producers) models, CO₂ is not considered a toxic substance and it has been analyzed as a low-concentration gas observed in fire, not able to cause significant effects on human health. At the same time, IOGP puts in evidence the possibility to reach higher carbon dioxide concentrations that stimulate respiratory rate. As already said, this effect enhances the amount of other toxic substances inhaled by people exposed to a released cloud of CO₂. The breathing rate increases of 50% for a CO₂ concentration of 2%, it doubles for 3% of CO₂ and at 5% it becomes so high that some people can experience breathing difficulties (IOGP Risk Assessment Data Directory, March 2010).

Inhalation of 4-5% of CO₂ for 15-30 minutes causes headache, increased blood pressure and breathing difficulties after few minutes. Mental depression starts at 5% of CO₂ for several hours of exposure. Inhalation of 5-7% CO₂ for 15-30 minutes increases the blood pressure, but a slight increase can be obtained even inhaling 1-2% CO₂ for 17-32 minutes. In general, for these values body's circulatory system is affected but no changes are shown in cardiac output.

After some experimental tests on astronauts (Wong King Lit, 1996), it has been proved that the 2.5% is the no-observed-adverse-effect level (NOAEL), for an exposure of 5-22 minutes. The 3-4% CO₂ is the threshold for slight hearing impairment, but also vision can be damaged by low concentrations of CO₂. For example, a 6-minute exposure to 6.1-6.3% of CO₂ can cause a reduction in hearing of 3-8%, while reduction of visual intensity occurs after few minutes exposed to 6% CO₂. The same test shows that a 7-10% CO₂ concentration is able to cause unconsciousness and near unconsciousness after few minutes. For these values dizziness, sweating, mental depression and visual and hearing dysfunction occur after 1-5 minutes.

A concentration of 10% is considered able to cause asphyxiation after 15 minutes, as established by NIOSH limits. The concentration of 1% can already stimulate respiration, but when reached the 8%, CO₂ depresses human respiratory system. The CO₂ concentration in the range of 10-15% will lead to drowsiness, muscle twitching and unconsciousness after 1 minute, while, for the same duration, a volumetric percentage in the range 17-30% can result in loss of controlled activity, unconsciousness, coma and death of exposed people (Holt, 2020). NORSOK Z013 standard has defined the relationship between concentration of CO₂ in air and time to develop unconsciousness (see Chapter 4.1.1.). According to NORSOK standard, unconsciousness is reported after 30 minutes if exposed to 10% of CO₂ and after 1 minute if exposed to a 15% concentration.

Putting together all the previous considerations, some common exposure values, reported in the following figure, are used to identify ranges of concentration able to cause different acute effects on human health, starting from headache and difficult breathing, until unconsciousness and death.

| CO ₂ Concentration in Air (% v/v) | Exposure | Effects on Humans |
|--|-----------------------------|---|
| 17 - 30 | Within 1 minute | Loss of controlled and purposeful activity, unconsciousness, convulsions, coma, death |
| >10 - 15 | 1 minute to several minutes | Dizziness, drowsiness, severe muscle twitching, unconsciousness |
| 7 - 10 | Few minutes | Unconsciousness, near consciousness |
| | 1.5 minutes to 1 hour | Headache, increased heart rate, shortness of breath, dizziness, sweating, rapid breathing |
| 6 | 1 - 2 minutes | Hearing and visual disturbances |
| | ≤ 16 minutes | Headache, difficult breathing (dyspnea) |
| 4 - 5 | Several hours | Tremors |
| | Within a few minutes | Headache, dizziness, increased blood pressure, uncomfortable breathing |
| 3 | 1 hour | Mild headache, sweating, and difficult breathing at rest |
| 2 | Several hours | Headache, difficult breathing upon mild exertion |

Figure 2 Health effects of inhalation of CO₂. (Holt, 2020)

In general, these described effects on humans and related CO₂ concentrations are shared and adopted as references in the common practice. However, some published projects based toxicity criteria on specific national guidelines, in order to define the iso-risk contours inside which a defined lethality value may be evaluated. For example, among all the published projects about CCUS risk assessment, the FutureGen project (U.S. Department of Energy - National Energy Technology Laboratory, November 2007) has adopted the US Environmental Protection Agency (EPA) and the US Department of Energy (DOE) guidelines, in order to identify exposure limits able to characterize a calculated risk contour.

The FutureGen results are obtained according to the EPA and DOE toxicity criteria of Maximum Exposure Limit (MEL). The MEL is fixed by the EPA agency at 3% of CO₂ inhaled for 20 minutes. If the exposure is prolonged or the concentration rises, the increasing of respiratory rate and other impactful effects are likely to occur. The MEL fixed by DOE is obtained for 15 minutes exposed to 4% CO₂ and also in this case, a higher dose is considered to be life-threatening. The EPA agency establishes the MEL also for a shorter duration and higher concentration (7% of CO₂ for less than 3 minutes), for which unconsciousness may occur. These MEL values have been used as references for the FutureGen project in order to identify the risk contours outside which no harmful effects are reported.

4.1.1. Occupational exposure limits

The acceptable concentration of a hazardous substance in a workplace has to be settled, usually by authorities and legislations. With the Occupational Exposure Limits (OELs), occupational safety and health are taken into account. For this reason, healthy and adult workers are considered to determine the maximum acceptable dose of a hazardous substance that is not valid for pregnant women and sensitive people. For example, the Time Weighted Average (TWA) concentration is referred to a limited value at which workers can be exposed for 8 or 10 hours a day, for a working life of 40 years and 200 working days per year, without consequences. Other limits are settled for short-term exposure concentrations (STEL), often referred to a 15-minute duration. Some substances have a Ceiling value that should not be exceeded at any time.

The OELs may assume a legal status in some countries. For example, the UK OELs have a legal status, managed by the COSHH Regulations and reported annually in the HSE publication EH40. In Norway the OELs are established by the Arbeidstilsynet Central Labour Inspectorate and the proposed TWA, STEL and Ceiling limits are only recommendations, without a legal value. Some published OELs are reported in figure 3.

| Exposure Time | % CO ₂ | Comment | Reference |
|---------------|-------------------|---|---|
| 10 hours | 0.50% | Time weighted average | NIOSH (US) |
| 8 hours | 0.50% | Time weighted average | OSHA (US) |
| | 0.50% | Occupational Long Term Exposure Limit (LTEL) | COSHH HSE (UK) |
| 60 min | 4% | Emergency Exposure Level for submarine operations | USA Navy |
| | 2.5% | Emergency Exposure Level for submarine operations | National (US) Research Council |
| | 5% | Suggested Long Term Survivability Exposure Limit | HSE (UK) |
| | 2% | Maximum exposure limit | Compressed Gas Association 1990 |
| 20 min | 3% | Maximum exposure limit | Compressed Gas Association 1990 |
| | 1.5% | Occupational Short Term Exposure Limit (STEL) | COSHH HSE (UK) |
| 15 min | 3% | Short Term Exposure Limit (STEL) | Federal occupational safety and health regulations (US) |
| | 4% | Maximum exposure limit | Compressed Gas Association 1990 |
| 10 min | 5% | Maximum exposure limit | Compressed Gas Association 1990 |
| 7 min | 5% | Maximum exposure limit | Compressed Gas Association 1990 |
| 5 min | 5% | Suggested Short Term Exposure Limit (STEL) | HSE (UK) |
| | 6% | Maximum exposure limit | Compressed Gas Association 1990 |
| 3 min | 7% | Maximum exposure limit | Compressed Gas Association 1990 |
| 1 min | 15% | Exposure limit | NORSOK (Norway) |
| <1 min | 4% | Maximum Occupational Exposure Limit | Federal occupational safety and health regulations (US) |

Figure 3 Occupational Exposure Limits for CO₂ (DNV-RP-J202, April 2010)

Some applicable limits are nowadays based on existing CO₂ OELs. For example, a concentration of 10000ppm (1%v/v) has been proposed as an average of long-term exposure limit (5000ppm for 8 hours defined by ACGIH in 2001 that appears to be well tolerable due to normal oxygen levels of 19-20%) and UK short-term exposure limit (15000ppm for 15 minutes). In addition, the NIOSH puts the IDLH (*Immediate Dangerous to Life and*

Health) limit, at a concentration of 40000ppm (4% v/v), already defined by the Federal occupational safety and health regulations as the Maximum Occupational Exposure Limit (Mazzoldi & Oldenburg, 2011).

Once the health effects of a given percentage of inhaled CO₂ have been discussed, associated probabilities of death have to be evaluated, in order to define useful vulnerability criteria in addition to the existing occupational exposure values. In general, the lethality induced by the inhalation of CO₂ is linked with concentrations higher than the 10%, for which unconsciousness occurs.

The UK HSE has proposed the following NORSOK Z013 (DNV TECHNICA/SVCANDPOWER A/S) 100% fatal limits:

- 100000ppm (10%v/v) for more than 30 minutes;
- 120000ppm (12%v/v) from 5 to 30 minutes;
- 150000ppm (15%v/v) for less than 5 minutes.

The value of CO₂ able to develop immediate unconsciousness and death is 250000ppm (25%v/v), established by NIOSH. Proposed thresholds for a QRA may be associated with limits of unconsciousness reported in figure 4, for which the probability of death is not mentioned.

| CO₂ Concentration | Responses |
|-------------------------------------|--|
| 45 000 ppm / 4.5% | Reduced concentration capability for more than 8 hours exposure, adaptation possible |
| 55 000 ppm / 5.5% | Breathing difficulty, headache and increased heart rate after 1 hour |
| 65 000 ppm / 6.5% | Dizziness, and confusion after 15 minutes exposure |
| 70 000 ppm / 7.0% | Anxiety caused by breathing difficulty, effects becoming severe after 6 minutes exposure |
| 100 000 ppm / 10% | Approaches threshold of unconsciousness in 30 minutes |
| 120 000 ppm / 12% | Threshold of unconsciousness reached in 5 minutes |
| 150 000 ppm / 15% | Exposure limit 1 minutes |
| 200 000 ppm / 20% | Unconsciousness occurs in less than 1 minute |

Figure 4 Unconsciousness due to carbon dioxide exposure. (IOGP Risk Assessment Data Directory, March 2010)

4.2. Asphyxiation due to oxygen depletion

A CO₂ concentration above 5% starts to be dangerous for human health before being the cause of asphyxia or of reduced oxygen transportation via blood. At normal conditions, air is characterized by 78% nitrogen, 21% oxygen, 1% argon and 0.038% carbon dioxide. An increase in CO₂ in air induces a proportional reduction of the other components including O₂. Normal human activity can continue until the oxygen concentration in air reaches values lower than 18%.

The first effect of oxygen depletion is the reduction of capability to exercise due to low levels of oxygen-saturated hemoglobin and the increasing of the flux of blood to the brain. In fact, reduction in inhaled oxygen is strictly correlated to the decrease in arterial saturation of oxygen. A O₂ concentration of 13.5% corresponds to a drop in blood saturation of 10%. This correlation depends also on the level of physical activity, so during escape action or emergency, in an ambient with 18% of oxygen concentration, the drop in saturation is of about 10%, while, exposed to 17% of oxygen, the drop in saturation is of 15%. Typically, cautious recoverable blood saturation level is fixed at 10%, while a threshold of 15% in reduction of saturation corresponds to harms and fatality (OSD3.2, January 2006).

Low level of oxygen concentration in air can be associated with some effects and symptoms, noticeable for O₂ concentrations below 17-18% in volume, as shown in figure 5.

| Percent of Oxygen in Air | Symptoms |
|--------------------------|---|
| 21-20 | Normal |
| 18 | Night vision begins to be impaired |
| 17 | Respiration volume increase, muscular coordination diminishes, attention and thinking clearly requires more effort |
| 12 to 15 | Shortness of breath, headache, dizziness, quickened pulse, effort fatigues quickly, muscular coordination for skilled movement lost |
| 10 to 12 | Nausea and vomiting, exertion impossible, paralysis of motion |
| 6 to 8 | Collapse and unconsciousness occurs |
| 6 or below | Death in 6 to 8 minutes |

Figure 5 Effects of oxygen depletion. (OSD3.2, January 2006)

According to HSE and IOGP studies (IOGP Risk Assessment Data Directory, March 2010), oxygen concentration below 15% can cause hypoxia, increased breathing, headache, lost muscular coordination for skilled movements and faulty judgment. Concentrations below 10% induces loss of judgment and consciousness that limit the ability to escape, with consequent death in few minutes. For this reason, if escape is not feasible in few seconds, death is likely to occur. Standard concentrations are generally used to detect the combined effect of carbon monoxide, carbon dioxide and oxygen depletion when people are exposed to fire and fumes. The consequences are described by the British Cryogenics Council and divided into four asphyxiation stages reported in figure 6.

| Asphyxiation stage | Oxygen concentration(% v/v) / Effects |
|--------------------|---|
| 1 st | 21 to 14% Reducing: Increased pulse and breathing rate with disturbed muscular coordination |
| 2 nd | 14 to 10%: Faulty judgment, rapid fatigue and insensitivity to pain |
| 3 rd | 10 to 6%: Nausea and vomiting, collapse and permanent brain damage |
| 4 th | Less than 6%: Convulsion, breathing stopped and death |

Figure 6 The four stages of asphyxiation. (OSD3.2, January 2006)

Immediate effects, as unconsciousness, are strictly related with both CO₂ and O₂ concentrations. Increasing the percentage of inhaled O₂, also the exposure time after which unconsciousness occurs, at constant CO₂ level, increases (see figure 7).

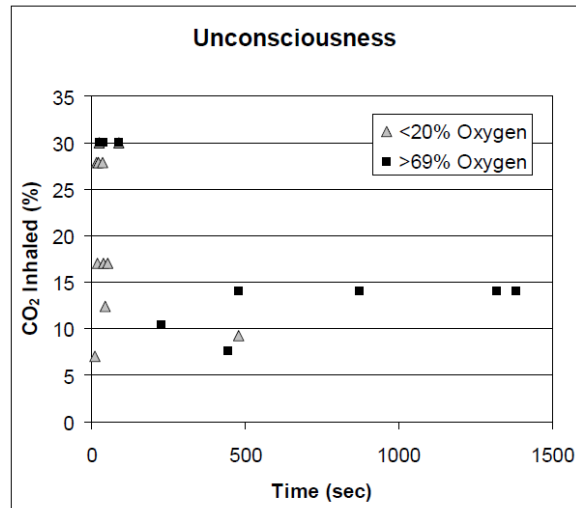


Figure 7 Time to unconsciousness for humans exposed to CO₂ in a low and in a high O₂ environment. (Rice, 2004)

Serious consequences occur by inhaling high concentrations of CO₂, even in the presence of high concentrations of O₂, i.e. without reaching a low level of O₂ capable of causing asphyxia. For example, after an exposure to 30% CO₂ and 70% O₂ for 38 seconds, most of patients exhibit ECG abnormalities, as premature ventricular contractions or nodal and atrial premature systoles. In case of monkeys exposed to 21% O₂ and more than 60% CO₂, death occurs due to acidosis with blood pH between 6.45 and 6.50 (Rice, 2004).

An atmosphere richer of O₂ can prevent some severe symptoms, even at sensible CO₂ percentage, but prolonged low-level CO₂ exposure can also induce acidosis even at very high O₂ concentrations. In particular, persistent effects have been identified in people after unconsciousness due to a high level of CO₂ exposure in a low O₂ environment, while after a spontaneous recovery from high level CO₂ coma, with adequate O₂ concentration, the individuals result to be not affected by a problematic acidosis (Rice, 2004).

These last results are not relevant for the evaluation of toxic effects related to accidental release of carbon dioxide because, in these emergency conditions, the oxygen concentration is expected to drop with the increasing of CO₂ in the interested area. For this reason, experimental data about simultaneous high concentrations of CO₂ and O₂ are not representative of a realistic release condition.

In controlled condition, low CO₂ concentrations have beneficial effects in presence of low oxygen. First of all, a higher-than-usual CO₂ percentage in air provokes the vasodilator effect on cerebral blood vessels that may be the cause of headache, but at the same time it may reduce any possible oxygen deficiency. In addition, in case of oxygen reduction, the increase of CO₂ enhances the ventilation rate of the lungs, promoting the oxygen delivery to the tissues. Also this situation is not representative of the leakage event, because these too low CO₂ concentrations are not typical of the dense plume released on the ground after the rupture.

In order to describe lethality of oxygen depletion, no probit functions have been found in literature, but it is possible to establish a correlation between CO₂ and O₂ concentration in air. For example, when the CO₂ volumetric percentage is of about 70%, the oxygen concentration will be of about 6% and that depletion is considered to be lethal. On the other hand, when effects of low O₂ concentration (15%) occur, as increased pulse and breathing rate or disturbed muscular coordination, a person will already be affected by high CO₂ concentration (30%) symptoms. In fact, severe health effects are obtained before reaching the 30% of CO₂ and the 15% of O₂. The decrease of inhaled oxygen and the corresponding increase of CO₂ percentage in air can be approximated by a linear relationship reported in the following graph.

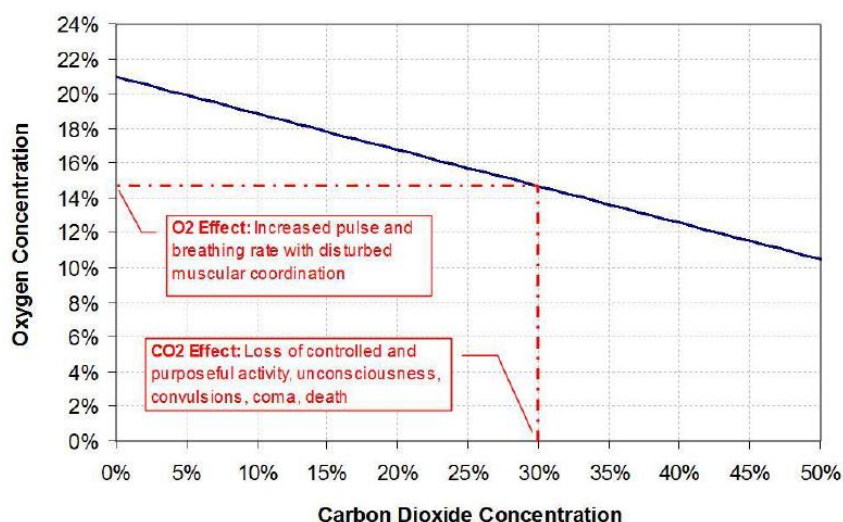


Figure 8 Relationship between CO₂ and O₂ in air. (Holt, 2020)

4.2.1. Summary of combined effect of O₂ depletion and CO₂ inhalation

It is possible to summarize all the previous results about concentrations, duration of exposure and effects on human health. In particular, following the above mentioned linear correlation between CO₂ and O₂ in inhaled air, the effects of a given dose of carbon dioxide have been divided in three different groups, changing the range of oxygen percentage.

- For a not dangerous concentration of oxygen in the range of about 21-20% and a consequent not lethal range of CO₂ of 0.5-5%, the health effects are reported in the following table.

Table 1 Health effects of CO₂ when O₂ concentration is high enough to not cause asphyxia

| CO ₂ Concentration in Air (% v/v) | Exposure | Effects on Humans and References |
|--|--|--|
| 0.5% | 10 hours 8 hours | Time weighted average NIOSH (US). ACGIH long term exposure limit, well tolerable with 19-20% oxygen. Time weighted average OSHA (US). |
| 1% | | Stimulation of respiratory system. Average value for OEL . |
| 1.2% | 5 days | Reduction of 20% of blood pressure. |
| 1.5% | 15 min | Occupational STEL UK. |
| 2% | 60 min Several hours | MEL (Compressed Gas Association 1990). Headache, difficult breathing upon mild exertion. Increase of 50% of ventilation rate. |
| 2.5% | 5-22 min 60 min | NOAEL (no observed adverse effect level). Emergency exposure level for submarine operations (National US Research Council). |
| 2.8% | 1 hour | Acidosis. |
| 3-4% | 30 min 15 min 20 min 1 hour 8 days | Headache. Hearing impairment. Dyspnea even at rest. STEL (Federal occupational safety and health regulations US). MEL (USEPA) Mild headache, sweating, difficult breathing at rest. Increase of 100% of ventilation rate. Important decrease of performance. |

| | | |
|--|---|--|
| <ul style="list-style-type: none"> • 4% | <p><1 min</p> <p>15 min</p> <p>60 min</p> | <p>IDLH (immediate dangerous to life and health) by NIOSH.</p> <p>Occupational MEL (Federal occupational safety and health regulations US).</p> <p>MEL (DOE).</p> <p>Emergency exposure level for submarine operations (USA Navy).</p> |
| <p>>4-5%</p> <ul style="list-style-type: none"> • 4.5% • 5% | <p>few min</p> <p>8 hours</p> <p>5 min</p> <p>7 min</p> <p>60 min</p> | <p>Headache, dizziness, increased blood pressure, uncomfortable breathing.</p> <p>Reduced concentration, possible adaptation.</p> <p>Increased ventilation rate so breathing difficulties.</p> <p>Suggested STEL (HSE UK).</p> <p>MEL (Compressed Gas Association 1990).</p> <p>Suggested Long Term Survivability Exposure Limit (HSE UK).</p> |

- For a not dangerous concentration of O₂ between 20% and 19% and a related harmful CO₂ concentration between 5.5% and 10%, the results are summarized in table 2.

Table 2 Health effects of CO₂ when depletion of O₂ starts to be perceived

| CO₂ Concentration in Air (% v/v) | Exposure | Effects on Humans and References |
|---|---|---|
| 5.5% | 1 hour | Breathing difficulties, headache, increased heart rate. |
| 6% | 1-2 min 5 min ≤ 16 min Hours | Reduced visual intensity. MEL (Compressed Gas Association 1990). Headache, dyspnea. Tremors. |
| 6.1-6.3% | 6 min | Reduction of 3-8% of hearing. |
| 6-5 % | 15 min | Confusion, dizziness. |
| 7-10% | Few min 1.5 min-1 hour | Unconsciousness, near consciousness. Headache, increased heart rate, shortness of breath, dizziness, sweating, rapid breathing. |
| <ul style="list-style-type: none"> • 7% • 8% • 10% | Few min 3 min 10-60 min 15 min 30 min | Unconsciousness, anxiety due to breathing difficulties (severe after 6 min). MEL (Compressed Gas Association 1990). Depression of human respiratory system. Acidosis. Asphyxiation. Unconsciousness, 100% fatal limit. |

- For a dangerous range of oxygen from 19% to 15% and for a concentration of CO₂ in between 10% and 30%, the effects are shown in table 3. For these values, even if first health effects due to oxygen reduction start to occur, no lethality can be linked with asphyxiation, while death, in less than 30 minutes, can be caused by a concentration of CO₂ higher than the 10% in volume.

Table 3 Health effects of CO₂ when asphyxia due to oxygen depletion starts to occur

| CO₂ Concentration in Air (% v/v) | Exposure | Effects on Humans and References |
|--|-----------------|---|
|--|-----------------|---|

| | | |
|--|---|--|
| >10-15% <ul style="list-style-type: none">• 12%• 15% (18% O₂) | 1 min 5-30 min 5 min <5 min 1 min | Unconsciousness, severe muscle twitching, dizziness, drowsiness. 100% fatal limit. Unconsciousness. 100% fatal limit. NORSOK Exposure limit. Unconsciousness. |
| 17-30% (17.5-15% O ₂) <ul style="list-style-type: none">• 17%• 20%• 25% | 1 min 1 min <1 min | Loss of controlled and purposeful activity, unconsciousness, convulsion, coma, death. Death. Unconsciousness. Immediate unconsciousness and death. |

All these results are compatible with the summarized effects of oxygen depletion, as reported in the following table.

Table 4 Health effects of oxygen depletion

| O ₂ Concentration in Air (% v/v) | Correspondent CO ₂ Concentration in Air (% v/v) | Effects on Humans |
|---|--|---|
| 21-20% | <5% | Normal activity. |
| 21-14% 1 st level <ul style="list-style-type: none">• 18%• <18%• 17% | <33.3% | Increased pulse and breathing rate with disturbed muscular coordination. Night vision impaired. During high activity drop in saturation of 10%(cautious recoverable blood saturation reduction). Reduced capability to exercise. Respiration volume increases, muscular coordination diminishes, difficult attention and thinking. During high activity drop in saturation of 15% (reduction of saturation for harm and fatality). |
| 15-12% | 28.6-42.9% | Shortness of breath, headache, dizziness, quickened pulse, effort fatigues quickly, muscular coordination for skilled movements lost. |
| <15% | >28.6% | Hypoxia headache, increasing breathing, lost muscular coordination, fault judgement. |
| <14-10% 2 nd level <ul style="list-style-type: none">• 13.5%• 10-12% | >33.3-52.4% | Fault judgment, rapid fatigue, insensitivity to pain. Drop in blood saturation 10% (cautious recoverable blood saturation reduction). Nausea vomiting, exertion impossible, paralysis of motion. |
| <10-6% 3 rd level <ul style="list-style-type: none">• <10%• 6-8% | >52.4-71.4% | Nausea, vomiting, collapse and permanent brain damages. Loss of judgment, limited ability to escape. Collapse, unconsciousness, nausea. |
| <6% 4 th level | >71.4% | Convulsion, breathing stopped. Death in 6-8 min |

Data shown in table 4 follow the linear correlation between O₂ and CO₂ whose effects correspond to those determined during the Texas Clean Energy Project (Quest Consultants Inc., 2010). According to this project, carbon dioxide is odorless gas whose major associated hazard is asphyxiation, not able to determine lethal level of acidosis. Analyzing these results, an oxygen concentration of 6-8% may be fatal after 8 minutes in 50 to

100% of cases or after 6 minutes in 25 to 50% of cases. If the 100% CO₂ fatal limits are observed (see Chapter 4.1.1), it can be said that the inhalation of CO₂ is lethal for concentrations lower than 71.4%, value that corresponds to the 6% of O₂ considered by the Texas Clean Energy Project able to cause 100% probability of death. It can be affirmed that, the effects of CO₂ inhalation are underestimated if acidosis is not taken into account.

In conclusion, it can be proved that the lethal effects of the inhalation of CO₂ predominate over health effects linked with the correlated oxygen depletion. For this reason, in the QRA calculations, the CO₂ concentrations of 12% and 15% are usually considered the lowest limits for which unconsciousness (and therefore potentially death) occurs after 5 and 1 minute, respectively.

5. Statistical probability of death due to CO₂ exposure

Due to the hundreds of thousands of tons of dense phase CO₂ potentially involved in CCUS technologies, a major release has a MAH (*Major Accident Hazard*) potential. In some countries, as in UK, there is a legal duty to demonstrate that a MAH risk, in terms of fatality numbers, is below an acceptable limit. For this reason, a QRA for CCUS applications is needed.

As part of risk assessment the definition of impairment ('vulnerability') criteria is fundamental to define the potential consequences of the hazardous scenarios. Generally, the fatality criteria for a MAH are based on the 50% mortality level. In order to evaluate the lethality of an exposure to a hazardous substance it is necessary to estimate the received dose, in particular the concentration and the duration of the exposure, and the related probability of death of a population or an individual, in a statistical way. In fact, the response to a given concentration and duration is not the same for all individuals and there is not a single value at which all people react in the identical way. For this reason, probabilistic methods can be applied, based on observed or experimental data about consequences on a large generalized population. This can be done by the determination of the harmful dose or by specific probability unit (probit) methods, based on normal distribution outcomes (HSE UK, 2020).

5.1. SLOT and SLOD Dangerous Toxic Loads

An appropriate source of statistic information about CO₂ major accident consequences is the UK Health and Safety Executive (HSE) that has also developed vulnerability criteria needed to determine limit doses and related effects. These criteria give information about the threshold above which protection is required against impairment of the human functions needed to escape, avoiding a fatality. Consequently, the UK HSE has also established a method to estimate the fatality obtained exceeding a dose without adequate protection.

In particular, the UK HSE's *Dangerous Toxic Loads* (DTLs) define the exposure conditions in terms of concentration and duration able to produce a defined level of toxicity. Two different limits can be distinguished: The *Specified Level of Toxicity* (SLOT) and the *Significant Likelihood of Death* (SLOD). These criteria are based on the fact that, within a toxic cloud there can be zones of higher and lower concentrations, so not everyone is exposed to the same dose. The SLOD and SLOT values express the toxicity by the determination of a functional relationship between the substance concentration in air and the duration of exposure. In order to identify this relationship, HSE uses an approach based on available data coming from accidental chemical exposures or direct relevant animal data (HSE UK, 2020).

The SLOT DTL is the dose for which vulnerable people are killed and a substantial portion of the exposed population needs medical assistance, while the remainder exposed individuals experience severe distress. This level reflects the condition of low probability of death, so the SLOT DTL can be associated with 1% of mortality, referred to LD1 or LD1-5 of toxic substances. The SLOD DTL is defined as the dose that can result in 50% of mortality (LD50) and, given the extent and the severity of consequences for a distributed population, it can be used to estimate the number of fatalities. This approach assumes that the number of people not died inside the

SLOD contour is balanced by the number of people who die outside the contour. Between SLOD and SLOT contours, people are assumed to be injured.

Even if the criteria for CO₂ classification as a dangerous substance are not reached, the following HSE relationships between concentration ‘c’ (ppm) and time ‘t’ (minutes) define the CO₂ Toxic Loads able to reach the SLOT and SLOD levels (Holt, 2020):

- SLOT DTL: $1.5 \times 10^{40} [ppm^8 \text{ min}] = c^8 * t$
- SLOD DTL: $1.5 \times 10^{41} [ppm^8 \text{ min}] = c^8 * t$

To define these correlations, in case of a substance with no acute toxicity as CO₂, the HSE experimental process exploits an exemplar substance. This toxicologically potent substance should have physical properties similar to those of the analyzed one.

The following concentration-duration graph shows the SLOT and SLOD DTL curves. The gap between them is small due to the fact that, above a value of 7% of carbon dioxide, human body is sensitive even to a small variation of CO₂ concentration in inhaled air, as already discussed. CO₂ concentrations for 1% and 50% of lethality and for a given exposure time differ by 33%.

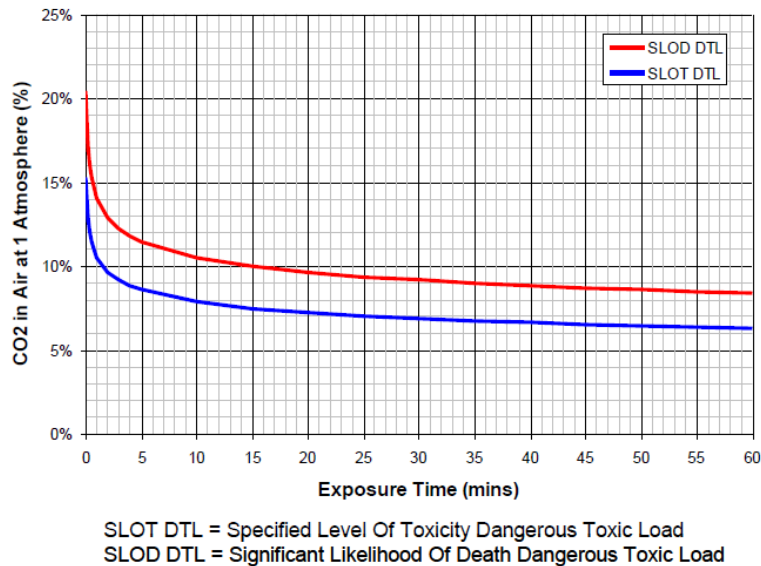


Figure 9 SLOT DTL and SLOD DTL curves. (Holt, 2020)

5.1.1. The effect of concentration fluctuations on toxic load

An approach able to account the effect of concentration fluctuations on toxic load is investigated by the UK Health and Safety Executive (Gant & Kelsey, 2011). This aspect may have a significant effect on calculated hazard especially for momentum-dominated free jets of CO₂, for which the HSE approach results to be conservative. On the other hand, if only mean concentrations are used to determine the toxic load, without any consideration about fluctuation, the hazard ranges result to be under-estimated. The conservative approach is based on the assumption that the concentration fluctuates by a factor of two with a square-wave variation over time. In this way, the concentration is assumed twice the mean value for half of the time and zero for the rest of the time. The methodology does not provide a realistic representation of the turbulence, but it includes the fluctuations in a simple way.

If a free jet produced by a CO₂ release is analyzed, comparisons between different approaches can be done, in order to predict the toxic load. In particular, the following three methods can be used:

- Calculation of the toxic load (TL) using the mean concentration, neglecting fluctuations, as:

$$TL = \int_0^T \tilde{c}^n dt,$$

where T is the duration of the exposure, \tilde{c} is the time-varying concentration and n is the ten Berge exponent equal to 8;

- Calculation of the toxic load (TL) using the PDF empirical model, as:

$$TL = \int_0^1 \tilde{c}^n p(\tilde{c}) \tilde{dc},$$

where $p(\tilde{c})$ is the concentration Probability Distribution Function (PDF), \tilde{c} is the time-varying concentration and n is the ten Berge exponent equal to 8. The shape of PDF is based on the mean and the variance of the concentration, but also on the turbulence intermittency (Gant & Kelsey, 2011);

- Assumption of a factor-of-two square wave concentration fluctuation about the mean level.

Considering an exposure of 30 minutes, the SLOD and the SLOD distribution curves are obtained from these three approaches. An example of the corresponding predictions of distribution of CO₂ concentration, generated by a release from a source with a diameter of 0.5 m and velocity of 50 m/s, is reported in the following figure.

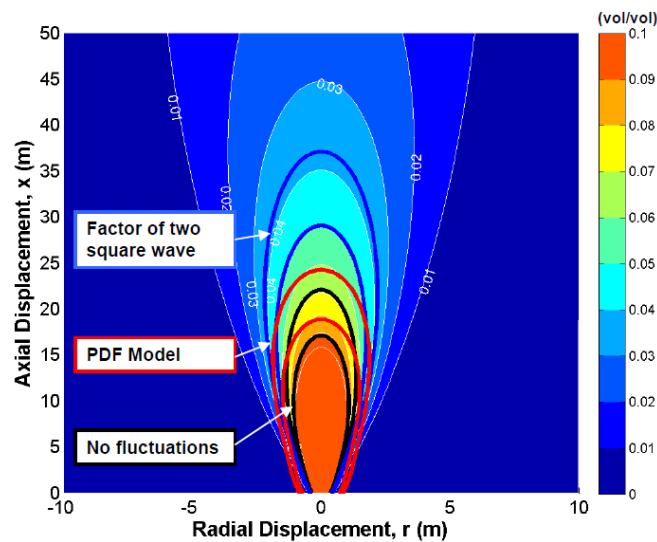


Figure 10 Prediction of mean concentration in a CO₂ jet. The three pairs of curves show the locations of the SLOD and SLOD calculated using different load models. (Gant & Kelsey, 2011)

The axial displacement obtained by a no fluctuations model is the lowest and the hazard area is the smallest among the three approaches. The factor-of-two square wave model results to be the most conservative, while the PDF obtained shape is the only one characterized by a wider area near the base of the jet. This is due to the fact that the intensity of fluctuations, usually higher in the periphery of the jet, can be well represented only by the PDF model, based on empirical evaluation of the turbulence intermittency and not only on the radial distribution of the mean concentration.

These considerations are valid only for free jets in a quiescent environment for which fluctuations are linked with turbulence. The turbulences can be generated by induced shear layers, frictional effects due to the rolling of dense layer on the ground, or by turbulence in the atmosphere. When a dense phase CO₂ is transported, also a low-momentum dense plume can be released. In these conditions the gravitational forces accelerate the cloud and the vertical density gradient reduces the turbulence, generating a uniform plume. No model in literature has been found able to describe the fluctuations in the dense plume, useful to calculate the toxic load. Data analysis, large-scale experiments and numerical simulations of the dense phase dispersion and concentration fluctuation are needed to not overlook this phenomenon in the definition of dangerous toxic loads.

The presence of turbulence has also been included in the prediction of consequences of a CO₂ pipeline release on building occupants (Lyons, Race, Hopkins, & Cleaver, 2015). This study wants to prove that nearby

buildings could act as a form of shelter against toxic and asphyxiating effects of CO₂. The source of release consists on a double-ended guillotine break of a 96-kilometer-long pipeline with an external diameter of 610 mm. In order to quantify the CO₂ concentration inside the building the “C-mean” and the “C-equiv” models are applied. This last equivalent value is an adjusted mean concentration that includes CO₂ fluctuations in neutral atmospheric conditions (5D Pasquill stability class). Results about mean and equivalent concentrations after the release, for different distances from the source, can be compared.

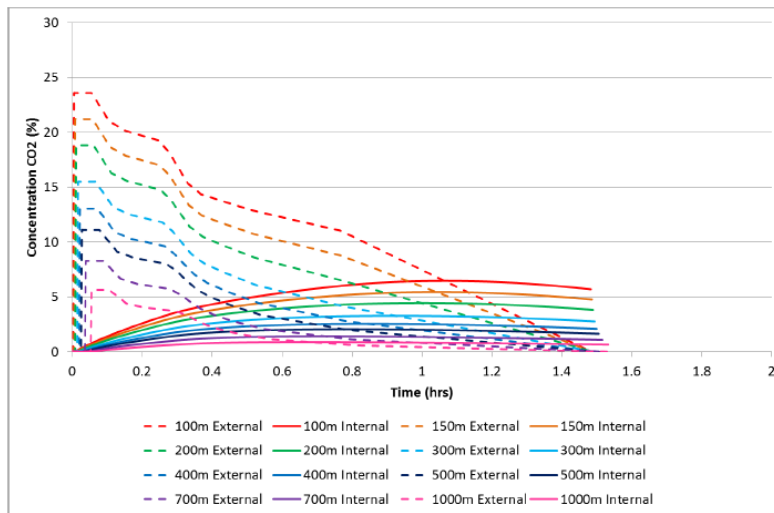


Figure 11 Change in mean CO₂ concentration with time and distance from the release point. (Lyons, Race, Hopkins, & Cleaver, 2015)

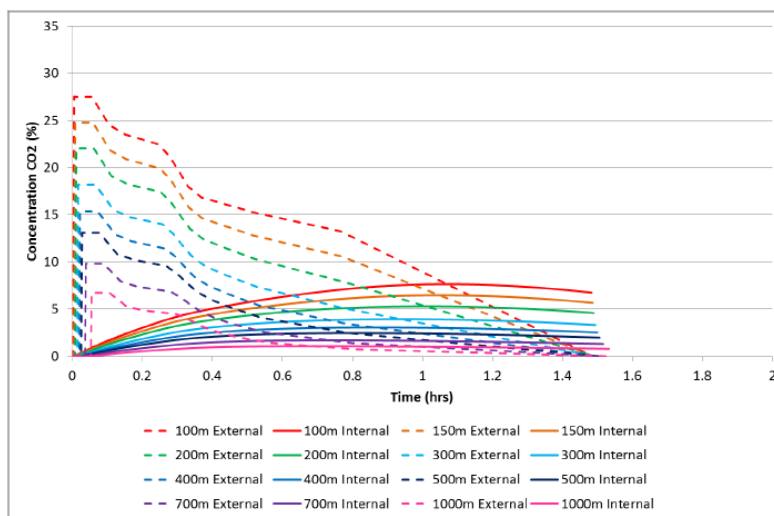


Figure 12 Change in equivalent CO₂ concentration with time and distance from the release point. (Lyons, Race, Hopkins, & Cleaver, 2015)

Observing figure 11 and 12, it can be said that, changing the concentration model, the shape of the obtained curve is preserved but, as proved before, the inclusion of turbulences makes the approach more conservative. In fact, for each dashed curve, the “C-mean” peak, reached few minutes after the release, is lower than the corresponding “C-equiv” peak. The equivalent curves result to be shifted to higher CO₂ values. This behavior is also preserved for internal concentration curves.

5.1.2. Application of concentration limits or DTL curves for QRA

The ultimate goal of the analysis of consequences and identification of vulnerability thresholds is the definition of the risk, a combination of frequency and casualty probability for each defined scenario of a given event. In order to define the effects of consequences on health of exposed people, some vulnerability thresholds have

been defined and used in literature. For CCUS experimental projects and simulations, the lethality is usually evaluated only considering the asphyxiating and toxic properties of CO₂, through the definition of critical doses or concentration values, as reported in Appendix A. Here some literature examples are analyzed.

LITERATURE EXAMPLES BASED ON CO₂ CONCENTRATION LIMIT VALUES

In most of reported cases the IDLH NIOSH limit value (4% v/v of CO₂) is used to determine the distance from the leak above which no mortality is expected within 30 minutes of exposure (Preeti, Prem, & Qingsheng, 2016) (Vianello, Macchietto, & Maschio, 2013) (Vianello, Macchietto, & Maschio, 2012). According to these studies, the safety distance is fixed at a proposed maximum concentration of CO₂, without any considerations about duration of exposure. For distances higher than that defined by this threshold, no severe consequences due to toxic CO₂ inhalation are expected. Also the 5% (Hill, Fackrell, Dubal, & Stiff, 2011) (Guo, et al., 2016) and the 7-10% range of maximum concentration may be applied to identify where the first symptoms and unconsciousness may occur, without taking into account the actual received dose (Mocellin, Vianello, & Maschio, 2016) (Ahmad, et al., 2015).

LITERATURE EXAMPLES BASED ON LETHAL DOSES

When the dose-based lethality is chosen, UK HSE's SLOT and SLOD DTLs parameters are usually adopted. The HSE SLOT 1% lethality is preferred to identify the maximum safety distance from the potential release. However, in some cases, instead of the UK HSE DTL-based correlation, other limit doses are defined. For example, the 3% mortality has been associated with SLOT dose value, following a modified correlation between lethality and received dose (Lyons, Race, Hopkins, & Cleaver, 2015).

Also the acceptability of the individual and societal risks may be determined through comparisons with some UK HSE dose criteria (Cooper & Barnett, 2014). According to evaluations about UK CO₂ pipelines, the proposed individual risk criteria correspond to 'broadly acceptable', 'tolerable if ALARP' and 'unacceptable' conditions, while for societal risk SLOD or SLOT-based curves are used as thresholds, referred to 1 kilometer pipeline. In this last case, the SLOT assessment results to be the most conservative one.

For individual risk evaluation the sum of all hazards has been considered in the study (Cooper & Barnett, 2014), assuming buildings occupied for 100% of the time and people outdoor present for 10% of the day and 1% of the night. The individual risk has been obtained for different distances from the potential release point, obtaining the risk transects, different lines perpendicular to the pipe at which constant risk value is expected. Also the societal risk has been determined. It evaluates the correlation between CO₂ effects and neighboring population, defining a F-N curve that relates the cumulative frequency F of the events able to generate N casualties, with the number of casualties N.

Thanks to COOLTRANS project's (Cooper & Barnett, 2014) dose evaluations, the individual risk-distance curve, merely based on CO₂ toxicity, has been compared with that obtained for flammable natural gas. The SLOT-based risk connected with natural gas results to be higher than that of CO₂ only in proximity of the release point. The CO₂ derived curve reaches lower peak of individual risk, because of lower failure frequency of CO₂ equipment and pipelines, but larger distances from the leak. This aspect underlines the capability of the emitted plume to reach a large number of people, increasing the societal risk. Because of the slow decay of risk with distance, the evaluations are strongly dependent on source conditions, dispersion behavior and population and shelter assumptions. For the same reason, according to COOLTRANS project, the QRA is preferred to be based on societal risk assessment, able to give information about recommended separation distances to different targets (through SLOT curves). This approach results to be more conservative than individual risk-based one (Cooper & Barnett, 2014) (Quest Consultants Inc., 2010).

5.2. The probit method

In order to obtain a larger range of mortality results, the probability unit method can be used to assess the response of a generalized population to a CO₂ exposure. In particular, thanks to a derived probit function, the fatality rate of people exposed to a given dose of a harmful substance can be calculated. This kind of function is in the form of:

$$Y = k_1 + k_2 * \ln(V)$$

Evaluated the probit value 'Y', that can vary from 2.67 to 8.09, the probability of death, that varies from 1% to 99.9%, can be extrapolated from a probit transformation chart. The 'V' value for toxic substances is evaluated as the product of concentration of the substance, elevated to 'n', and the exposure time, in predefined units. The 'n', 'k₁', 'k₂' constant values depend on the kind of substance analyzed.

The 'V' parameter takes the form of:

$$V = c^n * t$$

Where:

- 'c' is the concentration of the substance
- 't' is the exposure time
- 'n' is a constant that corresponds to ten Berge factor

5.2.1. The UK HSE probit correlation

The constant values 'k₁' and 'k₂', derived from UK HSE's SLOD DTL and SLOT DTL curves for CO₂ exposure, are respectively equal to -89.81 and 1. In this way, following a normal distribution, the SLOD DTL probit value is set to 5.00 and the SLOT DTL value is set to 2.67. The SLOT DTL can represent an exposure of 15 minute at 7.5% of CO₂, while the SLOD DTL corresponds to an exposure of 15 minutes to a 10% concentration. The SLOD and SLOT's derived probit correlation gives dose values for the following probability of death.

| Probit | Probability of fatality (%) | Concentration for one minute exposure (%) | Concentration for 10 minute exposure (%) | Concentration for 60 minute exposure (%) |
|--------|-----------------------------|---|--|--|
| 7,85 | 99,75 | 20 | 15 | 12 |
| 6,06 | 85,5 | 16 | 12 | 9,5 |
| 5 | 50 | 14 | 10,5 | 8,4 |
| 3,76 | 11 | 12 | 9 | 7,2 |
| 2,67 | 1 | 10,5 | 7,9 | 6,3 |

Figure 13 Probability of fatality for CO₂ based on SLOT and SLOD (UK HSE) data. (Energy Institute, 2010)

These data can be also shown graphically in the following figure.

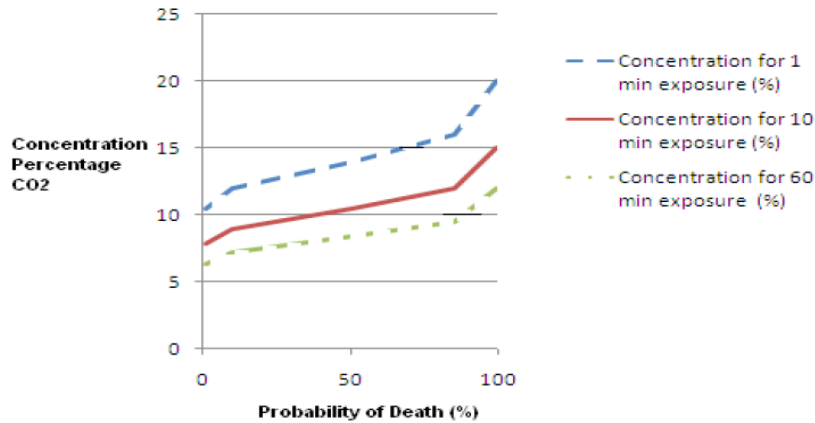


Figure 14 CO₂ dose-fatality correlation based on SLOD and SLOT (UK HSE) data. (Energy Institute, 2010)

During the period 2008-2009 the UK HSE has used the data collected by IDLH and DNV TECHNICA/SCANDPOWER A/S (2001) to reformulate the probit function in which ‘k₁’, ‘k₂’, and ‘n’ values are respectively -90.8, 1.01 and 8.

The relative concentrations and durations of exposure are reported in the following figure.

| Concentration / approximate exposure time for % lethality | | | | | |
|---|-------------------|-----|---------------|-------------------|-----|
| 1-5% lethality | | | 50% lethality | | |
| ppm | mg/m ³ | min | ppm | mg/m ³ | min |
| 63000 | 115290 | 60 | 84000 | 153720 | 60 |
| 69000 | 126270 | 30 | 92000 | 168360 | 30 |
| 72000 | 131760 | 20 | 96000 | 175680 | 20 |
| 79000 | 144570 | 10 | 105000 | 192150 | 10 |
| 86000 | 157380 | 5 | 115000 | 210450 | 5 |
| 105000 | 192150 | 1 | 140000 | 256200 | 1 |

Figure 15 Lethality levels UK HSE 2008. (W ter Burg, 2021)

Comparing results shown in figures 13 and 15, it can be proved that no significant variations in lethality are obtained if all different non-linear correlations, defined by UK HSE during the years, are used.

5.2.2. The Tebodin probit correlation

The Tebodin’s assumptions have been followed in order to assess the QRA for Barendrecht project (Gelderen, 2013). Because of the absence of an official probit relation for CO₂, Tebodin Consultants & Engineers performed a literature study and developed a probit relation based on experiments and accidents, able to quantify the lethality of a given exposure. The obtained probit relationship is:

$$Y = -98.81 + \ln(c^9 * t)$$

Comparing the obtained function with other ones reported in literature, the Tebodin correlation results to be the most conservative. The obtained probit is based on European directives and, for this reason, a 30-minute exposure has been considered (maximum duration for QRA in Netherlands). The relationship between concentration and time to unconsciousness is used to define the function’s constant values, starting from two reference concentrations evaluated after 30 minutes (Heijne & Kaman, 2008):

- 5% of CO₂ for no expected death
- 10% of CO₂ for 100% expected lethality

During the CATO program on 25/05/2010, the Barendrecht project has been criticized because of its unvalidated assumptions about the determined probit function. The critic concluded that the Tebodin QRA method does not provide a certified risk reduction (Gelderen, 2013).

5.2.2.1. Sub-lethal effects

Even if usually not considered in the QRA, the sub-lethal effects have to be described for a complete risk analysis. In particular, the highest concentration at which no adverse effects occur during a short term exposure (STEL) is evaluated. For a duration of 15 minutes, the HSE has proposed a STEL of 1.5% CO₂, while US DOE has chosen a concentration of 3%. Since none of these options can be considered the best choice, both of them may be used to identify levels of CO₂ able to cause sub-lethal effects, from headache to unconsciousness.

With a simplified approach, a probit correlation about sub-lethal effects may be obtained. The method consists in the adjustment of the Tebodin probit function, shifting the 1% lethality to the lowest CO₂ concentration able to cause sub-lethal effects (1.5% or 3% of carbon dioxide), changing the 'k₁' value. All the Tebodin equations are reported in the following table, from which a probit value of 2.67 can be obtained.

Table 5 Tebodin probit relations

| Probit | 'k ₁ ' value | Equation |
|-----------------|-------------------------|-----------------------------|
| Lethal | -98.81 | $Y = -98.81 + \ln(c * t)$ |
| 3% sub-lethal | -93.51 | $Y = -93.51 + \ln(c^9 * t)$ |
| 1.5% sub-lethal | -87.27 | $Y = -87.27 + \ln(c^9 * t)$ |

The artificial modifications of the Tebodin function also affect the mortality at higher concentrations. Therefore, only the region of the curve for expected sub-lethal effects is used. The obtained curves are reported in figure 16, in which also the original Tebodin probit function for 1% of lethality is represented.

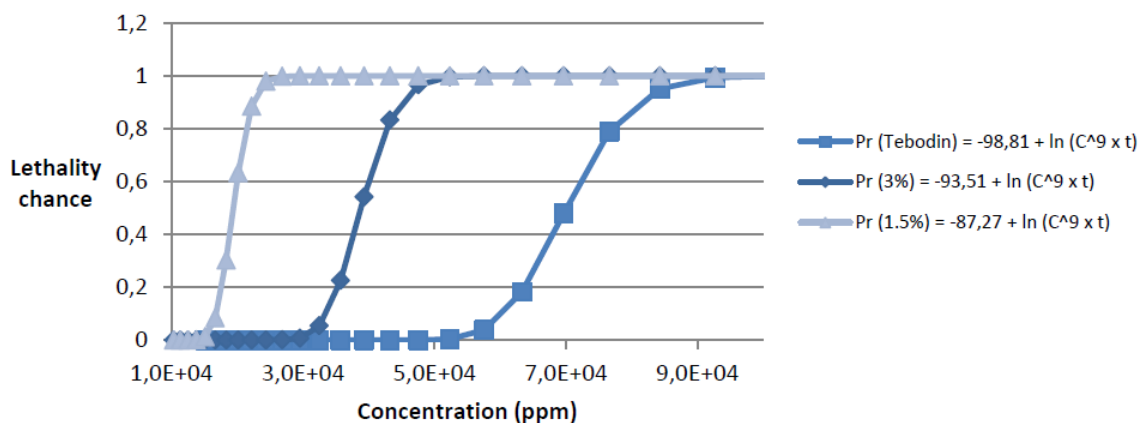


Figure 16 Probit relations to calculate sub-lethal effect areas. The 'k₁' values of all these functions are obtained considering an exposure duration of 30 minutes. (Gelderen, 2013)

5.2.3. Comparisons between different probit functions

Different CO₂ probit functions may be found in literature. These functions take into account levels of toxic and oxygen dissipating gases, considering the respiratory effects of them. The evaluation of 'n', 'k₁' and 'k₂' values starts from some mortality information referred to two or more couples of concentration and duration data. Here some examples are reported:

- Koornneef (TNO):
 - k₁=4.45; k₂=1; n=5.2 (Concentration expressed in [kg/m³] and time expressed in [s]);

- Referred to 1% of lethality for 5 [min] exposed to 100000 [ppm] and 99% lethality for 5 [min] exposed to 200000 [ppm].
- McGillivray, 2008 (HSE):
 - $k_1=-90.8$; $k_2=1.01$; $n=8$ (Concentration expressed in [ppm] and time expressed in [min]);
 - Referred to SLOT 1.5×10^{40} [ppm⁸ min] and SLOD 1.5×10^{41} [ppm⁸ min] values.
- Lievense, 2005 (OCAP):
 - $k_1=-0.91$; $k_2=1$; $n=2$ (Concentration expressed in [kg/m³] and time expressed in [s]);
 - Referred to lethality of 1% for exposure of 54647 [ppm] for 60 [min].
- Molag and Raben, 2006 (TNO):
 - $k_1=-63.3$; $k_2=1$; $n=5.2$ (Concentration expressed in [mg/m³] and time expressed in [min]);
 - Referred to 1% of mortality for 5 [min] exposed to 130000 [ppm] and 99% lethality for 5 [min] exposed to 320000 [ppm].
- Save, 2009 (OCAP):
 - $K_1=-23.37$; $k_2=1$; $n=2$ (Concentration expressed in [ppm] and time expressed in [min]);
 - Referred to 1% of mortality for 5 [min] exposed to 200000 [ppm] and 99% lethality for 5 [min] exposed to 1900000 [ppm]
- Tebodin, 2008:
 - $k_1=-98.81$; $k_2=1$; $n=9$ (Concentration expressed in [ppm] and time expressed in [min]);
 - Referred to lethality of 100% for 100000 [ppm] and no mortality for less than 50000 [ppm] in 30 [min];
 - Referred to lethality of 1% if exposed for 5 [min] to 70000 [ppm] and of 99% if exposed to 110000 [ppm] for 5 [min].

The last three options of probit function can be compared with the UH HSE’s correlation proposed in 2011, for which no value about 99% of lethality is obtained, due to the fact that it derives from SLOD and SLOT DTL curves. Also in this case, not evident differences between functions obtained by UK HSE in 2008 (by McGillivray) and in 2011 can be observed. Also the OCAP’s Lievense (2005) and Save (2009) correlations provide very similar results. The values of lethality extrapolated from ‘Molag and Raben, 2006 (TNO)’, ‘Save, 2009 (OCAP)’, ‘Tebodin, 2008’ and ‘UK HSE, 2011’ are reported in figure 17.

| Exposure duration (min) | Lethality chance (%) | Vol% CO ₂ TNO | Vol% CO ₂ OCAP | Vol% CO ₂ HSE | Vol% CO ₂ Tebodin |
|-------------------------|----------------------|--------------------------|---------------------------|--------------------------|------------------------------|
| 1 | 1 | 18 | 45 | 11 | 8 |
| | 50 | 28 | (*) | 14 | 10 |
| | 99 | 43 | (*) | - | 13 |
| 5 | 1 | 13 | 20 | 8 | 7 |
| | 50 | 20 | 62 | 11 | 9 |
| | 99 | 32 | (*) | - | 11 |
| 30 | 1 | 9 | 8 | 7 | 5 |
| | 50 | 15 | 25 | 9 | 7 |
| | 99 | 22 | 77 | - | 9 |
| 60 | 1 | 8 | 6 | 6 | 5 |
| | 50 | 13 | 18 | 8 | 6 |
| | 99 | 20 | 55 | - | 8 |

Figure 17 Lethality chance of CO₂ for different probit relations. (*) Values obtained from the too optimistic OCAP correlation are not representative because higher than the 100%. Data based on (Gelderden, 2013).

Observing all the different proposed functions, comparisons can be done. As reported in figure 18, the Lievense (OCAP) and TNO correlations result to be different in shape compared to Tebodin and HSE ones, due to higher ‘ k_1 ’ value and lower ‘ n ’ value. In particular, for the Tebodin and the HSE functions, mortality starts to assume significant values even before a 10-15% of CO₂, reaching the 100% before a concentration of 20%, for a 60-minute and for a 1-minute exposure. In general, it can be affirmed that TNO and Lievense

correlations depend more on the duration of the exposure than the other two functions, that are highly influenced by the value of CO₂ concentration.

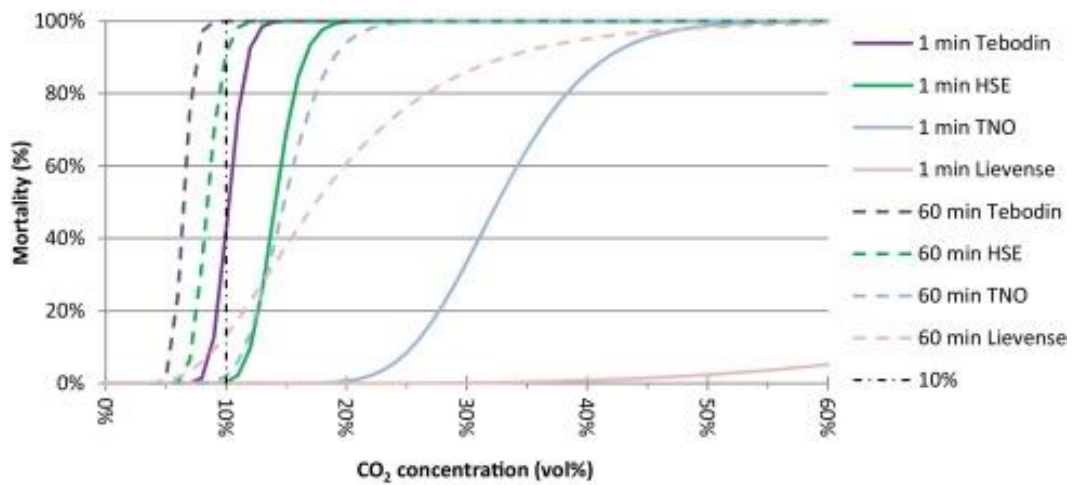


Figure 18 Comparisons between Tebodin, HSE, TNO and Lievense probit functions for exposure of 1 min and 60 min. (M. M.j. Knoope, 1 January 2014)

As shown in figure 19, a comparison between TNO and Lievense probit functions, both used in the Netherlands, can also be done. Analyzing the TNO curve, with the increasing of concentration, the increasing of probability of death is faster than that obtained with Lievense correlation, at the same duration of exposure. For this reason, Lievense function is more dependent on duration, while the TNO one is more dependent on concentration of CO₂.

Simulations have been conducted to compare results of a simulated release event by applying different methods in order to evaluate the connected risk (Koornneef, Spruijt, Ramirez, & Faaij, 2009). The obtained results show that following a TNO probit function, the distance for which a probability of death of 1×10^{-8} per year occurs is higher than the distance obtained using the Lievense method during the simulation. In addition, thanks to these studies, it is possible to prove that scenarios that include concentration thresholds, such as SLOT and SLOD DTL, result in a higher risk compared to simulations that use less conservative probit method.

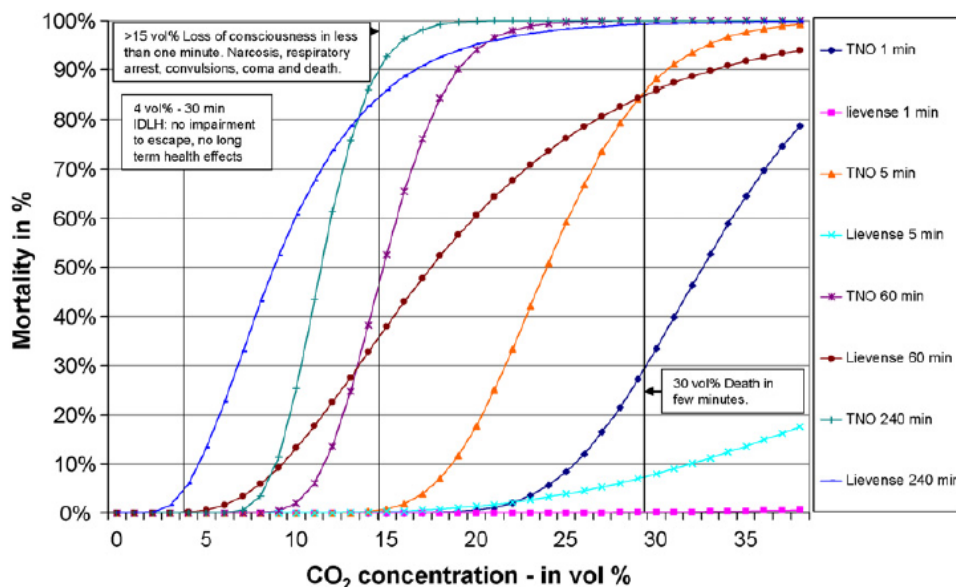


Figure 19 Comparisons between TNO and Lievense probit functions for exposure of 1 min, 5min, 60 min, 240 min. (Joris Koornneef, 2009)

In figure 19 three different dose limits are also reported. The first one refers to a concentration of 4% in volume of CO₂ for an exposure of 30 min, whose curve is not reported in the figure and that is representative of the condition of no impairment and no prolonged health effects. The second threshold is put at a concentration of 15% of CO₂ related to loss of consciousness in less than one minute, convulsions and death. This limit is not crossed by the TNO and Lievense probit functions referred to a 1-minute or 5-minute exposure. The last threshold of 30% in volume of CO₂ underlines the condition for which death occurs in few minutes and it is crossed by TNO 1-minute and 5-minute curves, by Lievense 5-minute curve, but not by Lievense 1-minute curve. This consideration is related to the fact that TNO probit is more dependent on percentage of CO₂ than Lievense function, so, even at the same value of concentration, the mortality percentage for a 1-minute exposure obtained by TNO is higher than both 1-minute and 5-minute mortality values expected using Lievense correlation.

For QRA analysis, mortality data about the first few minutes (1-5 min) are considered. For this reason, the too optimistic Lievense (OCAP) correlation cannot be proposed as a proper method to determine the lethality associated with the inhalation of carbon dioxide. TNO and OCAP probit functions do not fulfill the QRA's requirements. In fact, their 1-minute and 5-minute curves do not respectively cross the 15% and the 12% concentration lines, that are the lowest critical limits for which unconsciousness and death occur.

In conclusion, it can be said that all the proposed lethal levels of toxicity of CO₂ and probit correlations may only be taken as a suggestion, based on results of different studies over the time that adopt a less or more conservative approach.

The uncertainties in establishing a shared vulnerability model for CO₂ exposure are also due to the fact that CO₂ is not yet officially labelled as a toxic chemical by the Global Harmonized System (GHS) and by the European Classification, Labelling and Packaging (CLP). In fact, CO₂ is a "Not Classified" substance because its LC50 concentration is greater than 5000 ppm. The only way to classify the carbon dioxide is by referring to the European Chemical Agency (ECHA) in which all the labels proposed by companies are reported. According to them, CO₂ has been classified as "harmful if inhaled" (H332) or as "may cause a respiratory irritation" (H335). Also all conducted experiments about CO₂ toxicity have to be analyzed, even if they report less conservative levels of toxicity compared with doses proposed by companies or, for example, by the UK HSE. The uncertain toxic properties, the limited large-scale implementations of CO₂ projects and the lack of further information and knowledge make possible to consider CO₂, especially in its dense phase, a new substance whose connected risk has to be managed. In order to perform and compare different Quantitative Risk Assessments a standard probit correlation or some shared and accepted thresholds of CO₂ concentration are required.

6. Cryogenic effects of a CO₂ release

For CCUS applications, CO₂ can be transported in dense phase, in liquid or in supercritical conditions (above 73.8 bar and 31.1°C), in order to make the transportation more efficient. At atmospheric pressure, CO₂ can only exist as gas or as solid, so, depending on inventory and ambient conditions, after a release and a depressurization process of the fluid, a cryogenic or cold two-phase jet is obtained. In particular, defining the pure CO₂ rapid depressurization on the T-s diagram, starting from liquid or supercritical phase, the expansion line at constant enthalpy may enter the liquid-vapor and the solid-vapor region at which CO₂ is discharged.

According to the Joule-Thomson effect, in the over mentioned release process, the rapid reduction of pressure produces cooling effects in the discharge area, reaching temperatures of about -80°C. The two-phase plume can contain 20%-40% by mass of solid CO₂, with temperatures of about -78°C. When in atmosphere, the plume becomes warmer as warmer air is trapped and energy is absorbed from external sources. Increasing the distance from the release point, the temperatures inside and near the plume start to increase. Consequently, the solid particles are transported in the plume until their sublimation or loosing of momentum falling to the ground. In

this last case, the obtained dry-ice bank can take hours to completely sublimate, becoming an additional issue for humans, equipment and seals, especially in low wind speed conditions.

The cold released plume may be the cause of severe injuries/death of people outdoor and impairment of equipment. If the low temperatures insist on structures for minutes, the resulting cold surfaces of materials may cause cold burns of people, if touched during escape or operations. Also the internal structure of metals and polymers may be damaged by the cryogenic cloud.

6.1. Cryogenic effects on human health

The low temperatures reached near the release point, consequently to the fast depressurization, can become dangerous for people that, in case of inhalation of the cooled air in the range of -40°C and -70°C , may be affected by harms to respiratory system after few minutes. These effects are more severe in case of a release in a congested zone, where the cold plume can more likely engulf anyone present in the area.

Generally, when temperatures dip this low, hypothermia and frostbite may become health concerns. Hypothermia occurs if body's core temperature falls below 35°C . This condition may be induced by immersion in cold water or by a prolonged exposure to low temperatures, with an increased probability of death for people not able to take off their wet clothes (Le Cronache, 2017).

Human body exposure to low temperatures may cause permanent damages to organs until death. In literature, the cooling of the vital organs has been widely studied in terms of threat to an immersed person in cold water, but in this case the ingestion of water can modify the final probability of death. Nevertheless, the debilitating effect of cold can change the estimation of survival time in cold water, as reported by OTO 90 038 "Review of Possible Survival times for Immersion in the North Sea" (OSD3.2, January 2006).

The 'cold shock', due to immersion in cold water or exposure to cold air, is defined as a sudden drop in skin temperature that instinctively induces hyperventilation and abnormal cardiac output. After an involuntary gasp, the breath-hold times decrease and hyperventilation occurs. Heart-rate and cardiac output rise inducing a cardiac arrest in vulnerable people. Another effect is the shutdown of peripheral perfusion, by vasoconstriction, reducing the heat lost from the extremities of the body. In this way the temperature of vital organs is preserved and outer layers of tissues act as an insulating barrier. This mechanism is arrested above a critical temperature, causing the fall in core temperature and a spontaneous contraction of muscles. The metabolic fatigue occurs and the core temperature decreases with a greater rate due to lack of energy.

Thought thermoregulation mechanism the internal body temperature is maintained at 37°C , but in cold environmental conditions hypothermia may occur. Different levels of hypothermia can be reached, depending on temperature value and duration of the exposure (Istituto Superiore di Sanità, 2020):

- Mild hypothermia, until core temperature of 32°C . Shivers, increased heart rate and muscular and articular pain start to occur.
- Moderate hypothermia, in between 32°C and 26°C . Irregular heart rate and difficult breathing are reported. Confusion and drowsiness may occur.
- Severe hypothermia, for core temperatures lower than 26°C . Vital functions are impaired and unconsciousness and death occur due to cardiac arrest (24°C).

Wet people may experience hypothermia even at not severe conditions, with external temperatures in between -1 and 10°C , due to the fact that human body loses heat 25 times faster in water than in air. However, hypothermia is more likely to occur at subzero temperature. For example, an exposure of 10 minutes to -34°C is able to cause hypothermia, while the same effects may be obtained in 5-7 minutes at -40 or -45°C (Rettner, 2019).

During mild and moderate hypothermia, the cooling of extremities such as hands and feet may reach the frostbite condition (skin temperature of 0°C), with skin and soft tissue damaged by reduced oxygenation. Changing the temperature and the duration of the exposure, the frostbite effects vary, from loss of oxygen and blood flow in

tissues, to cellular death (necrosis) and gangrene, followed by bacterial attack that may be solved with amputation of the damaged part.

In healthy adults, hypothermia needs very low external temperatures to occur, while frostbite is possible even at less critical ambient conditions. Cooling effects are enhanced in case of exposure to water or humidity, due to higher thermal conductivity of water, or in case of wind exposure under heavy activity.

In general, below -15°C frostbite is more likely to occur. At -18°C , with wind at -28°C , frostbite is expected in 30 minutes, while with ambient air at -26°C and wind at -48°C , people can be frostbitten in 5 minutes. Frostbite condition is linked with cold environment exposure but it can also be caused by direct contact with ice, frozen metals or cold liquids (Rettner, 2019).

6.1.1. Correlations between temperature values and health effects

Due to the fact that a guidance for the management of cold burn injuries is not yet available, and that there are no existing comprehensive sets of methods and models, co-operation research projects were started. One of them is the program 'Barents Interreg IIA', developed by The European Regional Development Fund (ERDF) from 1999 to 2001 (Juhani Hassi, December 1999 - May 2001). The study focuses on the effects of cold on human body, dependent on environmental aspects (air temperature, wind, presence of water, radiation), degree of activity and clothing used. Results about local or whole body cooling are linked with individual factors (gender, age, health, fitness) and firstly consist in physical (muscular), manual and cognitive performance degradation. Thermal stress, considering the received cooling dose, determines different degrees of harm, starting from discomfort and pain, to cardiac, respiratory and circulation systems damages, passing through muscular and peripheral system injuries.

According to Barents project some thresholds about cold injuries are settled. For example, critical skin temperature for tactile sensitivity is fixed at a value in between 6 and 8°C . Finger dexterity is reduced when skin temperatures in the range 20 - 22°C are reached and it becomes too low at 15 - 16°C . Also hypothermia, is defined a kind of cold injury.

Some of the cold related health effects and symptoms are:

- Cooling decreasing physical performance;
- Respiratory symptom;
- Musculoskeletal symptom;
- Peripheral circulatory disturbances;
- Color change in fingers;
- Thermal discomfort and consequent decreasing mental performance;
- Exceptional sensitivity to cold;
- Cardiovascular symptoms;
- Cold urticarial;
- Serious frostbite.

The total injury rate, as sum of direct and indirect effects of cold, can vary a lot. For example, the probability of slip or fall accidents increases, decreasing the temperatures, and the impairment of the cold body will only enhance the risk of accidents.

Problems connected with touching cold materials are explored too. The study gives information about relationship between touched material's temperature, duration of the contact and related consequences, for different types of material (aluminum, steel, stone, nylon, wood). Graphs below represent the frostnip, the numbness and the pain thresholds for short contact periods with small skin surface, as function of material temperature (T_s), type of material and contact duration.

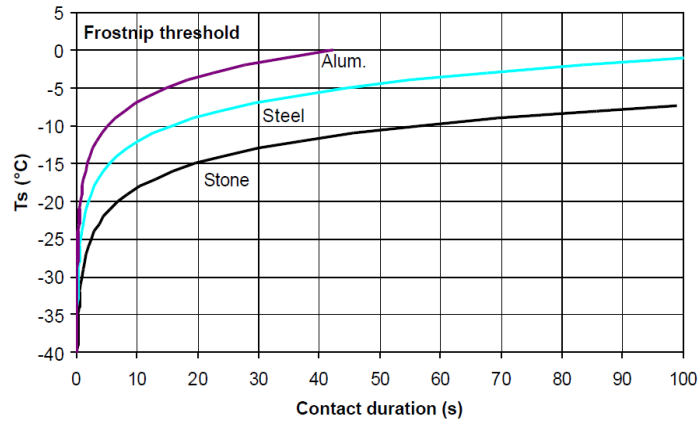


Figure 20 Surface temperature as function of time for frostnip (skin at 0°C). (Juhani Hassi, December 1999 - May 2001)

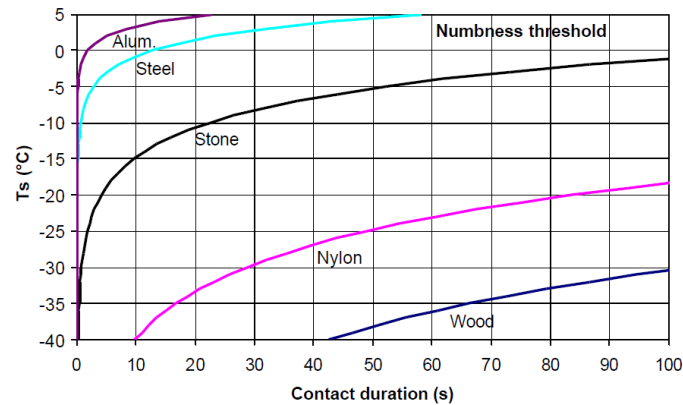


Figure 21 Surface temperature as function of time for numbness condition (skin at 7°C). (Juhani Hassi, December 1999 - May 2001)

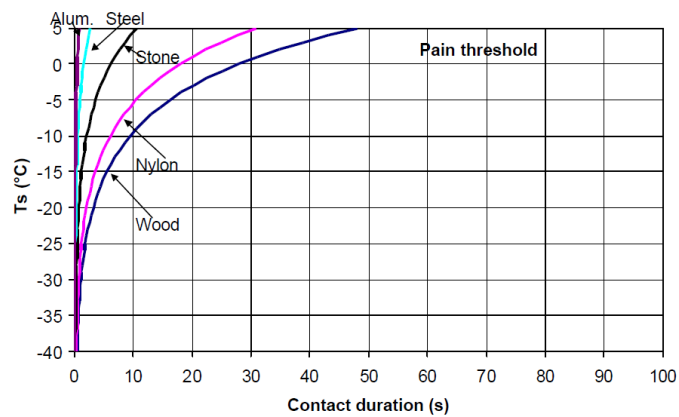


Figure 22 Surface temperature as function of time for pain condition (skin at 15°C). (Juhani Hassi, December 1999 - May 2001)

For a gripping condition, the pain threshold is defined for longer contact duration (up to 10 minutes) with a larger surface area of the skin. The following graph shows the correlation between the different materials' surface temperature and time needed to reach a painful condition.

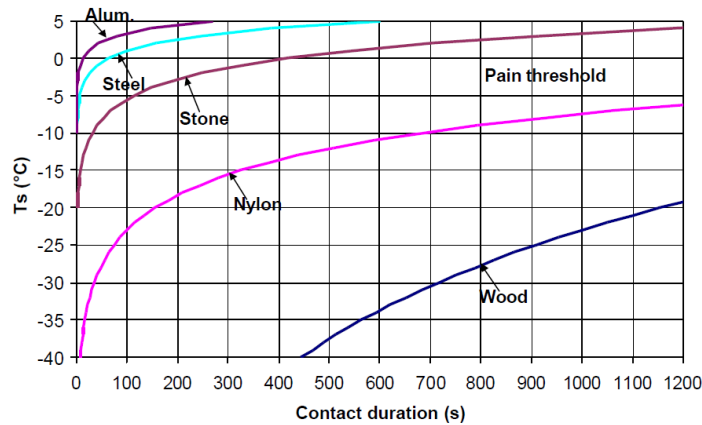


Figure 23 Surface temperature as function of time for pain condition during gripping conditions (skin at 15°C). (Juhani Hassi, December 1999 - May 2001)

These data can also be combined with results about how the drop in finger temperature occurs, depending on external air temperature, under low or high activity level. In particular, for an exposure to air at -40°C, under low activity, fingers reach 15°C (pain condition) within 30 minutes with a protection of 2 clo, while under high activity, finger skin temperature is of about 15°C after more than 35 minutes, with 1.4 clo of protection. The loss of tactile sensitivity (6-8°C), in the first situation, occurs after less than 50 minutes exposed to air at -40°C, while, in the second condition, it appears after about 70 minutes. This demonstrates that, even with a lower level of skin protection, the high activity level may preserve people from cold injuries, prolonging the time of exposure after which severe health effects are reported.

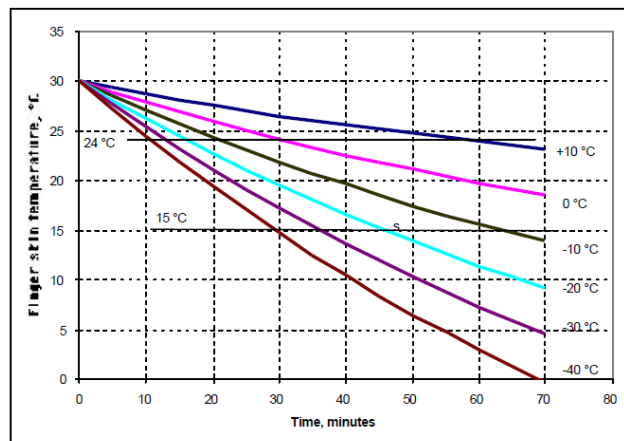


Figure 24 Drop in finger temperature with time, at low activity. Hand protection of 2 clo. (Juhani Hassi, December 1999 - May 2001)

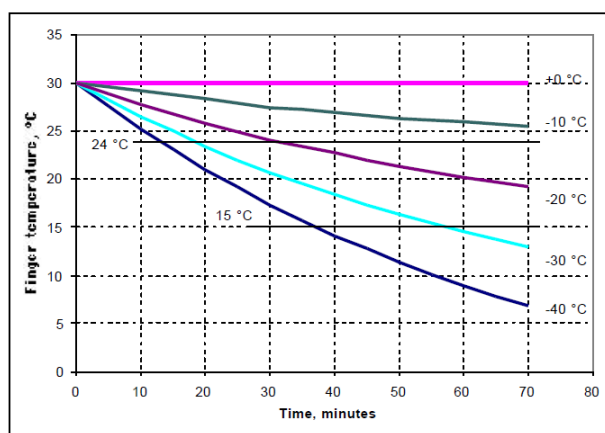


Figure 25 Drop in finger temperature with time, at high activity. Hand protection of 1.4 clo. (Juhani Hassi, December 1999 - May 2001)

In order to define how cryogenic conditions can affect the health of people present in the area of cold CO₂ release, these studies can be adopted for a general and qualitative analysis. More experiments are also needed to identify how the superficial temperatures of materials vary with external conditions, considering the possibility to interact with a liquid, solid or vapour cryogenic substance. In addition, near the release point, the distribution of the gradient of temperature is essential in order to establish the consequences due to exposure to cold air and due to contact with cold surfaces or cold solid CO₂. Solid CO₂ particles can also be ingested, causing significant health effects due to their very low temperature (-78°C) and their capability to transport dangerous substances in the human body. Even about these last aspects, no more precise experimental data are reported in literature.

6.1.2. Mortality thresholds for low temperatures exposure

According to studies analyzed in the previous Chapter, mortality within the cold plume may be predicted, in order to include this hazard in a QRA. As already said, no standard methodologies are present in literature, so some assumptions have been done.

First of all, probability of death of people suffering hypothermia is considered. The highest lethality level may be associated with severe hypothermia, for body core temperatures below 26°C. In this state, frostbite is a secondary effect that starts to assume importance for mild and moderate hypothermia. Consequently, known data about duration of exposure and temperature after which frostbite occurs may be linked with a lower probability of death.

Following the HSE suggested fatality criteria of ‘Onset of fatality’ and ‘Estimated 50% fatality’, which meaning may be compared with LC1 and LC50 for toxic effects (OSD3.2, January 2006), the 1% and 50% mortality of people exposed to a cryogenic fluid may be evaluated according to criteria reported in following table. Severe hypothermia has been set at 50% fatality, while frostbite after which hospitalization of substantial portion of exposed individuals may occur, has been associated to 1% fatality.

Table 6 Suggested fatality criteria for exposure to cryogenic conditions. Data based on (Rettner, 2019)

| 1% fatality | | 50% fatality | |
|------------------|----------------|------------------|----------------|
| Temperature [°C] | Duration [min] | Temperature [°C] | Duration [min] |
| -18 | 30 | -34 | 10 |
| -26 | 5 | -40 | 5-7 |

Cold stress is evaluable in terms of global cooling, influenced by definition of required thermal insulation, and local convective cooling, referred to wind chill temperature evaluation (Del Ferraro, Molinari, Moschetto, & Pinto, 2019).

Hypothermia associated to 50% fatality thresholds is a global cooling effect. According to European standard EN ISO 11079, when the required insulation is lower than the actual thermal insulation of clothing, the “*high strain condition*” for global cooling occurs. In particular, thresholds in table 6 consider people not properly dressed for the cold, with typical daily wear clothing characterized by a maximum thermal insulation of 1.5 clo (European Committee for Standardization, 2005).

Frostbite, as a form of local convective cooling, is evaluable starting from the definition of wind chill temperature, function of air temperature and wind speed. Through table reported in EN ISO 11079, for each wind chill temperature value, the expected risk and health effects may be determined. The 1% fatality thresholds in table 6 refer to frostbite risk class 2 (air at -18°C for 30 minutes) and 3 (air at -26°C for 5 minutes), for which wind chill temperatures of -28°C and -48°C are expected, respectively (Del Ferraro, Molinari, Moschetto, & Pinto, 2019).

6.1.3. Effects of impact with solid CO₂ particles

During a CO₂ release, in the surrounding area a temperature of about -80°C may be reached. In these conditions, before the cooling of vital organs of exposed people, in addition to the ‘cold shock’ cardiac reactions, also skin or tissues and especially eyes, in contact with cold air, are harmed. In particular, immediate cryogenic burns and pain affect people that may also be disoriented. Impact injuries and burns are not only caused by the contact with cold surfaces, but also by the impact with emitted solid CO₂ particles.

When supercritical CO₂ is released, a two-phase single or multi-component stream is discharged, therefore the formation of a solid phase has to be considered, especially in case of large leaks and full bore ruptures. The dry-ice particles present in the jet may snow out forming a bank on the ground, which will slowly sublime. This phenomenon may expose people to dangerous concentration of CO₂, whose consequences may be determined adopting over mentioned probit correlations. Changing release conditions, the particles can sublime during their fall to the ground. For horizontal releases, the lowest value of particle diameter for which deposition occurs is of about 700 μm. For slanting and direct downwards releases, the value drops to 150 μm and 120 μm, respectively (Vianello, Mocellin, & Maschio, Study of Formation, Sublimation and Deposition of Dry Ice from Carbon Capture and Storage Pipelines, 2014). Before their sublimation, transported dry-ice particles act as flying objects able to cause death of impinged people.

Even if no detailed data about emitted dry-ice particles are available, they can be considered as fragments and debris of a density of about 1562 kg/m³ and their presence can be simulated considering them as a variable mass fraction of the emitted cloud, depending on release conditions. Starting from mass of fragments and debris (m), the following probit functions, established by TNO (Roos, December 1989), can be used to determine the probability of death of hit people as function of the impact velocity (v_0):

- For mass of particles greater than 4.5 kg (debris high compressive stress criterion)

$$Pr = -13.19 + 10.54 * \ln(v_0);$$
- For mass of particles in between 0.1 kg and 4.5 kg (debris high compressive stress criterion)

$$Pr = -17.56 + 5.30 * \ln\left(\frac{1}{2} * m * v_0^2\right);$$
- For mass of particles in between 0.001kg and 0.1kg (fragments penetration criterion):

$$Pr = 38.83 - 2.08 * \ln(m * v_0^{5.115}).$$

Dry-ice particles able to penetrate the skin are considered fragments and their effect also depends on the possibility to protect the skin with appropriate clothes. On the other hand, solid CO₂ particles not able to cut the skin are considered debris that cause compressive stresses and bones fractures, or that can determine deformations and damages to internal organs.

Considering particles diameter and density values, it can be asserted that deposited dry-ice particles are characterized by a mass higher than 0.1 kg and, for this reason, they may be considered debris able to generate compressive stresses and fractures. On the other hand, smaller solid CO₂ particles, transported by the plume until sublimation, are characterized by a mass lower than 0.1 kg and, for this reason, they may be considered fragments able to penetrate skin and organs.

After the deposition of bigger particles, the sublimation of the obtained dry-ice bank acts as a delayed emission source able to generate a localized high concentration of gaseous CO₂ for long time after the release. In this way, after the rupture two emission sources are obtained: the first one, associable with the inventory depressurization, that prevails during the release, and the second one, generated from the bank sublimation, that prevails for hours after the leak. This last emission assumes dangerous CO₂ values only within a few meters from the ground level.

Due to CO₂ density of the sublimated cloud, higher than that of air, and its toxicological and asphyxiating properties, death of people involved in rescue and reactivation operations occurs, even after a short-term exposure. In the following figure, the time evolution of the CO₂ emitted from the release is compared with that of CO₂ emitted from the dry-ice bank.

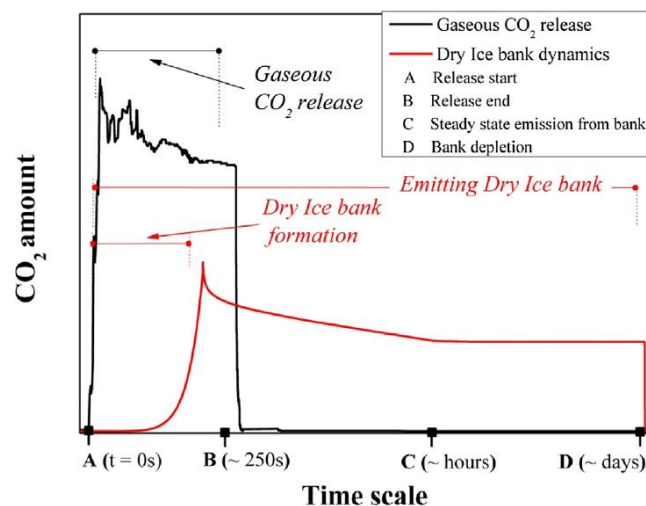


Figure 26 Pressurized CO₂ release and sublimating bank dynamics with reference to a general time scale. (Mocellin, Vianello, & Maschio, 2016)

As shown in a qualitative representation of the phenomena in figure 26, the peak of CO₂ concentration, caused by the discharge and reported at the beginning of the release, results to be higher than that obtained due to bank sublimation just few minutes before the end of the release.

While CO₂ immediate discharged plume reaches high concentration values only for few minutes, the dry-ice bank dynamic starts slowly and it is characterized by a more prolonged emission. This phenomenon becomes the major hazard for hours after the leak, in the near-field area, when the steady state emission begins.

6.1.4. Low temperatures and high CO₂ concentration

The suggested fatality criteria for cryogenic effects may be applied on large or small-scale experimental projects and simulations conducted in the past, in order to identify the extent of hazard represented by exposure to cryogenic conditions. In analyzed studies, the physical characteristics of released and dispersed plume have been defined. In most of the reported cases, the CO₂ concentration and the temperature

distribution in both near and far-field areas have been discussed, but damage areas due to cryogenic conditions have not been defined according to any vulnerability models.

LITERATURE EXAMPLES FOR OUTDOOR CRYOGENIC CONDITIONS

In literature, no health effects and vulnerability thresholds for exposure to the cold rich-CO₂ environment, generated by the Joule-Thomson effect, are reported. For this reason, the results obtained from analysis of state of the art could be applied to determine low temperature risk contours.

In some experiments the low temperature profile may be compared with dangerous dose-based contours, concluding that cryogenic critical conditions may be obtained only in the near-field region, for few seconds after the release. For example, according to some experiments (Vianello, Macchietto, & Maschio, 2012)., when the IDLH limit is reached at 750 m, cryogenic conditions (-20°C) are obtained only at the equilibrium plane, where the jet is fully expanded to atmospheric pressure.

Apart from the definition of temperature profile in the near-field analysis of an under-expanded CO₂ jet, the dangerous effects of cryogenic CO₂ in the far-field area, obtained from plume dispersion models and simulation, may be analyzed. In some large-scale experiments the -40°C limit distance from the source point could be determined, in order to compare cryogenic effects with toxic consequences on human health. For example, in the range between -40°C and -70°C the provoked respiratory symptoms may be compared with that caused by inhalation of 11% CO₂.

For each the literature experiment, the distance for which dangerous low temperatures are reached is lower than that at which the 5% of CO₂ is obtained (Hill, Fackrell, Dubal, & Stiff, 2011). In particular conditions (Ahmad, et al., 2015), -17°C are registered 50 m downwind from the release, but at the same distance a CO₂ concentration of 12% may already be associated to 100% probability of death within 30 minutes. For upwind evaluations, at the same conditions, -30°C and 16% CO₂ values are reported, leading to the conclusion that the definition of the damage area for populations is driven by toxicity of carbon dioxide.

Here, the (Guo, et al., 2016) study will be used to apply defined vulnerability thresholds to dispersion results. The experiment consists in the characterization of the jet and dispersion of supercritical CO₂ released from three different types of pipeline rupture: orifice of 15 mm, orifice of 50 mm and Full Bore Rupture. For each of these conditions, temperature and concentration's distributions are obtained in order to identify contours within which dangerous low temperatures and life-threatening CO₂ percentages are reached. The 258 m long pipeline is characterized by an internal diameter of 233 mm and it is located 1.3 m above the ground.

The three scenarios differ for initial atmospheric conditions, inventory properties and size of the orifice, as reported in the following table.

| Number | Test1 | Test2 | Test3 |
|--------------------------------|-----------|--------|--------|
| Pressure (MPa) | 7.6 | 7.9 | 8.0 |
| Temperature (°C) | 35.1 | 33.4 | 36.9 |
| Orifice (mm) | 15 | 50 | FBR |
| Inventory (tons) | 3.14 | 6.27 | 3.59 |
| Environmental pressure (kPa) | 101.02 | 100.75 | 100.01 |
| Environmental temperature (°C) | 0.2–2.2 | 4.7 | 26.6 |
| Humidity (%) | 52.4–52.5 | 75.9 | 62.8 |
| Wind speed (m/s) | 5.5–7.2 | 1.5 | 0.8 |
| Wind direction | 290–348 | 188 | 198 |
| Atmospheric stability | D | B | B |

Figure 27 Environmental and experimental conditions of the three different release tests. (Guo, et al., 2016)

The results reported in figure 28 and 29 show that along the release direction the temperature increases and the CO₂ concentration decreases, due to the reduction of solid CO₂ content in the plume and to the expanding velocity. The values registered in the near-field and in the far-field can vary a lot changing the parameters of the simulation. Increasing the number of tons of the inventory and the dimension of the orifice, the drop in temperature is higher and faster and the dangerous CO₂ dispersion area is larger.

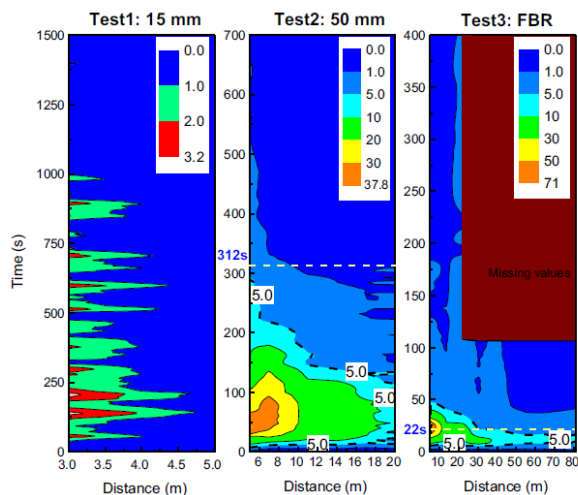


Figure 28 CO₂ concentration evolution along the axial line. (Guo, et al., 2016)

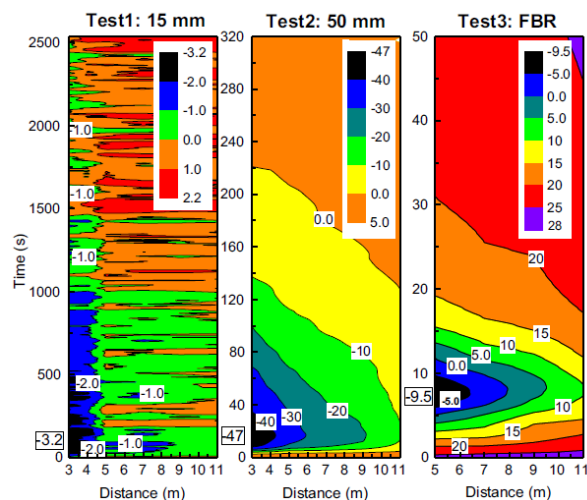


Figure 29 Temperature evolution along the axial line. (Guo, et al., 2016)

Critical cryogenic conditions are obtained during test 2, as shown in figure 29, for which -47°C are registered near the release point. Considering -40°C as the threshold for significant harm to the respiratory system and hypothermia in 5 minutes, the corresponding contour delimits the area extended for less than 5 meters along the jet axis and less than 0.5 meters in the horizontal direction. The minimum temperatures obtained during test 1 and test 3 cannot be considered dangerous for exposed people.

As evident in figure 28, a violent fluctuation of CO₂ concentration is obtained only in test 1, characterized by a strong wind speed and small diameter of the rupture. In test 2 and 3, no fluctuations are considered and larger areas of dangerous concentration are defined, due to a reduced dilution of the plume. During test 2, for which the cryogenic effects cannot be neglected, also the distribution of CO₂ concentration along the jet axis has to be considered. An axial distance of about 20 meters defines an area for which a 5% concentration, able to cause the first evident symptoms (Guo, et al., 2016), is kept for a duration of about 5 minutes. This dangerous area is larger than that delimited by the -26°C line, value for which the 1% fatality may be expected.

In case 2, people within the 5-meter contour experience -40°C for about 40 seconds, but they are exposed to a 30% concentration of CO_2 , higher than the value able to cause immediate unconsciousness and death (25%). In conclusion, even if the inventory and release conditions are able to develop a harmful low-temperature environment near the rupture, the distance for which death firstly occurs due to inhalation of a too high concentration of CO_2 is higher than that for which damages to respiratory system due to low temperatures can be obtained.

The registered temperatures generally turn out to be critical, for few minutes, only within few meters from the leak, where maximum CO_2 concentrations are experienced. However, changing the characteristics of the release event, the cryogenic effects on human health can assume higher or lower impact on the QRA evaluations compared with toxicity of CO_2 .

LITERATURE EXAMPLE FOR INDOOR CRYOGENIC CONDITIONS

In order to define the safety distance between high pressure CO_2 pipelines and habitable dwellings, the over mentioned European project about consequences of a release on building occupants (Lyons, Race, Hopkins, & Cleaver, 2015) can be analyzed. According to this study, the consequences of the unlikely rupture of a CO_2 pipeline are linked to the fact that the released gas is toxic and acts as an asphyxiating, but both CO_2 concentration and temperature behavior are taken into account. The goal is to verify, through the infiltration model, if the nearby buildings can offer shelter against CO_2 effects, until the conditions inside match that of the external environment.

It is assumed that the initial value of internal concentration is the typical one registered in atmosphere (0.039%) and the initial internal temperature is the typical project room temperature (20°C). The external concentration and temperature are assumed to change with time due to a constant and continuous CO_2 release. The description of the external temperature behavior is necessary to establish the difference with the internal values that drives the ventilation flow rate of the building itself. The simulated results show the variation with time of external conditions and of internal concentration and temperature of buildings placed at a distance of 100 m, 150 m, 200 m, 300 m, 400 m, 500 m, 700 m, 1000 m from the release. At these locations the released solid CO_2 particles are assumed to be sublimated.

In the following figure, the internal and external change in temperature is reported for each distance at which buildings are located.

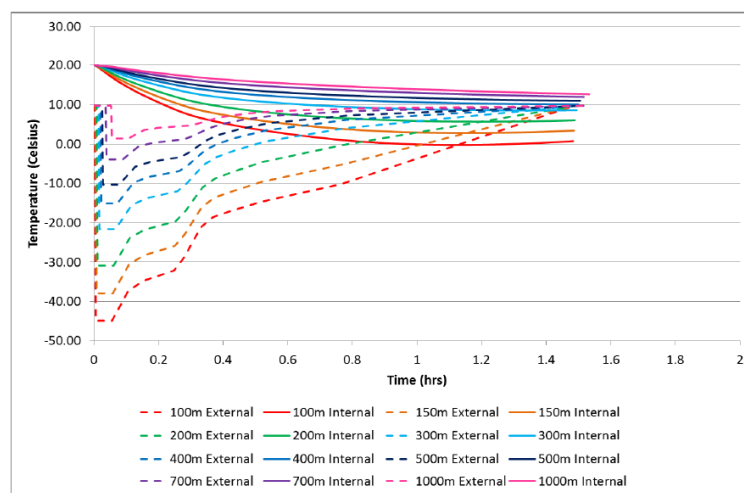


Figure 30 Change in internal temperature with time and distance from the release point. (Lyons, Race, Hopkins, & Cleaver, 2015)

Results in figure 30 show that indoor populations are repaired from external cryogenic conditions and they are never exposed to temperatures low enough to cause severe damages to organs and respiratory system. Apart

from that conclusion, the external temperature evolution can be compared with the “C-equiv” curves reported in figure 12 and used during the simulation to determine the toxic dose. From this analysis it can be concluded that even if dwellings are able to protect people from too low external temperatures after a release, they cannot prevent occupants from inhaling too high CO₂ concentration (>5%).

At a distance of 100 m from the release point, a temperature of less than -40°C is reached outside for less than 5 minutes during which a lethal concentration higher than 25% is maintained. For higher distances, from 150 m to 1000 m from the leak, the Joule-Thomson consequent low temperatures are not able to cause high probability of death, because the -40°C threshold is not reached and -34°C are not maintained for more than 20 minutes. On the other hand, a lethal dose of 15% of CO₂ for less than 5 minutes is inhaled by people outdoor, even at 400 m from the rupture. At this distance the limit of -26°C is not overtaken and -18°C are not preserved for 30 minutes, so no lethality due to cryogenic conditions is expected. If the less conservative “C-mean” values are considered, the same dose is registered at a shorted distance of 300 m. Also in this case, the 1% probability of death due to low temperatures is not obtained.

6.2. Cryogenic effects on equipment

The exposure to low temperatures may be an issue also for materials that, below critical conditions, will exhibit some changes in their physical and mechanical properties. In particular, the cryogenic embrittlement of metals can occur. It consists in a reduction of metals’ temperature that, below their ductile to brittle transition temperature, causes the failure of them, if put under load. When the solid cold CO₂ particles or other fragments produced by the rupture of a containment of CO₂, enter in contact with structures and critical instruments, they can determine the catastrophic failure of them, due to the loss of integrity enhanced by the very low temperatures reached within the released cold plume. Consequently, also people can be harmed by the escalation of dangerous events, due to material failure and possible consequent collapse of pressurized containment systems or walkway supports.

Electrical systems may be compromised by cryogenic conditions. For this reason, also gas detectors and alarms will be able to work even at very low temperatures. Apart from the material’s exposure to the cryogenic released cloud, also the prolonged contact with cold solid particles can determine a localized embrittlement of the involved materials.

Evaluations about embrittlement of materials could be done not only for equipment invested by the cold plume, but also for components that contains pressurized CO₂. In this case the embrittlement causes the enhancement of the dangerous event scale (‘escalation’ or ‘domino effect’).

6.2.1. From the leak to the break of the pipeline due to embrittlement

All materials used in pipelines and CO₂ infrastructures are designed to avoid brittle failure, but this event can happen due to a fast depressurization of the inventory, after a huge leakage of CO₂, and the associated impact of structures with cold released plume and solid CO₂ particles. Usually, the low temperatures are likely to be observed during line venting, down to -20°C, or during a leakage event, down to -80°C. In particular, when the inventory temperature falls, consequently to its depressurization, the reduction in pressure will reduce the likelihood and the consequences of a brittle failure of its containment, but in this condition localized failures cannot always be avoided, due to the fact that the toughness of involved steel drops when the temperature decreases a lot.

The potential risk that a leak may evolve into a break is possible due to the fact that the sudden pressure drop causes the drop in temperature also in the area near the release point. For these reasons the pipeline steel can be affected by local embrittlement and high local stress that enhances the running fracture propagation. In particular, a brittle failure can be observed when the crack propagation speed is close to the speed of sound in the metal (400+ m/s), faster than the depressurization front in the pipeline in which the release occurs. The crack will continue until there is a changing in material toughness thanks to fracture arrestors or block valve.

Another secondary possible cause of brittle failure of a pipeline is the creation of a two-phase inventory at saturation point. In fact, for the evaporation, caused by the inventory release, part of the needed energy comes from the cooling of the liquid inside the pipeline. If the pressure reaches the triple point of 5.12 bar, solid CO₂ starts to be deposited throughout the pipeline length causing the internal embrittlement of it. It is important to put in evidence that the presence of impurities can change the triple point pressure of the stream (Holt, 2020).

6.2.2. The embrittlement of metals and sealants

Apart from cryogenic embrittlement of the pipeline after a leak, all the materials invested by the generated cold cloud can change their behavior.

In general, the embrittlement of structures involved in the cryogenic release of dense CO₂ determines the loss of ductility of metals, due to chemical or physical changes, that induces the propagation of a crack without any plastic deformation. The cryogenic embrittlement of body-centered cubic metals is linked with the changing of their original ductile behavior into a brittle one. In this condition the hardness, yield and tensile strength, elastic modulus and fatigue resistance of metals and alloys are reduced. Consequently, structures fabricated with these materials may fracture and shatter unexpectedly at low temperatures.

Metals that remain ductile at subzero conditions are based on nickel, copper, aluminum, silver and lead. Also titanium and some of its alloys exhibit high ductility in cryogenic environment. For these face-centered cubic metals the fracture strength increases at a rate equal to or greater than that of the flow strength. This means that the deformation occurs before the fracture. In CCUS applications, the usually used low temperature carbon steel is able to reach temperatures of about -40°C or -46°C without losing ductility, thanks to its proper lattice structure. All aluminum alloys can be used at temperatures below -45°C, except series 7075-T6 and 7178-T6, and titanium alloys 13V-11Cr-3Al and 8Mn. Also copper and nickel alloys can work at these temperatures.

For CCUS applications reaching temperatures below -78°C, some materials are preferred, such as low alloys, quenched and tempered steels and ferritic nickel steels. In fact, also microstructure affects low-temperature toughness of alloys. For example, heat treatments to a tempered martensitic structure increase mechanical properties at subzero environments. Also low carbon (0.20-0.35% of carbon) martensitic steels show good performances at these working conditions. In fact, apart from geometry, rate of load and sharpness of notches, some metallurgical factors may influence the temperature at which the ductile to brittle transition occurs. For example, increasing the carbon content of alloy steels, the transition temperature increases. Also a nickel percentage above 13% may affect low-carbon cryogenic properties. Consequently, steels with 9% of nickel are usually employed for cryogenic fluid storage tanks and equipment.

Nonmetallic inclusions, oxygen, nitrogen, sulfur and phosphorus content and coarse-grained microstructure usually reduce mechanical properties of metals at low temperatures, also increasing the transition level.

The material property that defines the resistance to failure of a material in presence of a stress concentrator, is the toughness. If the low temperature fracture toughness of various cryostat metals is observed, it is possible to notice that some high-strength steels and alloys pass through a sort of phase transition that reduces their toughness of about 25%. As shown in figure 30, below 100 K some steels experience a huge decreasing in toughness, exception done for stainless steel AISI 316 and 310. These too low temperatures are not reached in the area in which the CO₂ is dispersed after a leak. In fact, if the behavior of represented metals around 190 K is observed, even for body-centered cubic nickel steels, the ductile to brittle transition temperature is not reached, but fracture toughness preserves its original ambient temperature behavior.

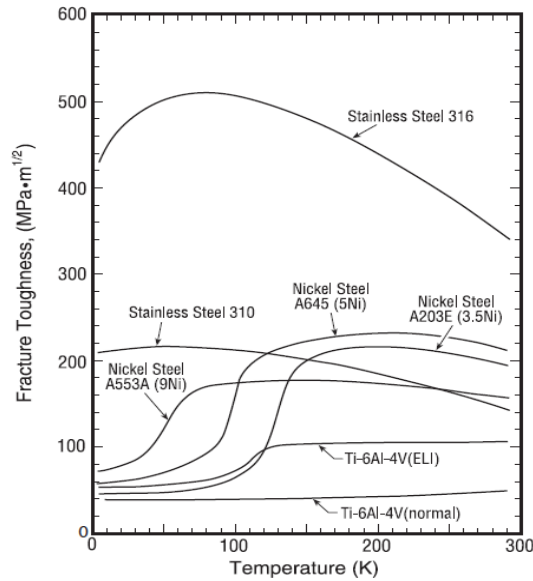


Figure 31 Fracture toughness of various metals at low temperatures. At low temperatures, nickel steels (b.c.c.) decrease in toughness and become brittle, whereas austenitic stainless steels (f.c.c.) such as AISI 310 and AISI 316 remain tough reducing temperature. Ti-6% and Al-4% (h.c.p.) toughness drops more moderately. (Data compiled from Tobler and McHenry 1983, Mann 1978, and Fowlkes and Tobler 1976.)

An exhaustive description of mechanical and physical properties of metallic and nonmetallic materials is reported in the “Cryogenic Materials Data Handbook”. Revision of these results is made by the General Dynamics/Astronautics analysis (Hurlich). The obtained metals suitable for critical applications at reduced temperatures are reported in the following figure. This way of presentation lists steels and alloys suitable for each range of temperature. For carbon dioxide applications, metals reported below HY-TUF and HY-80 3.5% Ni steel result to be a safe option because able to face critical temperatures equal to or lower than -80°C.

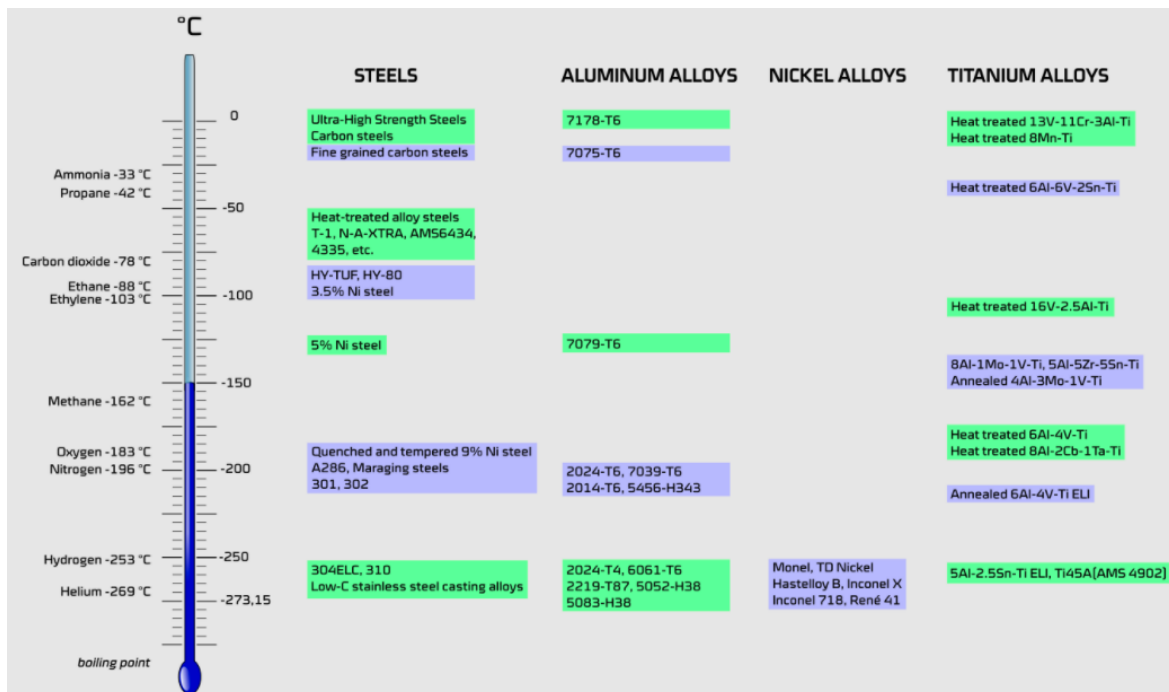


Figure 32 Materials resistant to extremely low temperatures. (Gasparini, 2019)

When vulnerability criteria for equipment exposed to cryogenic environment are needed, the first aspect to be considered is how the propagation of heat from materials to cryogenic gas occurs. In order to do that, a thermo-

fluid dynamic approach through a CFD (Computational Fluid Dynamics) model may be applied. It can describe how the surface temperature of a material changes, until reaching the ductile to brittle transition temperature, when immersed in a cold gas plume. During this kind of analysis, the varying of material thermal properties with the decreasing of temperature has to be considered. For a typical ferritic steel, for example, the transition occurs within a range of 30°C (Billingham, Sharp, Spurrier, & Kilgallon, 2003). Thanks to thermo-dynamic calculations the time needed to cool the component may be evaluated.

Another aspect to be considered is the variability of the temperature limit value. Especially for metals, as already described, the transition temperature is not a constant property, but it varies in a range of values depending on thermal treatments, microstructure and other intrinsic characteristics of the component, including the thickness and geometry of the analyzed part. Consequently, the commonest way to avoid a brittle failure is to choose materials with transition temperature below the operating conditions. However, the large number of variables does not guarantee that no failure of structural components occurs, below critical temperature, due to cryogenic embrittlement (Billingham, Sharp, Spurrier, & Kilgallon, 2003). As usually done for CO₂ cryogenic processes, a Minimum Design Metal Temperature (MDMT) of -100°C may be chosen for selection of critical components materials (Amiza, 2019).

Low temperatures are a big issue also for seals and rubber parts of components. The exposure to a very cold environment can affect elastomers, resulting in a decreasing of their maximum percentage of deformation and consequent loss of containment, if used as sealants. For example, rubber needs to be able to deform in order to provide good performance as seal, also at low temperatures, without becoming less flexible and brittle. Plastic materials and elastomers have to be tested to define a design low limit temperature, at which they harden without a desired deformation. For CCUS applications, the brittleness point of different materials can be determined testing them between -40°C and -65°C. For example testing five samples of different materials, in critical conditions, the Carboxylated Nitrile results to fail below -65°C, while 2 samples on 5 tested of Low-temperature Epichlorohydrin will fail at -60°C, together with all the 5 samples of Low-temperature nitrile (Apple Rubber, 2015). Lists of elastomeric seals and plastic materials able to face cryogenic conditions may be found in literature (Weitzel, Robbins, & Herring, 2015) (Hechtel, 2014).

Elastomers and rubbers minimum operating temperature has a big influence on vulnerability of components insulated and coated to resist critical conditions (Keane, Schwarz, & Thernherr, 2013). For flexible components, not only brittleness but also hardening of coatings has to be tested at low temperature. For this application silicon rubbers are preferred, whose working conditions are in the range of -60°C to 180°C. For insulating rigid components PVC is typically used, whose limit temperature is of -15°C (ELAND, 2020).

The identification of vulnerability criteria for structures, safety systems and other equipment is fundamental for the assessment of Escape, Evacuation and Rescue Analysis (EERA). The first step of the analysis is the definition of facilities and arrangements able to ensure that people not involved in the initial accident are still able to escape and evacuate the area. The EER facilities comprehend personal equipment, muster areas and temporary refuges where personnel are protected against asphyxiating and toxic concentrations, escape and evacuation routes, emergency communication and alarm and rescue facilities. When an accidental release occurs, the availability of these required facilities has to be determined.

The criteria for loss of integrity of EER facilities for CCUS installations have to consider the embrittlement of materials and consequent unavailability of escape routes and temporary refuges. In addition, also the loss of functionality of emergency and safety systems has to be analyzed for cryogenic effects in the EERA, defining for example the safe location of Emergency Shutdown equipment.

For electrical equipment and safety instruments the cryogenic conditions supported by structural materials cannot always be tolerated and their functionality could be limited also by higher external temperatures. For safety equipment, the functionality is the first area of concern and, for this reason, some existing standards about components operating temperature must be followed.

For explosion-proof equipment the minimum temperature of -50°C is adopted according to U.S. (UL 1203) and Canadian (CSA C22.2) standards, but these thresholds refer to enclosure resistance and do not ensure functionality of inner components. Generally, components inside a certified enclosure may show a reduced functionality at higher temperatures, that limit the minimum allowed temperature of the entire component. The IEC 60079-0 standard certifies equipment for explosive environment until -20°C . The U.S. and Canadian standards for hazardous location refer to the same limit, adding considerations about manufacturer specifications.

For example, the thermal-magnetic circuit breakers are usually protected by low temperature tested Ex-d explosion-proof enclosures. They are designed to resist temperatures of -25°C , or -40°C in case of expensive cryogenic breakers, for which engineered materials and lubricants are used. These values are lower than the minimum allowed for enclosures (-50°C) and for this reason breakers limit the operating conditions of the panel. If standard (-20°C) breakers are used, the panel is equipped with heater to increase inner temperature, as proposed by the IEC 60079 standard. In conclusion, -20°C could be considered as a limit value below which functionality of panels is not yet preserved. If circuits activate safety equipment, the panels must be located outside the area in which these low temperatures may be reached, otherwise more expensive components have to be used. For emergency equipment activated by electric motors, the lowest external temperature below which the engine stops to work may be defined from data about operating conditions reported in practical installation guidance (WEG, 2018). Generally, an electric engine preserves its performances for temperatures in the range between -20°C and 40°C .

For safety reasons, also emergency lighting must resist cryogenic conditions, especially if useful for highlighting escaping routes (HSE UK, 2020). Lighting functionality may be compromised when, due to low temperatures, lighting is not able to start because of impairment of drivers, or it cannot operate at its regime. For external application, incandescent lighting results to be the best option, preserving its ability to start and operate at all temperature levels. For High Intensity Discharge (HID) lighting, the operability is not an issue, but the starting is not guaranteed below -30°C or -40°C . LED lighting is expected to preserve operability and durability even at low temperatures. Also in this case, the only drawback is the use of limited drivers for starting. For this reason, their application is limited to -30°C or -40°C , as for HID. Otherwise there exist developing drivers for LED able to resist -55°C . The worst option for lighting are the fluorescent lamps, not proposed for external applications, for which a 50% reduction in performance is expected for temperatures below -20°C , while a negligible output is obtained at -40°C (Keane, Schwarz, & Thernherr, 2013).

Also the installation of Blow Down Valves (BDVs) and Shut Down Valves (SDVs) has to follow safety criteria in order to avoid the loss of functionality of safety systems. When exposed to cold gases, valves can experience reduction in body temperature below 0°C , that causes the formation of ice from atmospheric moisture on their external surface (Mofrad, 2018). This phenomenon may prevent the component manipulation from operators. For this reason, valves have to be externally protected with anti-condensation coatings. Apart from moisture solidification, also the materials used for BDV and SDV body have to resist cryogenic conditions. Valves typically used for low temperature applications are able to face a minimum external temperature of -30°C (Schubert&Salzer, 2020).

7. Visibility issues

Another consequence of a release of pressurized CO_2 is the lack of visibility due to a vapor cloud formation. In particular, if the dense phase CO_2 is released at ambient pressure, it will reach a temperature of about -80°C , forming a plume in which warmer air can be trapped, causing the increasing of plume temperature, diluting the CO_2 concentration. If air cools below its dew point, the condensation of water present in it occurs, allowing the formation of a fog with liquid water droplets or small water ice crystals. It is important to put in evidence that, because of invisibility of CO_2 vapor, the only visible phenomena of a CO_2 release are the visible cloud of condensed water and the solid CO_2 particles precipitation. Apart from these visible effects, the

strong noise emitted by a high pressure release can make possible to initiate emergency procedures, even without the perception of this visible cloud.

During some conducted experiments the evolution of the visible cloud has been recorded with digital HD cameras or drones. According to a study conducted in 2011, the minimum concentration of CO₂ for which the plume can be considered visible is set to 100000ppm (10%v/v). This result depends on the reached low temperatures and consequent condensation of water, but also on the obtained degree of air plume dilution (Mazzoldi & Oldenburg, 2011). At this concentration, after some minutes, unconsciousness and asphyxiation have already caused the mobility impairment, reducing the ability to escape.

On the contrary, if considered the simulations conducted by the Energy Institute, the indicative minimum value of CO₂ concentration, that makes the plume visible, is set in between 1 and 1.5% (10000-15000 ppm), with ambient air at 10°C and 70% of relative humidity (Energy Institute, 2010). In this last case, the extent of the visible cloud is higher than that of the area for which a dangerous concentration of CO₂ is reached.

With the Phantom 2 Vision aerial drone, the visible cloud extent of a gas and of a dense CO₂ release is recorded (Guo, et al., 2016). The full bore rupture (FBR) of a 258 m long pipeline and ruptures with orifice diameters of 15 and 50 mm are studied, changing the inventory properties from gas to dense phase. During the gas tests, the visible cloud reaches its maximum development after the rapid expansion, preserving the shape until the end of the metastable second phase, when its dimensions start to decrease. The maximum visible cloud lengths for gas tests are:

- 12 cm for 15 mm orifice after 52.5 s
- 12 m for 50 mm orifice after 5 s
- 40 m for FBR after 0.8 s

During dense phase tests, the duration of the cloud is longer compared with that of the gas phase produced one. In dense cases the visible cloud is more widely dispersed and it contains higher amount of dry-ice particles and condensed water. The maximum visible cloud lengths for dense tests are:

- 40 m for 15 mm orifice after 9 s
- 80 m for 50 mm orifice after 6 s
- 150 m for FBR after 5 s

According to the same experiments (Guo, et al., 2016), the 5% CO₂ threshold is the limit above which adverse effects to human health are observed and, for this reason, it is used to define toxic contours. The maximum distances at which dangerous CO₂ concentration of 5% is reached during gas tests are:

- 9.2 m for 15 mm orifice
- 12 m for 50 mm orifice
- 25 m for FBR

The maximum distance at which 5% CO₂ is measured during dense tests are:

- 20 m for 15 mm orifice
- 60 m for 50 mm orifice
- 160 m for FBR

Tanks to these examples it can be affirmed that the presence of the visible cloud at a given distance from the release cannot give precise information about the level of lethality of the reached CO₂ concentration.

The visible plume cannot be considered a good indicator of CO₂ harmful extent in every situation also because, when the plume warms above the air's dew point temperature, no water vapor is obtained. Some parts of CO₂ cloud remain invisible and dangerous, especially when accumulated on the ground or inside buildings, due to CO₂ density higher than that of air.

The temperature for which the air-carbon dioxide mixture is above 100% of humidity can vary changing the initial ambient conditions. For example, in winter, the water in ambient air difficultly remains in the vapor phase and the generated plume is invisible, if the dry-ice initially trapped is not considered. For this reason, training and information to the public is needed.

The visibility within a CO₂ formed fog is very limited and it may be reduced to less than 30 cm, as tested by a Shell camera. It is consequently necessary to evaluate the visible cloud extent in order to manage the emergency response plans, considering obstructions and restricted access ways, and establishing a good level of lighting of the escape routes. In addition, also the reduction of capability of making decisions due to CO₂ exposure must be considered in the design of escape routes. In fact, the lack of visibility can cause impairment especially if added to other critical effects due to CO₂ inhalation and exposure, like disorientation when eyes are affected by cold air.

For QRA purposes, persons outdoor are expected to attempt escape, moving crosswind or inside buildings, at an average speed of 2.5 m/s or to remain in their original position, with a 50% of probability for each of these two options. For vulnerable people, the escape velocity is reduced to 1 m/s (Cooper & Barnett, 2014). This commonly used values should be corrected considering the reduced visibility of the plume.

In addition, if a significant dense or supercritical CO₂ release occurs in proximity of a road, the lack of visibility inside the large generated cloud can be the cause of an escalation of events until, for example, a multiple vehicle crash.

8. Health effects of generated physical blast

The expansion of dense phase CO₂ into the atmosphere generally releases a large amount of energy, due to the fact that the expansion ratio between liquid and vapor is of about 500. The effects of the physical blast linked with an instant failure of a CO₂ containment can cause harm to people and damages to adjacent equipment and structures.

It is usually assumed that the blast effects have an impact only close to the rupture (meters) and for a short time period (hundredths of a second) after the considerable loss of high pressure CO₂. After the instantaneous peak overpressure, the pressure value starts to decrease, reaching zero passing through small negative values. This uncontrollable release of energy, associated with a sudden drop in pressure due to the leakage, can cause damages to people and structures that have to face the consequent shock wave and the impact with the generated flying objects.

Generally, the release resulting from a catastrophic rupture of a pipeline or vessel at high pressure is a rapid process for which a spherical pressure front is generated. The resulting damage levels can be compared with those caused by an explosion of a given amount of Trinitrotoluene (TNT), from which similarities can be exploited in order to evaluate effects of the actual blast-front amplitude, at a given distance from the “detonation source”. A ton of TNT is assumed to release a quantity of energy of 4.184 GJ, the unit used to identify the equivalent energy generated by the explosion under investigation (Mazzoldi & Oldenburg, 2011).

The human body is able to adapt to a gradual increase of pressure, compensated by the dilatation or contraction of organs, but when a sudden overpressure is perceived, this compensation is not effective and damages of organs occur. As reported in the technical guidance of the Energy Institute (EI), a physical blast and connected overpressure can determine primary effects on human organs like ears and lung, but also secondary effects linked with impact with fragments and debris, or with the collapsing of structures. Due to the speed of the overpressure, also the whole body displacement can occur, causing human body impact with other obstacles that in this case, at the same time, can be characterized by a very low superficial temperature able to cause additional severe cold burns. In order to consider all these phenomena, an empirical approach can be used, establishing some overpressure upper boundaries connected with some percentages of fatality (Energy Institute,

2010). Vulnerability of outdoor or indoor populations exposed to a given overpressure is reported in figure 33 and 34.

| mbar | psi | Assumed effect criteria |
|------|------|-------------------------|
| 68,9 | 1,0 | 0 % fatality assumed |
| 689 | 10,0 | 100 % fatality assumed |

Figure 33 EI effect criteria for outdoor populations. (Energy Institute, 2010)

| mbar | psi | Assumed effect criteria |
|------|-----|-------------------------|
| 34,5 | 0,5 | 0 % fatality assumed |
| 138 | 2,0 | 100 % fatality assumed |

Figure 34 EI effect criteria for indoor population. (Energy Institute, 2010)

The indoor vulnerability is additionally affected by possible collapse of buildings that enhances the probability of death for an assumed level of overpressure, compared with that calculated for outdoor populations at the same distance from the rupture. In fact, it is proved that the human body is more resistant to overpressure than rigid structures. Also equipment and parts of plant, such as elements and furniture of buildings, increase the probability of death, providing missiles during the blast event.

8.1. Direct effects of blast

The succession of compression and decompression of the blast wave causes the dangerous transmission of pressure waves on human body through junctions and at interface between tissues and airspace. Muscles and systems containing air are the most vulnerable.

For this reason, the proposed pressure upper limits can firstly be related to lung damages, able to cause death. When exposed to sudden overpressures, the pressure outside lung is higher than the inner pressure and, for this reason, the thorax is pressed inwards, damaging lung, depending on the extent of the impulse provoked by the shock wave. Also the position of the body influences the lung damage, due to the fact that the result of reflection and flow around a person during a shock wave can be higher than the simple maximum overpressure. The TNO (Roos, December 1989) provides graphs and probit functions able to explain the correlation between survival probability, actual peak overpressure and impulse of the wave, dependent on the atmospheric pressure and body weight.

If all overpressure values, reported in figures 33 and 34, are compared with the lower limit curve of the TNO pressure-impulse graph for lung damage, it can be seen that the Energy Institute vulnerability limits are all under this curve, for each value of scaled impulse. So, death due to lung damages is expected at EI thresholds. The compared maximum peak overpressure associated with 100% fatality for outdoor population, scaled on ambient pressure of 100 kPa (data reported in the simulation of EI), is equal to 0.69, as reported with the red line in figure 35.

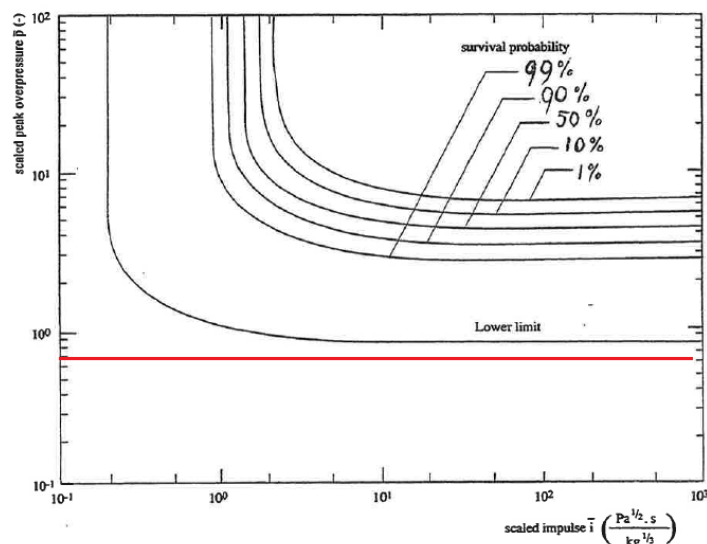


Figure 35 Pressure-impulse graph for lung damage according to TNO Green Book. The red line is the highest scaled overpressure value proposed by EI, associated with 689 mbar. (Roos, December 1989)

A more sensitive to overpressure and impulse organ is ear. The rupture of ear-drum can be linked with the perceived overpressure peak (signals with at least frequencies of about 10 kHz), but not precise needed correlations between peak duration and impulse value, generated by the CO₂ release, are quoted in literature. However, following the probit function defined by TNO, some probabilities of ear-drum rupture can be associated with a given overpressure peak. In this case, only the EI peak value of 689 mbar is in the range of overpressure able to cause damages. It corresponds to a probability of rupture of ear-drum of about 20.65% (value obtained with probit function reported in the Green Book (Roos, December 1989)).

Lung damage is a serious injury that, if not fatal, requires hospitalization, while ear-drum rupture often requires no treatments. As a consequence, mortality is deeply influenced by consequences of lung damages. An example of consequences of lung damages by the Australian Petroleum Production & Exploration Association Limited (APPEA) is proposed in the following table.

Table 7 Overpressure effects. (HSE UK)

| Overpressure [mbar] | Consequence |
|---------------------|--|
| 210 | 20% probability of fatality inside |
| | 0% probability of fatality for in open |
| 350 | 50% probability of fatality inside |
| | 15% probability of fatality in open |
| 700 | 100% probability of fatality inside |

Peak overpressure values lower than that reported in table 7 are able to cause non-lethal injuries such as non-lethal lung damages or eardrum rupture. Also for this APPEA standard, the peaks that corresponds to 0% mortality outdoor and 100% mortality indoor are higher than the corresponding ones proposed by the Energy Institute.

Due to the fact that the overpressure levels able to cause injuries to lung and ear-drum can be defined as function of peak without regard to exposure time, the following probit relationship, proposed by the Health and Safety Executive (HSE UK), can also be used for definition of mortality thresholds:

$$Y = 5.13 + 1.37 * \ln(p)$$

Where ‘*p*’ is the peak overpressure in *bar* units, and no distinction is made between outdoor and indoor conditions. According to this probit it can be affirmed that medical treatments are typically required for injuries caused by direct blast effects that are produced by peak values between 100 and 340 mbar (HSE UK).

In particular, through the HSE probit function the 1% of mortality is associated with a peak of 0.17 bar, while a peak of 3.00 bar determines a mortality of 95%. Comparing these values with that proposed by the Energy Institute, it is evident that the HSE UK 1% and 95% peak values are higher than the 0% and 100% EI ones, for both outdoor and indoor conditions. This consideration can be explained considering that the conservative Energy Institute thresholds also refer to indirect blast effects that are predominant over direct ones.

In conclusion, comparing TNO, APPEA and HSE UK thresholds with that proposed by EI, it can be proved that lung damages and rupture or ear-drum alone are not able to generate the lethality considered by the over mentioned Energy Institute’s vulnerability thresholds.

8.2. Indirect effects of blast

There is a slight possibility that blast effects directly cause fatality. Typically, more severe injuries can be caused by impact with fragments and disintegrated buildings and structures, or by falling and flying of people, hitting solid objects. For this reason, in risk analysis the most important effects are:

- Flying objects hitting people
- Whole body displacement and impact damage
- Damage caused by collapsed structures

In general, the air particles in the area of a shock wave are characterized by a velocity, in the same direction of the blast. That generates an explosion wind able to displace a human body. During this event, injuries and death can be caused not only by the falling of people on the ground, but also by collision with objects. The lethality depends on velocity of the impact, hardness and shape of objects, and on what part of body is involved, considering that the skull is defined as the most vulnerable part of the body.

Both the probit and the graphic TNO methods need to identify the extent of the shock wave impulse, in order to determine the impact velocity and the related probability of death in case of whole body collision or of skull-base fracture. In addition, fragments and debris, generated by the explosion source or from structures damaged by the shock wave, can harm involved people. In particular, fragments (mass lower than 0.1 kg) are more dangerous than overpressure itself and they can cause the penetration of skin and organs if inhaled. The DNV (NORSOK Z013) skin laceration thresholds are reported in table 8. Also debris are considered in risk analysis because they are responsible of high compressive stresses on bodies (mass in between 0.1 kg and 4.5 kg) or skull-base fracture (mass higher than 4.5 kg).

Table 8 Injuries from fragments. (HSE UK)

| Injury | Peak overpressure [mbar] |
|--------------------------------------|---------------------------------|
| Skin laceration threshold | 70-150 |
| Serious wound threshold | 150-200 |
| Serious wounds near 50% probability | 250-350 |
| Serious wounds near 100% probability | 500-550 |

The Energy Institute overpressure values for indoor conditions, whose effects vary from 0% to 100% of fatality, are included in the first threshold reported in the previous table, for which only skin laceration due to fragments may occur. Otherwise, for outdoor populations, the Energy Institute wide range of overpressure does not correspond to any of the proposed DNV threshold, so fragments may cause skin laceration, when the 0% of mortality is reported, or serious wounds near 100% probability, when the 100% probability of death is expected following the Energy Institute’s evaluations.

As said before, the observed overpressure, damaging buildings, is able to harm indoor populations because of the impact with glass fragments of windows and collapse of structures. The risk depends on the age of people and on size and age of the building itself. Also in this case, the consequences on buildings depend on the peak overpressure that reaches the structure. As lowest threshold, the DNV (NORSOK Z013) analysis of explosion provides indicative pressure values needed to break a common glass. The 1% of the glass breakage is reached at 17 mbar, while the 90% is obtained at 62 mbar (HSE UK).

Considering the EI 0% fatal limit for indoor populations of 0.5 psi (34.5 mbar), the worst consequence on structures consist on occasional damages to windows frame, with only 10% of windows broken. Reaching the 2.0 psi (138 mbar) of overpressure, partial collapse of walls and roofs of houses occurs, determining the 100% of probability of death for indoor populations (Quest Consultants Inc., 2010).

All previous information about direct and indirect effects of a blast are putted together in order to compare standard correlations between consequences on human health and vulnerability thresholds with that proposed by the Energy Institute and reported in figures 33 and 34. The EI empirical evaluations result in a conservative approach compared with TNO, HSE UK and other shared technical guidance and standards.

8.3. Blast effects compared with toxic effects of CO₂

For most of analyzed literature examples about CO₂ release, the overpressure peak evolution is generally reported for near-field evaluations and only the Energy Institute study (Energy Institute, 2010) considers the propagation of the blast wave, generated by the jet expansion, for a maximum distance downwind equal to that used for toxic cloud dispersion calculations. Apart from the Energy Institute guidance, no other methods have been found in literature to correlate mortality to overpressure generated by a rapid CO₂ depressurization. However, in this Chapter some simulations and experimental works will be discussed to identify the entity of this physical effect for different storage and release conditions.

ENERGY INSTITUTE SIMULATION FOR FAR-FIELD EVALUATIONS

Some CO₂ concentration exposure limits and shock wave fatality thresholds have been applied in the Energy Institute simulation (Energy Institute, 2010) in order to determine which one of these hazards generates the larger impact area, driving the risk assessment.

The Energy Institute has modelled a rapid release of a dense phase CO₂ inventory (at 117 barg and 10°C) through a full bore rupture of a 54 km long pipeline. Three scenarios are simulated with pipeline diameter of 203 mm, 406 mm and 711 mm, respectively. Exploiting the PHAST method, different overpressure-distance graphs and isopleths of CO₂ concentration have been obtained (Energy Institute, 2010). Comparisons of these results are useful to evaluate if the distance associated with lethality due to physical blast is lower or higher than that obtained measuring the probability of death due to toxic CO₂ effects. The Energy Institute dispersion model and consequent considerations cannot be applied to low momentum releases.

With ambient air temperature of 10°C, humidity of 70% and a wind speed of 5 m/s, the post expansion temperature of -87.5 °C is reached in each of the three simulated cases. The not directional blast effects, caused by the shock wave produced by the energy released during the expansion, have a limited duration. For this reason, the effective involved amount of released gas results to be very low.

In case of FBR of a pipeline with a diameter of 203 mm and a center-line 1 m above the ground, the lowest overpressure value, above which fatalities occur (0.035 bar, see figure 34), is registered at 35 m from the rupture. This distance is lower than that evaluated, in the same release conditions, for the 1% probability of death caused by toxicity of CO₂ (100 m from the rupture). Considering that the 100% fatal limit due to overpressure (0.7 bar, see figure 33) is obtained within the 5-meter contour, the blast effects can be classified as severe only near the release point.

Analyzing the consequences of a FBR of a pipeline with a diameter of 711 mm, the 100%, 10% and 1% fatality limits for outdoor population, due to inhalation of toxic CO₂ concentrations, have been compared with the maximum distances for which peaks of 0.7 bar (mortality of 100%) and 0.07 bar (mortality of 0%) are reached. The fatality footprint and the peak-distance curve are shown in the following figures.

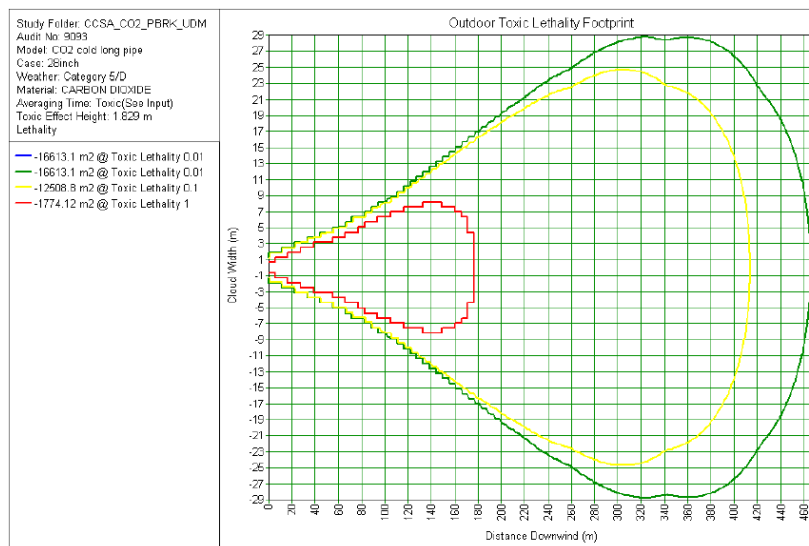


Figure 36 117 mm pipeline release outdoor fatality footprint (red=100%; yellow=10%; green=1%). (Energy Institute, 2010)

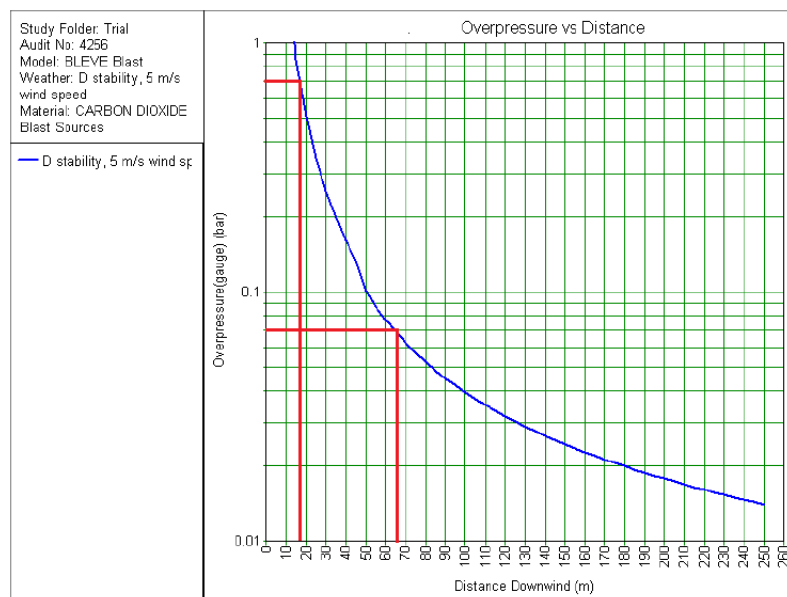


Figure 37 Blast-distance relationship for 117 mm line rupture. (Energy Institute, 2010)

Figure 36 indicates that the maximum distance, for which due to CO₂ inhalation there is the 100% probability of death, is 180 meters, while there is practically no risk of fatality for people beyond 500 meters from the release point. In figure 37, the 100% of fatality results to be possible for people exposed to overpressure within 17 meters from the release and there is no risk due to blast effects for populations beyond 65 meters from the pipeline FBR.

For each of the three reported cases, the 100% and the 0% fatality distances calculated for blast effects are lower than the corresponding distances evaluated for toxicity of the released cloud. If added the consideration that EI overpressure thresholds are more conservative than standard TNO, HSE and APPEA approaches, it can be concluded that the dangerous effects of exposure to high concentration of CO₂ prevail over that of a physical blast, whose additive contribution is effective only near the release point.

LITERATURE EXAMPLES FOR NEAR-FIELD EVALUATIONS

Other numerical simulations and experiments have been conducted to define the shock wave structure considering the Mach disk, the barrel shock and the reflected shock. These laboratory small-scale experiments, here described, aim to characterize the near-field kinetic effects of an accidental CO₂ release from a pressurized pipeline.

At the UK Health and Safety Laboratory (HSL), investigations about CO₂ release behavior have been done (Pursell, 2012). The pressure of the inventory is in between 40 and 55 bar, while the initial temperatures are 11.6 °C or 2 °C for liquid phase and 10.4 °C or -3.5°C for gas phase, not included in the range of temperatures usually involved in onshore pipeline transportation of CO₂ (30-40 °C). According to this experimental setup, after the rupture, the fluid expands isenthalpically from internal pressure to ambient pressure, after which the mixing with air reduces the concentration and the expansion velocity of the jet. Both gaseous and liquid releases from a 2 or 4 mm orifice generate an expansion zone of a length in the range 10-20 mm. The overpressure wave propagation continues until the experimental boundaries without generating dangerous peak values.

The near-field behavior of the shock wave generated from a supercritical pipeline release has also been studied (Li, et al., 2017). The experiment consists in a release from a 1 mm orifice of supercritical CO₂ (initial pressure of 8 MPa) transported through a 10 meters long pipeline. The obtained rapid depressurization causes an explosive expansion outside the leakage nozzle, followed by a sudden decrease of nozzle pressure to about 6 MPa. The discontinuity of parameters, like pressure, caused by the compression effect of the jet passage through the Mach disk has been evaluated. The propagation of the shock wave is perceived within centimeters from the release point and no dangerous peak overpressure is expected within the tested area.

Comparing these literature results about CO₂ discharge from gas, liquid or supercritical inventories, it can be affirmed that only large or full bore ruptures of large-scale dense CO₂ pipelines are able to generate relevant blast effects, due to the huge release of energy. However, also in these cases, the 1% and 50% mortality due to overpressure could be obtained only in proximity of the release point.

9. Effects of impurities on human health

During a leak, when the supercritical CO₂ changes to the gaseous state without any solvent capability, all the impurities contained in the flow may be released, posing a threat to health, safety and environment. When impurities are transported within CCUS streams, they are also able to induce some transformation on the CO₂ thermo-physical behavior. These substances change transport properties of CO₂, affecting its hydraulics, changing the number of compressors and compressor power needed. When transported, some of them alter pipelines fracture propagation, corrosion rate and properties of non-metallic components. Also the capacity of the pipeline itself is affected. The presence of impurities and their concentration increase critical temperature and pressure of the stream, changing its density and viscosity too.

Dangerous concentrations of impurities are usually associated, in literature, with a combustion process and, for this reason, the existing knowledge can be exploited to characterize their presence in accidentally released CO₂ streams, coming from power plants and industrial processes. A secondary phenomenon, that can occur long time after the release event, is the sublimation of the deposited solid particles of CO₂ and the related dispersion of impurities contained in them near the release area, or in human body after the dry-ice particles ingestion.

The composition of the released stream depends on the source from which CO₂ is captured. The contained substances and their volumetric percentages vary, changing the type of power plant and the capture technology, or considering the different industrial sectors, such as steel or cement industries from which CO₂ is produced. The DNV-RP-J202 Recommended Practice has developed the following summary of indicative composition of CO₂ streams, depending on the source type.

| Component | Coal fired power plant | | | Gas fired power plants | | |
|-------------------------------------|------------------------|----------------|----------|------------------------|-----------------|----------|
| | Post-Combustion | Pre-combustion | Oxy-fuel | Post -combustion | Pre- combustion | Oxy-fuel |
| Ar/ N ₂ / O ₂ | 0.01 | 0.03-0.6 | 3.7 | 0.01 | 1.3 | 4.1 |
| H ₂ S | 0 | 0.01-0.6 | 0 | 0 | <0.01 | 0 |
| H ₂ | 0 | 0.8-2.0 | 0 | 0 | 1 | 0 |
| SO ₂ | <0.01 | 0 | 0.5 | <0.01 | 0 | <0.01 |
| CO | 0 | 0.03-0.4 | 0 | 0 | 0.04 | 0 |
| NO | <0.01 | 0 | 0.01 | <0.01 | 0 | <0.01 |
| CH ₄ ⁺ | 0 | 0.01 | 0 | 0 | 2.0 | 0 |
| Amines | - | - | - | - | - | - |
| Glycol | - | - | - | - | - | - |

Figure 38 Indicative composition of dried CO₂ streams (IEA GHG). Unit % volume. (DNV-RP-J202, April 2010)

The Polytec research about state of the art of CO₂ pipeline transport (Oosterkamp & Ramsen, 2008) has led to another definition of the expected composition of the CO₂ mixtures, captured from post-combustion, pre-combustion and oxyfuel processes. In this case also information about purity of the stream is reported in terms of carbon dioxide volumetric concentration. In figure 39, the maximum levels of components are reported, considering that these values can be reached if purification and co-capture of other substances are not conducted.

| | Post-Combustion | Pre-Combustion | Oxyfuel |
|------------------|-----------------|----------------|------------|
| CO ₂ | >99 vol% | >95.6 vol% | >90 vol% |
| CH ₄ | <100 ppmv | <350 ppmv | -- |
| N ₂ | <0.17 vol% | <0.6 vol% | <7 vol% |
| H ₂ S | Trace | <3.4 vol% | trace |
| C2 ⁺ | <100 ppmv | <0.01 vol% | -- |
| CO | <10 ppmv | <0.4 vol% | Trace |
| O ₂ | < 0.01 vol% | Trace | <3 vol% |
| NO _x | < 50 ppmv | -- | <0.25 vol% |
| SO _x | <10 ppmv | -- | <2.5 vol% |
| H ₂ | Trace | <3 vol% | Trace |
| Ar | Trace | <0.05 vol% | <5 vol% |
| COS | | ? | |

Figure 39 Compounds from different power production methods with CO₂ capture. Indicative maximum values. (Oosterkamp & Ramsen, 2008)

The Polytec study also investigates the CO₂ mixture coming from natural sources. These streams typically transported by the existing USA pipelines are characterized by the presence of N₂, H₂S, water and hydrocarbons and by no traces of Ar, NO_x, SO_x and H₂, that instead are transported during CCUS processes as reported in figure 39.

The US Department of Energy (Herrom & Myles, 2013) has investigated what are the Carbon Capture Utilization and Storage (CCUS) technology-specific contaminants. For pre-combustion capture from an integrated gasification combined cycle (IGCC), in the produced stream organic impurities and sulfur compounds are still present, because the combustion process takes place after the CO₂ separation. The stream from post-combustion contains fewer numbers of different impurities, compared with pre-combustion captured one. NO_x, SO_x and particulate are a problem if the stream is not pre-treated. Oxy-combustion produced stream is characterized by an excess of oxygen of about 3% in volume, but also Ar and N₂ are present in higher percentages compared with the other two CO₂ capture technologies.

Impurities have an effect upon toxicity and, when leaks occur, their small concentrations may determine the safe exposure limit at the fluid instead of CO₂ concentration itself. This is the case of H₂S and SO₂. For the hazard management of these substances it is useful to understand their impact, both as isolated substances and combined with CO₂ and other elements contained in the stream. H₂S and SO₂ can be defined as irritants, affecting eyes, upper part of the respiratory system, impairing escape capability, until causing death due to lung damages. Other elements as CO and NO are classified by UK HSE as narcotic gases and analyzed for their toxicity (HSE UK, 2020).

Carbon monoxide (CO) is classified as an asphyxiating gas, able to cause tissues hypoxia by limiting the amount of oxygen transported by blood. All factors that increase the respiration and circulation rate can enhance the carboxyhaemoglobin formation and CO effects. For this reason, the simultaneous inhalation of CO₂ promotes hypoxia caused by CO. High concentration of CO may determine damages similar to a toxic substance, but in CCUS applications CO volumetric percentage is too low to provoke significant effects. Only in case of a coal fired power plant, in pre-combustion mode, the CO concentration reaches dangerous values, able to generate, after the rupture, a lethal envelope larger than that defined by a 5% of CO₂. In fact, the Time Weighted Average (TWA) limit for CO, set by NIOSH, is 35 ppm, for an exposure of 8 hours a day in a 40-hour work week. The IDLH concentration for CO is 1200 ppm, lower than the corresponding IDLH of CO₂. Some examples of concentrations of CO able to cause death are shown in the following table (OSD3.2, January 2006).

Table 9 Lethal levels of CO exposure by UK HSE and TNO

| Lethality | 1% lethality | 1% lethality | 1% lethality | 1% lethality | 50% lethality | 50% lethality | 50% lethality | 50% lethality |
|----------------------------|--------------|--------------|--------------|--------------|---------------|---------------|---------------|---------------|
| Duration [min] | 10 | 10 | 30 | 30 | 10 | 10 | 30 | 30 |
| Typology | HSE SLOT | TNO probit | HSE SLOT | TNO probit | HSE SLOD | TNO probit | HSE SLOD | TNO probit |
| Concentration [ppm] | 4013 | 2063 | 1338 | 688 | 5700 | 21203 | 1900 | 7068 |

Thanks to the very low percentages of impurities, the NORSOK Z013 lethal concentrations of SO₂ are not exceeded, exception done for CO₂ stream captured from oxy-fuel coal fired power plant that can contain 5000 ppm of SO₂, able to generate a too large damage area after the release characterized by a concentration higher than the NORSOK lethal limit of 800 ppm. The IDLH for SO₂ is 100 ppm, set by Vattenfall entity. The co-sequestration of CO₂ and H₂S is the scenario with the lowest percentage of SO₂ because the reaction of H₂S with SO₂ results in a dangerous deposition of Sulphur and pretreatments are always performed. Examples of other lethal concentrations of Sulphur Dioxide are reported in table 10.

Table 10 Lethal levels of SO₂ exposure by UK HSE and TNO

| Lethality | 1% lethality | 1% lethality | 1% lethality | 1% lethality | 50% lethality | 50% lethality | 50% lethality | 50% lethality |
|----------------------------|--------------|--------------|--------------|--------------|---------------|---------------|---------------|---------------|
| Duration [min] | 10 | 10 | 30 | 30 | 10 | 10 | 30 | 30 |
| Typology | HSE SLOT | TNO probit | HSE SLOT | TNO probit | HSE SLOD | TNO probit | HSE SLOD | TNO probit |
| Concentration [ppm] | 683 | 1327 | 394 | 840 | 2729 | 3504 | 1576 | 2217 |

SO₂ dangerous concentrations released with the CO₂ stream are able to cause respiratory irritation for exposed asthmatics (0.1 ppm for 60 min) and for healthy people (1.0 ppm for 60 min). Also the lowest SO₂

concentration registered by DNV Practice (10 ppm) may cause severe effects on the respiratory tract if directly inhaled.

Among nitrogen oxides, the presence of NO₂ has to be analyzed because even low levels of this toxic substance can cause unconsciousness and death. The IDLH for NO₂ is 200 ppm. Lethal doses by TNO and UK HSE are reported in table 11.

Table 11 Lethal levels of NO₂ exposure by UK HSE and TNO

| Lethality | 1% lethality | 1% lethality | 1% lethality | 1% lethality | 50% lethality | 50% lethality | 50% lethality | 50% lethality |
|---------------------|--------------|--------------|--------------|--------------|---------------|---------------|---------------|---------------|
| Duration [min] | 10 | 10 | 30 | 30 | 10 | 10 | 30 | 30 |
| Typology | HSE SLOD | TNO probit | HSE SLOD | TNO probit | HSE SLOD | TNO probit | HSE SLOD | TNO probit |
| Concentration [ppm] | 9600 | 90 | 3200 | 67 | 62400 | 168 | 20800 | 125 |

For nitrogen monoxide, some Short Term Exposure Limits are defined in literature. For example, a concentration of 25 ppm is the commonest limit for an exposure of 8 hours. This value is usually never reached after a release, whatever the CO₂ stream source is. The IDLH limit for NO is 100 ppm, that after the release and dispersion of the cloud must never be exceeded.

9.1. Health effects of high concentration of H₂S

A further analysis is required for H₂S stream content. Apart from oxygen depletion, also a high concentration of hydrogen sulfide (H₂S) can cause a dangerous reduction of oxygen saturation in blood. For this reason, a 60-minute exposure to 60 ppm of H₂S can subject individuals to possible impairment and death as the dose increases. The effects on human health of H₂S are reported in the figure 40 (HSE UK).

| Concentration (ppm) | Effect |
|---------------------|--|
| 20 - 30 | Conjunctivitis |
| 50 | Objection to light after 4 hours exposure. Lacrimation |
| 150 - 200 | Objection to light, irritation of mucous membranes, headache |
| 200 - 400 | Slight symptoms of poisoning after several hours |
| 250 - 600 | Pulmonary edema and bronchial pneumonia after prolonged exposure |
| 500 - 1000 | Painful eye irritation, vomiting. |
| 1000 | Immediate acute poisoning |
| 1000 - 2000 | Lethal after 30 to 60 minutes |
| > 2000 | Rapidly lethal |

Figure 40 Effects of exposure to hydrogen sulfide. (OSD3.2, January 2006)

Also for hydrogen sulfide, some lethal limits can be defined. The IDLH by NIOSH is 100 ppm, a concentration from which escape may be made in 30 minutes without irreversible health effects and severe impairment to escape. This value is in between 10 ppm, the TWA set by NIOSH, and 200 ppm, a limit based on health and safety effects obtained applying a safety factor of 5 on the maximum exposure limit of 1000 ppm. The lethal doses proposed by HSE and TNO are reported in the following table.

Table 12 Lethal levels of H₂S exposure by UK HSE and TNO

| Lethality | 1% lethality | 1% lethality | 1% lethality | 1% lethality | 50% lethality | 50% lethality | 50% lethality | 50% lethality |
|-----------|--------------|--------------|--------------|--------------|---------------|---------------|---------------|---------------|
|-----------|--------------|--------------|--------------|--------------|---------------|---------------|---------------|---------------|

| | | | | | | | | |
|----------------------------|----------|------------|----------|------------|----------|------------|----------|------------|
| Duration [min] | 10 | 10 | 30 | 30 | 10 | 10 | 30 | 30 |
| Typology | HSE SLOT | TNO probit | HSE SLOT | TNO probit | HSE SLOD | TNO probit | HSE SLOD | TNO probit |
| Concentration [ppm] | 669 | 371 | 508 | 208 | 1107 | 1265 | 841 | 709 |

The concentrations of H₂S in the typical CO₂ streams could be higher than that imposed as safety limits. Depending on source of captured CO₂, the H₂S concentration varies from 0 ppm to 6000 ppm. Some CO₂ lethality thresholds have been compared in literature with concentrations of toxic H₂S able to cause death (Liu, Godbole, Lu, Michal, & Venton, 2015). According to this experimental study reported in Appendix A, the effects of inhalation of 5% CO₂ are also obtained if a person is exposed to 0.02% of H₂S, while the 8% CO₂ gives the same degree of lethality of a 0.05% of H₂S.

9.1.1. The Mattoon Site project evaluations

The presence of impurities such as H₂S and CO in CO₂ stream has been considered in some experimental risk assessments in order to evaluate the impurities' concentrations below which the risk profile is dominated by the toxicity of CO₂.

According to the FutureGen Project for the Mattoon Site (U.S. Department of Energy - National Energy Technology Laboratory, November 2007), in the case of pre-combustion coal fired power plant the dangerous concentrations of hydrogen sulfide may generate, after a leak, a 200 ppm H₂S envelope higher than the 5% CO₂ envelop imposed as safety limit. This consideration may be done also comparing substances occupational limits. In fact, if STEL values of 30000 ppm for CO₂ and 15 ppm for H₂S are considered in the risk assessment, with an initial concentration of 100 ppm of H₂S in the inventory, the limiting factor will be the presence of hydrogen sulfide.

In particular, the distance for which the exposure limit value of H₂S is reached seems to be higher than that evaluated for CO₂ released during the same event. In this case, at a distance of about six times higher than that considered for CO₂ exposure risk, the impurities may dominate the evaluation of the external safety.

In order to evaluate all the consequences connected to Mattoon Site plant, it has been defined a conservative Region of influence (ROI) for human health and safety within 16.1 kilometers of boundaries of plant, sequestration site and CO₂ pipeline. Potential health effects have been evaluated both for workers and general public exposed to CO₂ and H₂S.

The exposure limits used for Hydrogen Sulfide are:

- NIOSH REL C (Recommended Exposure Limit): concentration of 10 ppm for 10 min exposure (ceiling). It should not be exceeded any time;
- OSHA PEL C (Permissible Exposure Limit): concentration of 50 ppm for 10 min exposure (maximum peak, ceiling). It must not be exceeded during any part of the workday;
- IDLH (Immediate Dangerous to Life and Health): 100 ppm.

The main provoked symptoms are dizziness, headache, insomnia and lassitude, as for CO₂ inhalation, but in addition, H₂S can cause irritation of eyes, lacrimation, abnormal visual intolerance to light and gastrointestinal disturbances. Also apnea, coma and convulsions can occur. Because of inhalation or skin and eye contact with H₂S, the eyes, the respiratory system and the central nervous system may already be altered by a concentration of 50 ppm.

The CO₂ exposure limits considered in the FutureGen Project are:

- NIOSH REL ST (Recommended Exposure Limit): concentration of 30000 ppm for 15 min exposure (short-term exposure limit);
- OSHA PEL TWA (Permissible Exposure Limit): concentration of 5000 ppm to not be exceeded during an 8-hour work shift of a 40-hour workweek;
- IDLH (Immediate Dangerous to Life and Health): 40000 ppm.

In order to evaluate the risk associated with separation, compression and transportation of CO₂ for FutureGen Project, the pipeline rupture, the leakage through a 19.4 cm² puncture and the rupture of a wellhead injection equipment have been simulated. The supercritical initial conditions of the stream, made of 95% of CO₂ and 100 ppm of H₂S, are characterized by a pressure of about 138 bar and a temperature of 32.2 °C.

Apart from physical trauma due to high flow rates and high speeds of the released flow, asphyxiation, toxic effects and frostbite, due to the rapid CO₂ expansion, are observed for workers near the rupture point. If considered a distance of 24 meters, the workers are exposed to a too high concentration of CO₂ (170000 ppm) that can cause death in a minute. If more extended area needed to be considered, the NIOSH CO₂ and H₂S limits have to be adopted (30000 ppm of CO₂ for 15 min and 10 ppm of H₂S for 10 min). The simulation results are shown in the following table.

| Release Scenario | Frequency Category ² | Exposure Time | Gas | Area of Exceedance |
|--------------------------------|---------------------------------|-----------------------|------------------|--------------------------------------|
| Pipeline Rupture | EU | Minutes | CO ₂ | None |
| | | | H ₂ S | Within plant boundaries ³ |
| Pipeline Puncture ⁴ | EU | Approximately 4 hours | CO ₂ | Near pipeline only ⁵ |
| | | | H ₂ S | Near pipeline only ⁵ |
| Wellhead Rupture | EU | Minutes | CO ₂ | None |
| | | | H ₂ S | Near wellhead only ⁵ |

¹ Occupational health criteria used were the NIOSH REL ST and NIOSH REL C for CO₂ and H₂S, respectively. See Table 4.17-4.

² EU (extremely unlikely) = frequency of 1x10⁻⁴/yr to 1x 10⁻⁶/yr;.

³ Within 820 feet (250 meters) of release.

⁴ 3-inch by 1-inch rectangular opening in pipe wall.

⁵ Distances for a pipeline puncture are: 372 feet (113.4 meters) for CO₂ and at least 548 feet (167 meters) for H₂S; for a pipeline rupture is at least 131 feet (40 meters) and a wellhead rupture at least 216.5 feet (66 meters).

Figure 41 Exceedance of occupational health criteria for workers. (U.S. Department of Energy - National Energy Technology Laboratory, November 2007)

Analyzing the results of FutureGen project results, when for few minutes the dispersion of the mixture occurs, caused by the rupture of the pipeline or of the wellhead, even if there are not areas for which the NIOSH REL C values of CO₂ are reached, the presence of H₂S is analyzed to evaluate the effects of inhalation on people within the plant boundaries (250 meters) or near the wellhead (66 meters). In fact, in these conditions the NIOSH REL ST dose of hydrogen sulfide of 10 ppm for 10 minutes is exceeded.

Apart from occupational limits, other concentration limit values are applied to identify three different categories of damage. After an exposure of minutes to CO₂ and H₂S, the health effects are reported in figure 42.

| Exposure Time | Gas | Effect Category | Concentration (ppmv) | Hazard Endpoint ¹ |
|---------------------|------------------|----------------------|----------------------|------------------------------|
| Minutes (Pipelines) | CO ₂ | Adverse | 30,000 | TEEL 1 |
| | | Irreversible adverse | 30,000 | TEEL 2 |
| | | Life threatening | 40,000 | TEEL 3 |
| | H ₂ S | Adverse | 0.51 | TEEL 1 |
| | | Irreversible adverse | 27 | TEEL 2 |
| | | Life threatening | 50 | TEEL 3 |

Figure 42 Type of effects and hazard endpoints for receptors. (U.S. Department of Energy - National Energy Technology Laboratory, November 2007)

The considered health effects from accidental chemical releases are:

- Adverse effects: effects ranging from mild and transient effects (headache, sweating);
- Irreversible adverse effects: permanent effects that generally occur at higher concentrations. They include death, impaired organ function (central nervous system damages) and impairment of everyday functions;
- Life threatening effects: subset of irreversible effects due to high concentrations that may lead to death.

The used hazard endpoints that indicate the Temporary Emergency Exposure Limits (TEEL), established by EPA (2006) and DOE (2006), are (U.S. Department of Energy - National Energy Technology Laboratory, November 2007):

- TEEL 1: The maximum concentration in air below which exposed individuals experience only transient health effects, without perceiving the presence of substance through a defined odor
- TEEL 2: The maximum concentration in air below which exposed individuals are not expected to develop irreversible or serious health effects that impair their ability to take protective action
- TEEL 3: The maximum concentration in air below which exposed individuals do not experience life-threatening effects

Through this comparison it can be affirmed that, for the same duration of exposure, the same adverse health effects obtained inhaling a given CO₂ concentration could be experienced by individuals at a H₂S concentration 1000 times lower than CO₂. In addition, H₂S may be perceived before reaching dangerous values of 27 ppm, while when individuals begin to perceive the CO₂ presence, the inhaled concentration of 30000 ppm is already able to cause significant health effects.

In general, even if the issues related to the presence of impurities in CCUS streams during the release event are considered not dangerous for human health, some of them assume higher importance if a long distance risk analysis has to be conducted because of their capability to affect individuals' health also through low volumetric percentages in air. Depending on the initial concentration of impurities inside the stream, relevant consequences may result, not only linked with the presence of dangerous substances in the cold cloud, but also due to the delayed sublimation of generated solid CO₂ particles that contain them.

9.2. Acceptable concentrations of impurities

The potential reactions between impurities and their individual negative effects after a release have to be investigated. An agreed specification needs to be approved for allowable amount of impurities in the CO₂ captured, transported and stored stream, in order to obtain a risk profile driven by toxicity of CO₂ and not by the presence of other toxic components of the stream.

Thanks to the CO₂ Europe project, an example of acceptable concentrations of impurities in the stream has been developed. The values, proposed by the Dynamis study (L. Buit, May 2011), are shown in figure 43, in comparison with other two proposed CO₂ specifications, the Kinder Morgan and the Ecofys ones, already applied for in operation lines. According to Dynamis specifications, impurities have not more harmful effect on people compared with pure CO₂ as long as remaining below the values reported in the table.

| Compound | Specification (Kinder Morgan) | Specification (Ecofys) | Specification (Dynamis) |
|------------------|---|------------------------|---|
| CO ₂ | Min. 95% | Min. 95% | Min 95,5 % |
| N ₂ | Max 4% | Max 4% | Max 4 % (combined all non cond. gases) |
| CH ₄ | Max 5 % | Max 4% | Max 4 % (Aquifer) Max 2 % (EOR) |
| H ₂ O | 257 ppm wt | Max 500 ppm | Max 500 ppm |
| O ₂ | 10 ppm wt | Max 4 vol % | Max 4 % (Aquifer, combined all non cond. gases) Min 100 - 1000 ppm (EOR) |
| SO _x | - | - | Max 100 ppm |
| NO | - | - | Max 100 ppm |
| H ₂ S | 10-200 ppm | - | Max 200 ppm |
| H ₂ | - | Max 4 % | Max 4 % (combined all non cond. gases) |
| Ar | - | Max 4 % | Max 4 % (combined all non cond. gases) |
| CO | - | - | Max 2000 ppm |
| Glycol | Max 4*10 ⁻⁵ l/m ³ | - | - |
| Temperature | Max 50 °C | Max 30 °C | |

Figure 43 Proposed limits of impurities concentrations. (Johnsen, Holt, Helle, & Sollie, 2009)

When all these substances are mixed, the obtained harm level can be less than, equal to, or greater than the sum of all individual ones (Holt, 2020). In order to assess the combined effect of a mixture, the simple additive approach can be used. This method is too conservative and it can be used only if substances attack the same organs in a similar mode. In order to apply the additive approach, data about individual impairment criteria for all stream harmful components are needed. For a consistent comparison the impairment criteria of impurities have to be based on recognized data sources such as HSE COSHH Levels or International Exposure Levels. In particular, evaluations about substance toxicity can be done analyzing the SLOD and SLOT UK HSE curves. As expected, each LD50 and LD1 concentration value calculated for CO, SO₂, H₂S and NO₂, individually considered, is below the LD50 and LD1 values of CO₂ respectively, due to the fact that their toxicity levels are higher than that of carbon dioxide.

For this reason, concentrations of contaminants have to be monitored. If their percentages are under the values reported in figure 43, their presence as individual toxic elements and as part of the mixture has less impact on human health than CO₂ after an accidental release. However, following the Dynamis project additive approach, the release of pure CO₂ present in the mixture is able to generate the largest damage area, due to the fact that the small percentages of impurities are not able to significantly increase the CO₂ toxicity.

When higher concentrations are transported, impurities in CO₂ stream may have an impact on risk assessment, linked to their toxicity (as H₂S and CO) or their ability to enhance internal corrosion. For this reason, some oxy-fuel and pre-combustion capture units require a pre-treatment, in order to decrease the high percentage of NO_x, SO_x, H₂S and CO. Apart from these last components of the stream, the presence of other substances is limited by the proposed specification. For example:

- N₂, O₂, Ar, CH₄ and H₂ concentrations should be limited in order to avoid the increasing of compression work.

- The presence of N₂, CH₄ and H₂ is limited because these components can affect pipeline strength, increasing the ductile fracture potential because of their critical temperatures, lower than that of pure CO₂.
- O₂ should be limited for EOR applications to eliminate exothermic reactions with hydrocarbons. O₂ with free water increases cathodic reaction.
- Water content has to be limited to avoid acids formation with CO₂ and SO₂.
- N₂, H₂ and CH₄ concentrations should be controlled to maintain the correct miscibility pressure during EOR operations.

In the Polytec overview (Oosterkamp & Ramsen, 2008), that also provides expected initial compositions reported in figure 39, the European Dynamis project's results are compared with the other two fluid specifications for CO₂ pipelines, the Kinder Morgan USA specification and the Dutch Ecofys proposed conditions, as reported in figure 40. The first stream composition is obtained from operated pipelines in USA for which a specified maximum and/or minimum concentration of impurities as nitrogen, hydrocarbons, water, oxygen and glycol is obtained. The Dutch study takes into account the stream composition of the mixture coming from a coal fired power plants, for which there are not proposed maximum concentrations for SO₂, NO and H₂S. Comparing different specifications, the Dynamis requirements result to be less restrictive than Kinder Morgan ones, but more specific than Ecofys proposed specification. Dynamis composition is the reference model because of its ability to reduce the cost of the capture process preserving the safety conditions.

The recommended ranges obtained from a literature review for each stream component are reported in the NETL quality guidelines (Herrom & Myles, 2013) for EOR or saline reservoir CCUS, as shown in figure 44. The CH₄, N₂, Ar, H₂O and H₂ concentration limits proposed by Dynamis project match the ranges and the design values of the NETL study. The O₂ Dynamis limit correspond to the upper bound of the NETL range. The SO_x and NO_x concentrations proposed by the two studies are the same and they correspond to the IDLH value of 100 ppm. The CO and H₂S Dynamis maximum concentrations are in the literature ranges but the values results to be less conservative than that proposed as highest limits in the NETL evaluations.

| Component | Unit (Max unless Otherwise noted) | Carbon Steel Pipeline | | Enhanced Oil Recovery | | Saline Reservoir Sequestration | | Saline Reservoir CO ₂ & H ₂ S Co-sequestration | | Venting Concerns (See Section 3.0) |
|------------------|--------------------------------------|-----------------------|---------------------|-----------------------|---------------------|--------------------------------|---------------------|--|---------------------|---|
| | | Conceptual Design | Range in Literature | Conceptual Design | Range in Literature | Conceptual Design | Range in Literature | Conceptual Design | Range in Literature | |
| CO ₂ | vol% (Min) | 95 | 90-99.8 | 95 | 90-99.8 | 95 | 90-99.8 | 95 | 20 - 99.8 | Yes-IDLH 40,000 ppmv |
| H ₂ O | ppmv | 500 | 20 - 650 | 500 | 20 - 650 | 500 | 20 - 650 | 500 | 20 - 650 | |
| N ₂ | vol% | 4 | 0.01 - 7 | 1 | 0.01 - 2 | 4 | 0.01 - 7 | 4 | 0.01 - 7 | |
| O ₂ | vol% | 0.001 | 0.001 - 4 | 0.001 | 0.001 - 1.3 | 0.001 | 0.001 - 4 | 0.001 | 0.001 - 4 | |
| Ar | vol% | 4 | 0.01 - 4 | 1 | 0.01 - 1 | 4 | 0.01 - 4 | 4 | 0.01 - 4 | |
| CH ₄ | vol% | 4 | 0.01 - 4 | 1 | 0.01 - 2 | 4 | 0.01 - 4 | 4 | 0.01 - 4 | Yes-Asphyxiate, Explosive |
| H ₂ | vol% | 4 | 0.01 - 4 | 1 | 0.01 - 1 | 4 | 0.01 - 4 | 4 | 0.02 - 4 | Yes-Asphyxiate, Explosive |
| CO | ppmv | 35 | 10 - 5000 | 35 | 10 - 5000 | 35 | 10 - 5000 | 35 | 10 - 5000 | Yes-IDLH 1,200 ppmv |
| H ₂ S | vol% | 0.01 | 0.002 - 1.3 | 0.01 | 0.002 - 1.3 | 0.01 | 0.002 - 1.3 | 75 | 10 - 77 | Yes-IDLH 100 ppmv |
| SO ₂ | ppmv | 100 | 10 - 50000 | 100 | 10 - 50000 | 100 | 10 - 50000 | 50 | 10 - 100 | Yes-IDLH 100 ppmv |
| NO _x | ppmv | 100 | 20 - 2500 | 100 | 20 - 2500 | 100 | 20 - 2500 | 100 | 20 - 2500 | Yes-IDLH NO-100 ppmv, NO ₂ - 200 ppmv |

Figure 44 CO₂ stream compositions recommended limits. (Herrom & Myles, 2013)

Some of the recommended limits are based on toxicity of the substance, for example in case of CO and H₂S that become dangerous if released with CO₂, and for SO₂ and NO_x, whose design values correspond to their IDLH limits. For most components, the minimum and maximum concentrations only represent the range of values found in literature and not a recommended limit proposed by NETL. Some values reported as conceptual design limit of a substance match the most restrictive constraint found in literature.

No internationally accepted standard for composition of CO₂ mixture exists, so a link between Dynamis, Kinder Morgan, Ecofys specifications and other governmental project results is needed. This process's aim is to identify a required level of CO₂ quality, taking into account all the other components of the stream and their possible effects on the CCUS system, in order to develop a more specific risk assessment.

It is also clear that following Dynamis specifications does not ensure that in each condition the impurities will not be able to drive the long distance toxic risk. As a result of it, it has been proved that 100 ppm of H₂S, in FutureGen project defined stream, are able to generate larger risk contours than released CO₂, even if the stream content matches the design value (see figure 44) and the Dynamis specifications (see figure 43). Once the CO₂ impact has been defined, analysis of damage caused by impurities is recommended.

10. Secondary engineering hazards

Even if installations near the inventory are designed to resist very low temperatures, they could be damaged by some secondary hazards associated with specific characteristics of the released plume.

The composition of the transported stream and its behavior during discharge and dispersion phases need to be better understood, to assess vulnerability of exposed materials and structures. Knowing the characteristics of the stream during releases, for CCUS projects, the selection of sealants, instruments, electrical systems, safety-critical components and nearby installations should be done considering, not only the intense cooling effect obtained in the release area, but also all possible damages caused by other secondary engineering hazards (Podger, 2006) (Crivellari, Pelucchi, Ramus, Rossi, & Hantig).

Specific data about the CO₂ stream effects on materials, considering all impurities, are not available, but the following secondary engineering hazards may be evaluated in order to know their influence on equipment vulnerability.

The use of dry-ice for heavy-duty surfaces scouring reflects the potential for released solid CO₂ to cause erosion and serious structural damages to nearby structures and instruments. The release of solid CO₂ particles can be an issue because of their low temperatures and high mass and velocity values reached during the leak, able to create damages to the hit surfaces. The generated solid particles may be considered as high velocity projectiles that could damage systems, acting as initiating events of a ductile failure or a brittle one, in case of cryogenic embrittlement of materials. Due to the fact that CO₂ discharged stream is characterized by different percentages of different impurities, some of them could combine with solid CO₂ to form particles with greater abrasive capability than solid CO₂ alone. This effect, called dry-ice "grit blasting", may cause erosion of pipelines and equipment near the area of the release event, with a combination of thermal and kinetic action. The solid CO₂ formation is dangerous also for relief system, causing: the valves blockage with consequent pressure build up, the embrittlement with consequent loss of containment and the erosion of valves and pipework not properly coated.

When a material is exposed to a CO₂ stream, the most relevant effects are the low temperature embrittlement and the consequences of collision with erosive solid CO₂ particles. When the release is arrested and the cold plume is dispersed, the area affected by the precipitation of solid CO₂ particles can be exposed to a huge concentration of CO₂ and impurities, after the sublimation at ambient conditions. In general, the high concentration of vapor CO₂ in air is able to reduce the performance of internal combustion engines, causing their stoppage. This can also be a serious hazard for power electrical generators or air compressors near the

release zone, but also for vehicles, ships and aircrafts. The CO₂ percentage able to stop engines depends on different aspects of design and management of them, but more precise considerations are needed in case of emergency generators, fire trucks or ventilators.

Emitted vapor CO₂ also attacks lubricants and in general non-metallic materials, changing properties or damaging them, causing jamming of blocks and rotating equipment near the release area. Apart from the cryogenic embrittlement resistance, the chosen elastomers have to show good performances also in contact with vapor CO₂ and impurities, transported by the jet and dispersed after the localized sublimation of solid bank. Especially petroleum based and synthetic greases are deteriorated by CO₂. Among elastomers, nitrile, polyethylene, fluoroelastomers, chloroprene and some ethylene-propylene compounds have to be avoided. In general, it is important to select materials able to operate in contact with CO₂ and impurities at different temperature and pressure conditions.

The hydrate formation is a possible secondary effect of a localized dispersion of carbon dioxide. The CO₂ hydrates are the result of interaction between free water and carbon dioxide, white material that seems like snow and that can cause the blockage of needed instruments, with consequent safety issues. Some studies have been conducted on the conditions needed to generate hydrates. Hydrates are a confirmed problem if gaseous CO₂ and free water can enter in contact, for example after a consistent leakage of CO₂. The following figure shows the dark region for which hydrate coexistence with solid water and gaseous CO₂ is possible. Above the highest quadruple point (10.5°C and 4.41MPa) no CO₂ hydrates can be formed (Annesini, Augelletti, De Filippis, Santarelli, & Verdone, 2013).

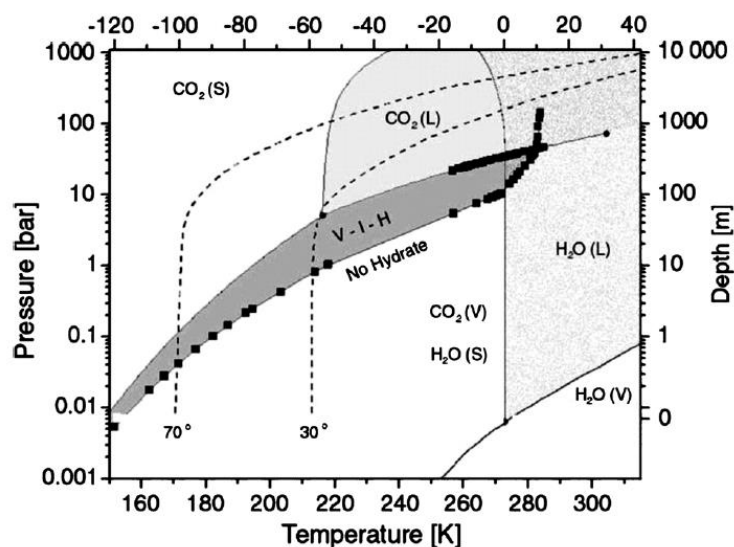


Figure 45 CO₂ hydrate phase diagram. Abbreviations: L - liquid, V - vapor, S - solid, I - water ice, H - hydrate. (Mike Bilio, 2009)

Within the cold plume, the interaction between released gaseous CO₂, impurities and free water can determine the enhancement of some chemical and physical phenomena. Even if in transported supercritical/liquid CO₂ no free water is present, in the vapour phase, the trapped atmospheric water and impurities could interact, generating CO₂ hydrates from which the formation of carbonic acids occurs. Sulfuric and nitric acids, produced by some impurities present in released stream, such as SO_x and NO_x and H₂S, increase deterioration rate of materials (Holt, 2020).

Corrosion could only occur after a prolonged exposure to CO₂ and impurities. This condition may be representative of a not arrested dry-ice bank sublimation, potentially able to expose materials to a denser-than-air CO₂ plume for days after the release event.

Increasing the temperature, the corrosion speed decreases due to the formation of protective FeCO₃ and reduced substances solubility. In addition, the corrosion rate changes depending on the involved phase of water. In

presence of water vapor, the corrosion is slower than in presence of water in its condensed state (Cabrini, Lorenzi, Marcassoli, Pastore, & Radaelli, 2012). Corrosion could be a secondary hazard for structures not originally designed for CCUS applications and for components coated with anti-corrosive materials that, after a release, will lose their protective external layer due to low temperatures and erosive particles attack.

When hydrogen is present as impurity in CO₂ stream, the H₂ embrittlement of structures can occur. In these conditions, the consequent ‘Hydrogen Stress Cracking’ effect determines the crack initiation or the growing of a subcritical crack, able to cause the failure of the affected components. In case of a CO₂ prolonged release from deposited banks, the generated cloud could be characterized by a huge amount of hydrogen, depending of the origin of the CO₂ stream itself. In these conditions, when the pipelines, valves and infrastructures near the release point are surrounded by the CO₂ cloud, their embrittlement may be obtained. This can be avoided choosing more resistant materials, such as steel with a lower sulfur content or higher nickel percentage (higher than 12.5%) (Jacob Leachman, 2019). Hydrogen embrittlement is promoted by high impact pressure, otherwise the H₂ is not able to attack materials. In addition, at low temperatures registered during a carbon dioxide release, the slowed chemical reactions and the enhanced chemical barriers may reduce the severity of the H₂ attack.

11. Summary of proposed vulnerability thresholds

In the previous Chapters, physical effects of a CO₂ release have been discussed in terms of consequences and impact on human health and surrounding structures. The extent and behavior of these phenomena may be summarized as follows.

Starting from the first seconds after the supercritical CO₂ release, in the near-field, one of the first considered effects is the physical blast and all the direct and indirect consequences of an exposure to the obtained overpressure peak. It can be affirmed that even for large-scale inventories, dangerous overpressure values may be reached only in the proximity of the release and consequently the risk results to be dominated by the CO₂ toxicity. At Energy Institute’s imposed vulnerability thresholds, according to TNO and UK HSE standards, no mortality caused by direct blast effects is expected. Only issues connected with the rupture of the ear drum can be associated with the highest proposed overpressure limit of 689 mbar. In general, the Energy Institute’s thresholds are a conservative result of the superposition of all possible direct and indirect blast effects.

Increasing the duration of the exposure, in the proximity of the release point, the CO₂ toxicity has to be taken into account. Different areas with different percentages in volume of CO₂ can be defined. The toxicity of inhaled CO₂ and the connected asphyxiation are able to cause death starting from a value of 10% of carbon dioxide in the cold plume, in which people may be engulfed. Apart from the peak value of CO₂ concentration, the lethality and the provoked health effects also depend on the duration of the exposure, that can be easily increased if the cognitive, muscular and manual performances are reduced. For this reason, the impairment of escape routes has to be determined.

For a QRA and EERA assessment, the low temperatures distribution, generated by the fast depressurization during a release, has to be considered. It is known that, inhaling air at temperatures in between -40°C and -70°C, damages to the respiratory system may be reported in few minutes, inducing a ‘cold-shock’ and a cardiac arrest in vulnerable people. If the whole body displacement, caused by exposure to overpressure, is coupled with the possibility of contact with cold surfaces, risk of cold burns has to be evaluated. Also the lack of visibility within the cold plume can increase the duration of exposure, limiting the possibility to escape. Changing the parameters of the discharge, the generation of limiting fog may occur for different values of CO₂ percentage in the cloud. In fact, the visible plume is not representative of the danger connected with toxicity.

For each discussed hazards, a literature analysis has been conducted to identify proper vulnerability models for individuals and materials. Here, the main results of this analysis are summarized.

In general, vulnerability of people linked with inhaled CO₂ concentration, cryogenic conditions and generated overpressure may be evaluated considering significant thresholds or probit functions. Existing probit methods may be applied to consider toxic and asphyxiating effects of CO₂. The UK HSE 2011 probit correlation results to be the most used in literature and a good compromise between too optimistic (Lievense, TNO) and too conservative (Tebodin) proposed functions. Assuming the UK HSE criteria (OSD3.2, January 2006), for each hazard, two different limit values may be defined, one representative of 1% of lethality and the other one associable with the 50% probability of death. For toxic hazard of CO₂ inhalation, the LC1 and LC50 thresholds may be extracted from the HSE chosen probit function.

When no probit functions have been found in literature to consider the consequences of physical effects of a CO₂ release, the thresholds method may be applied. For exposure to low temperatures, the 1% and 50% estimated fatalities have to be evaluated from literature examples. Data about limit temperature values and time after which frostbit and hypothermia occur may be exploited. The chosen thresholds for subzero temperatures exposure could be obtained from medical literature and studies about consequences on workers in critical environmental conditions. Values of temperature for an exposure in the range of 5-30 minutes could be collected. To evaluate the effects of an instantaneous overpressure obtained after a CO₂ release, Energy Institute's 0% and 100% mortality thresholds, may be used. Summary of proposed fatality criteria is reported in the following table.

Table 13 Proposed fatality criteria

| Hazard | 1% fatality | 50% fatality |
|------------------------------|-----------------------------|-------------------------------|
| Cloud temperature [°C] | -18 (30 min) -26 (5 min) | -34 (10 min) -40 (5-7 min) |
| Carbon Dioxide [%] | 7 (30 min) 8 (5 min) | 10 (10 min) 11 (5 min) |
| | 0% fatality | 100% fatality |
| Overpressure [bar] (outdoor) | 0.069 (instantaneous) | 0.689 (instantaneous) |

In particular conditions some secondary effects cannot be neglected. First of all, toxic impurities inside the CO₂ stream can represent a danger. For example, H₂S can be life-threatening above a value of 50 ppm, while CO, an irritant gas, is able to affect the upper part of the respiratory system and cause death for a concentration of about 700 ppm. For this reason, some proposed limits can be adopted, so that the effects on human health of these substances cannot be more severe than that evaluated for the inhalation of the corresponding concentration of CO₂. The optimum composition of the stream and concentrations of the impurities requires a balance between different technological requirements, cost and safety implications. For this reason, the Dynamis project stream specification is usually adopted for CCUS applications. Also the impact with solid CO₂ particles may determine the impairment of people, if considered as fragments and debris or if ingested, but deeper evaluations about mass and velocity are needed. In order to define vulnerability thresholds for these secondary consequences, the knowledge about oil and gas industrial explosion events can be exploited, considering the potential interaction between CO₂ and other released substances.

Once considered the cold plume effects on human health, the cryogenic embrittlement of metals and the degradation of polymers and sealants could be analyzed. The temperature profile in the dispersion area may be used to identify the distance at which equipment and neighboring sensible parts of plant are damaged by generated subzero temperatures.

The design and the evaluations about vulnerability for CO₂ facilities, and pipelines in particular, can follow the DNV proposed general guidance (DNV-RP-J202, April 2010). Nevertheless, the Minimum Design Metal Temperature of -100°C is usually applied for cryogenic CO₂ application in the selection of materials for plant components. Once designed metallic and structural components, limit operating temperatures for more vulnerable equipment types may be proposed. In the following table temperature thresholds for parts of safety

system and insulators are reported, in order to define a safety distance between components and potential release points.

Table 14 Some vulnerability thresholds for safety system materials. Temperatures in breakers refer to advanced technologies for cryogenic applications.

| Equipment type | Limit cloud temperature |
|----------------------------------|--------------------------------|
| PVC insulation | -15°C |
| Silicon rubber insulation | -60°C |
| Electric motor | -20°C |
| Thermal-magnetic circuit breaker | -25°C (-40°C advanced) |
| Ex-d enclosure | -50°C |
| HID lighting (escape routes) | -30°C |
| LED lighting (escape routes) | -30°C (-55°C advanced) |
| BDV and SDV | -30°C |

If materials can resist low temperatures (from about -20°C to -80°C) or these dangerous cryogenic conditions are not reached during the release, secondary engineering hazards may still occur. Hydrates and solid CO₂ particles can determine the plugging of critical components. Formed dry-ice and impurities present in the stream are able to enhance erosion of surfaces invested by the plume. In general, it can be affirmed that for assessing the effects of a CO₂ plume on equipment near the release point, the considered hazards have to be effective after a duration in the range of 5 to 30 minutes, time applied for a QRA and EERA.

Degradation of materials in contact with the released plume can cause severe consequences to people, generating the starting point for an escalation of dangerous events. For this reason, the cryogenic embrittlement of metals and degradation of sealants, the erosion and the blockage of safety systems both caused by solid CO₂ and the stoppage of combustion engines are all aspects whose impact needs to be evaluated, starting from common industrial and hydrocarbon database, exploiting specific information coming from experimental CCUS projects.

12. Application to the case study

In this section, the results about vulnerability and impairment thresholds for individuals and equipment are applied to a case study, a prototype of an Allam cycle plant. The scope is to identify the safety distances obtained considering consequences of different physical effects of accidental release of a gaseous, liquid or supercritical CO₂ inventory. The analysis will be divided in different chapters:

- In Chapter 12.1., the Allam cycle will be described, by focusing on its three main parts: Air Separation Unit (ASU), CO₂ Purification Unit (CPU) and Power Brayton cycle.
- In Chapter 12.2., the used methodology will be reported. Firstly, the parameters of the simulation conducted through DNV GL software Phast 8.23 will be discussed. Fixed inputs, used to model mixtures properties and stream behavior during discharge and dispersion phases, will be defined. In this Chapter the system modelling will also be described, by focusing on definition of simulated release scenarios. Data used for the plant modelling will be taken from the Process Flow Diagram (PFD) extracted from documentation about Eni's previous activities on Allam cycle prototype. Finally, the methodology used for post-processing of outputs of the simulation will be defined.
- In Chapter 12.3, outputs of the simulation will be reported. Results of the conducted sensitivity analysis will be presented, focusing on the influence of chosen release direction, storage conditions, turbulence mechanism and averaging time on characteristics of dispersed plume of CO₂. Additional considerations about temperature and solid fraction within the plume before and after the atmospheric expansion will be obtained. The concentration and temperature distribution during dispersion are the

main outputs of the simulation. The damage areas obtained applying vulnerability thresholds to these results will be compared, identifying the most critical component of the plant. Consequences of supercritical CO₂ release will be finally compared with those of a release of CH₄, also processed in the Allam cycle plant.

12.1. Allam cycle description

The Allam-Fetvedt cycle plant is an oxy-fuel semi-closed Brayton cycle which uses supercritical CO₂ as working fluid. It includes a natural gas combustor fed by a mixture of high-purity oxygen stream and recycled CO₂. As a NET Power cycle it results to be a competitive option to CCS post-combustion applications on typical gas-fired power plants. According to a technical and economic analysis conducted during the IEA Greenhouse Gas R&D program, this kind of cycle is able to reach an efficiency of about 59%, higher than that obtained from a new generation post-combustion capture process that uses amines as solvent (52%). Due to high efficiency, the NET Power cycle shows the best economics among other CCS solutions and a cost of CO₂ avoidance similar to that of an amine-based post-combustion process (Ferrari, et al., 2016).

As an oxy-fuel supercritical CO₂ plant, the Allam cycle, reaching high purity level of used oxygen, is able to avoid the formation of nitrogen oxides in produced fumes. In addition, the high degree of heat recuperation of the regenerative heat exchanger reduces the net energy required for the process, also re-using the hot air released from the Air Separation Unit (ASU) compressor. Another characteristic that increases the efficiency of the Allam cycle is the use of supercritical fluid that reduces the plant footprint and dimensions of equipment, leading to a significant drop in investment and operating and maintenance costs of plant.

A simplified Process Flow Diagram (PFD) of the cycle is reported in figure 46, from which also the pressure and temperature values, for inlet and outlet flows from the main components of plant, are taken. A more detailed PFD is reported in Appendix B in order to obtain information about single components and precise configuration of the ASU, CO₂ Purification Unit (CPU) and power cycle.

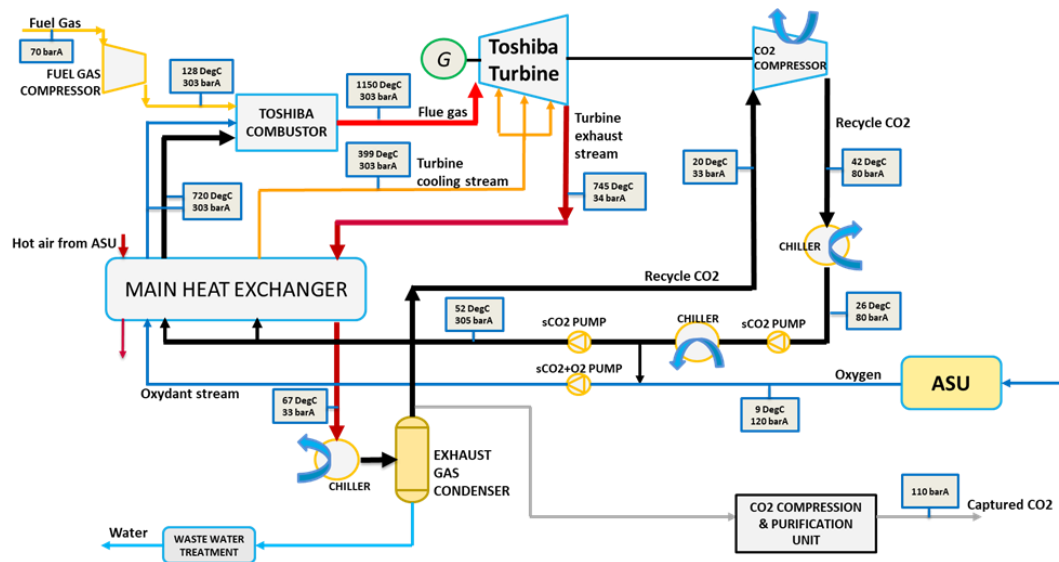


Figure 46 Simplified PFD of Allam Cycle

THE ASU SYSTEM

The cryogenic separation of air is an energy expensive process that requires to reach very low temperatures (-195°C). In the Allam cycle the double column ASU system is used. In the Air Separation Unit air is compressed from ambient pressure to 120 bar through the three-stage main air compressor and the four-stage booster air compressor, that acts on more than 53% of the total processed air (Chaturvedi, Kennedy, & Metew,

2021). From the main compressor air at 5.9 bar reaches the first column. Here the separated liquid part is extracted and conducted to the second column, where due to Joule-Thomson effect, the deposition of oxygen-rich liquid at the bottom of the column occurs. The system may produce a 99.5 mol% O₂ stream with a rate of 159301 kg/h.

The heat released from the intercoolers of main and booster compressors is used to heat the recycle CO₂ stream in the heat exchangers E-602, E-603, E-604 and E-605. This low temperature contribution compensates the imbalance between the heat released by the 34 bar exhaust gases coming from turbine and that needed for heating the 303 bar recycle CO₂ stream. Due to the high temperatures of the power cycle, the ASU system needs an additional cooling flux of water that allows stream of the intermediate stages of compression to reach required low temperatures (Chaturvedi, Kennedy, & Metew, 2021). Even if heat exchange increases the power consumption of the compressor, the net effect is positive, thanks to the reduction of fuel energy input.

THE CPU SYSTEM

The low temperature CO₂ purification unit is necessary to follow the purity requirements of the exported flow. Starting from the exhaust gas condenser (ET-100), a CO₂-rich stream in between 106.28 and 108.68 t/h (5% of the total CO₂ flow) enters the coalescing filters, to reduce the percentage of H₂O and O₂, and reaches low temperatures able to remove other impurities such as N₂ and Ar. The obtained pure CO₂ stream (99.6-99.8%) is compressed from 28.9 bar to 110 bar and exported from the Allam cycle in supercritical conditions.

The volumetric compositions of the stream after coalescing filters and low temperature purification are known. After passing through filters, the stream is characterized by 98.4% in volume of CO₂, 0.13% of H₂O, 0.57% of O₂ and 0.9% of Ar. Only after low temperature purification the 99.8% of CO₂ may be obtained, limiting the water content to 100 ppm.

The removing of impurities implies a loss of a small percentage of pure CO₂ that reduces the capture efficiency. For a NET Power cycle, increasing the level of purity of the stream, from 97.9% to 99.8%, the effective amount of captured CO₂ may vary from 100% to 90%. As a result, the Allam cycle loss of purified CO₂ is about the 10% of the total. If higher percentage of capture and simultaneous low percentage of impurities are needed, a post processing of the vent gas may be done using a membrane unit (Ferrari, et al., 2016).

From the stream analysis it can be affirmed that the exported stream follows the Dynamis project specifications. In fact, the water presence is reduced below 100 ppm (less than limit of 500 ppm) and the percentage of CO₂ results to be higher than the minimum value of 95.5%. In addition, the sulfur derived components and the nitrogen oxides are not present in the stream, thanks to the chosen fuel and the adopted high level of oxygen purity.

THE POWER CYCLE

In the Allam cycle the natural gas combustion occurs in a Toshiba combustor (B-100) at 303 bar. The fuel enters at 128 °C and reacts with an oxidant stream, a mixture of pure O₂ and 41% of the total recycle CO₂ that reaches the combustion chamber at 720°C, once heated in the main heat exchanger. The 48% of the remaining part of recycle CO₂ is used as diluent for oxidant stream. The dilution with CO₂ is needed in order to reduce the theoretical high temperatures reachable with a pure oxy-fuel combustion, able to damage the combustor materials.

The fume's outlet temperature of 1150°C is the highest obtained during the entire cycle. The exhaust gas composed of H₂O and CO₂ enters the double shell turbine (GT-100) in whose cave, in between inner and outer

casing, a CO₂ stream at 399°C flows in order to reduce the turbine blades' superficial temperature. This cooling stream, the 11% of the recycle CO₂ not mixed with oxygen, comes from the low temperature end of the main exchanger. The critical turbine conditions are possible thanks to the nature of the supercritical CO₂ that results to be non-flammable and less corrosive than typical stream. Due to physical properties of the processed flow, the chosen turbine is a hybrid between steam and gas turbine.

The expanded fumes enter the exchanger, transferring heat to over mentioned cooler streams and starting the condensation process. Thanks to a mixer and a coalescing water separation (FT-100), a low water content CO₂ stream is obtained. The 5% of this product is exported and purified, in order to preserve the cycle mass balance. The 95% is brought up to 80 bar through a three-stage intercooled compressor (C-200). When refrigerated at 26°C, the recycle dense CO₂ is pumped, reaching 120 bar (P-400). After the separation of the 41% of the stream, the remainder is pumped until 305 bar and 52°C (P-200), conditions at it which enters the three-section multi-flow heat exchanger.

12.2. Methodology

Through the PFD of the plant prototype, possible release points have been identified. Description of physical effects of these releases has been obtained from the analysis of consequences conducted with software Phast 8.23. The parameters of the simulation have been set with the aim of collecting reliable data about concentration and temperature distributions near the release point.

Once defined proper discharge and dispersion simulation parameters, the influence of variable release and storage conditions has been assessed, in order to identify conditions able to generate the longest damage distance. This has been possible thanks to the application of temperature and concentration lethal values reported in Chapter 11. When software's limitations make it impossible to properly estimate characteristics of released plume, some assumptions have been done to exploit Phast's outputs without overestimating or underestimating the entity of the associated damage. Additional analysis has been proposed to evaluate effects of a CH₄ release from compressor of the Allam cycle plant.

12.2.1. Modelling with Phast 8.23

Firstly developed for oil and gas industries, Phast is able to model discharge, dispersion and release consequences of a large database of explosive, flammable and toxic materials. The evaluation of release effects on the area surrounding the leak source may be exploited during design and operation of the plant, proposing modifications and mitigation measures.

The different CO₂-rich streams that characterize the Allam cycle have been modelled as toxic mixtures. For the modeling of CO₂ properties and behavior during discharge and dispersion phases, some assumptions may be done, in accordance with the Phast's ability to describe supercritical CO₂ releases.

The Phast workspace is organized in different tab sections within which simulation's input data can be inserted: Models section, Weather section, Parameters section, Materials section and Map section. All these tabs are part of the Study Tree pane. In this Chapter, the proper setting of "Parameters" section is discussed.

COMPONENTS AND MIXTURES MODELLING

For modelling the Allam cycle through Phast 8.23, the carbon dioxide-rich stream, the exhaust fumes and the oxidant stream have to be defined as mixtures of different substances, according to the "pseudo-component" (PC) model. This approach consists in associating to the mixture the thermodynamic behavior of a pure component, whose properties are an average of all contained substances.

The chosen pseudo-component method preserves the mixture composition during each stage of the release, so, as a pure material, the dispersed cloud has the same composition of the original stored stream. This method, preferred to describe the carbon dioxide releases, is not representative of the real two-phase mixture behavior.

In fact, the PC model does not consider that the liquid part contains higher percentages of heavier components while the vapour one is rich in less dense substances.

A more precise multi-component (MC) approach is able to follow the changing of equilibrium composition of the liquid and vapour coexisting phases. However, when a MC configuration has been used for modelling heavy CO₂, even if the rainout is set by user as a possibility, the results are inaccurate and the simulation fails due to convergence problems. This is due to the fact that the solid generation at the orifice plane is expected by the software for CO₂ releases, but the multi-component modelling is not able to consider it. In fact, for modelling of supercritical CO₂, a heavier than air and non-volatile stream for which the rainout significantly changes the dispersion results, the PC model has been preferred, even if it produces significant errors in the prediction of temperature and composition of the two-phase stream, during discharge and dispersion modelling (Witlox H. , Harper, Topalis, & Wilkinson, 2005).

The properties of simulated materials have been evaluated according to the default “PhastMC” template. Pure CO₂ and other streams may be defined choosing between “Components” and “Mixtures” options (Harper & Witlox, 2017). Some properties of a mixture or a component such as enthalpy, entropy and density cannot be calculated from a database, but they are obtained from equations of state. These “derived properties” are calculated by Phast through the XPRP property system. The XPRP consists of three sections. The first one contains the phase equilibrium algorithm, the second section sets the pure components properties from the DIPPR database and the last one derives mixture thermodynamic characteristics (Stene J. , 2020).

DISCHARGE AND ATMOSPHERIC EXPANSION MODELLING

In “Parameters” tab section, options used for modelling of release scenarios are set as shared parameters for all “Models”. In the “Discharge parameters” sub-section, the inputs of DISC and ATEX Phast models have been defined.

With Phast it is possible to model continuous or instantaneous dispersion from a short pipe or vessel. The discharge from a vessel may be a leak from an orifice or a catastrophic rupture. When the rupture of a vessel has to be modelled, the continuous discharge of substances is described through the so called DISC model, considering a constant or model-calculated flow rate. In general, this DISC approach describes steady-state release, while the TVDI model follows a time-varying process.

The input parameters for DISC orifice model are mass or volume of inventory and initial temperature and pressure values within the storage. Also the orifice dimensions have been set, considering that all the mass in the vessel is released from the defined area (Stene J. , 2017). The outputs of the discharge simulation are the stream conditions at the orifice plane and the release duration, data that become input for atmospheric expansion model (ATEX). This model may describe the evolution of instantaneous or non-instantaneous releases. The ATEX approach models the behavior of released toxic or flammable materials during the expansion, from pipe or vessel orifice plane to conditions for which atmospheric pressure is reached. The ATEX outputs are used as input for the Unified Dispersion Model (UDM) for toxic components, and for jet-fire model for flammable ones. In general, at the orifice the thermodynamic equilibrium is obtained, exception done for liquid release, for which metastable condition is preserved. The ATEX results are: area of the jet, temperatures, liquid fraction, density, enthalpy and velocity of the stream before dispersion. Thanks to this model, the “conservation of momentum” and the “isentropic” expansion methods may be applied.

The “conservation of momentum” uses equations of state, for the density and enthalpy definition, and conservation of mass, energy and momentum, for evaluation of mass flow rate, equivalent diameter and speed at equilibrium plane. The “isentropic” model uses the conservation of entropy instead of that of momentum. Another expansion approach can be selected in Phast as “results closest to the initial conditions”. This model chooses the conservation equation that better preserves initial temperatures.

In general, the “conservation of momentum” is applied to modelling of vapour releases with no liquid fraction and to all CO₂ releases, because of the assumption that solid deposition cannot occur. In fact, for both high pressure gas jets and flashing liquid jets, the “conservation of momentum” approach gives better prediction of concentrations of toxic substances, if rainout is assumed to not occur. This assumption may also be applied for two-phase flashing releases, even if the consistent rainout will affect the accuracy of results. As a result, to better predict concentration distribution of the two-phase expected release of CO₂, the “conservation of momentum” option has been chosen, obtaining results about jet characteristics at atmospheric pressure.

In addition, in order to fit experimental results according to which the solid formation inside the pipeline or vessel is a confirmed consequence of supercritical CO₂ rapid expansion, the “Allow phase change (equilibrium)” approach has been selected in the “Discharge parameters” section. Within discharge section also the droplet mechanism needs to be set. For simulation of the Allam cycle case study, the “Do not force correlation” and “Mechanical correlation” options have been used, as required by Phast warnings, depending on initial conditions of simulated release scenario.

DISPERSION MODELLING

The “Dispersion parameters” sub-section allows to fix parameters needed to evaluate CO₂ concentration and its variability in time and space. Through the Unified Dispersion Model (UDM) correlations, the dispersed plume characteristics have been obtained, with particular attention to percentage of CO₂ and reached low temperatures.

The UDM describes the jet dispersion, the droplet evaporation with possible rainout, the possible pool vaporization, the heavy gas dispersion and the final passive dispersion. The UDM may be used to describe continuous, instantaneous, time-varying or constant releases. The aim is to generate a continuous profile without discontinuities and evident transitions between the different stages of the modelled process.

The UDM model can be applied to ground level or elevated pressurized releases and it is also able to model pure CO₂ releases, describing the solid formation within the jet. The method accepts solid formation only for carbon dioxide and uses liquid aerosols for all the other materials. This is possible thanks to the DIPPR database of CO₂ properties that defines a fictional phase with liquid or gaseous characteristics depending on temperature. According to DIPPR, when material’s triple point pressure is higher than ambient pressure (as for CO₂), the triple point temperature is used as limit value between possibility of a solid-vapour or liquid-vapour equilibrium. When expanded to atmospheric conditions, the CO₂ is below its triple point and, for this reason, no liquid but only a solid-vapour mixture can be obtained. Consequently, at atmospheric pressure the software considers solid CO₂ each time that “liquid” adjective is printed as result. In the “Liquid” section of “Dispersion parameters”, the “No rainout, equilibrium” droplet evaporation model has been selected, in accordance with the chosen PC modelling of CO₂.

Starting from equilibrium plane, the dispersion model traces the cloud behavior from the near-field to the far-field, according to the presence of different vertical profiles of wind and atmospheric characteristics, contained in the same model. The 8.0 version of Phast also incorporates in its dispersion model the along-wind diffusion (AWD) and the gravity-spreading effects, in order to improve footprint estimations. For near-field and far-field dispersion models, the default parameters have been used during the simulation. However, in “Far-field” section the criterion for stopping dispersion calculations may be changed. In general, the dispersion calculations continue until the dangerous toxic load, imposed in “Material” tab section, is reached. The simulation has also been forced to give results for lower concentration values, expanding the modelled dispersion zone, according to a “Concentration of interest”. The lowest useful concentration has been set to 40000 ppm, if the IDLH distance has to be evaluated, and to 15000 ppm, if the STEL distance is needed. Without any fixed “Distance of interest” only one stopping criterion has to be met during the simulation.

12.2.1.1. DISC, ATEX and UDM models validated on CO₂ releases

The Phast modelling of CO₂ behavior during discharge and dispersion phases was validated during the CO2PIPETRANS project, by comparing the simulation results with experimental ones about a flashing two-phase jet (Witlox & Stene, 2015).

The Shell and British Petroleum (BP) experiments have been analyzed as part of the CO2PIPETRANS validation project. The experimental tests consist on steady-state or time-varying liquid releases and on time-varying supercritical releases from a vessel connected with a pipework. The leakage is simulated through a nozzle along the pipeline with variable diameter, through which horizontal non-impinging releases occur.

Even if not all default Phast parameters are changed to fit the experimental setup, the software models result to be accurate. The predicted flow rates have an accuracy within 10%, while the concentration footprints obtained from UDM result to be more compatible with the BP and Shell experimental results. The distribution of temperature at the release area is well predicted if the Peng-Robinson equation of state (PR EOS) is used, especially for values near the critical temperature (31.06°C) during Shell tests. The steady-state orifice release is modelled with DISC method, while for time-varying ones the TVDI is used. In this last case, the BP flow rate results refer to 20-second averaged values, while for Shell comparisons the initial value is used.

The first aspect analyzed is the possibility of modelling with Phast the flashing of liquid inventory during the discharge and the expansion from storage to orifice plane. Setting a non-equilibrium model, the liquid expansion generates a pure liquid phase at the exit, without any changing between storage and orifice conditions. On the other hand, if flashing is allowed by user, the equilibrium at the orifice is obtained and the phase changing may occur even before the release plane. During the Shell and BP validations, the flashing condition is allowed, considering the possibility of phase changing before the orifice plane. In particular, using PR EOS in Shell tests the difference in results between flashing and non-flashing option are not so evident. On the other hand, when used the default density option of saturated liquid, as for BP validation, the flashing option gives more accurate results.

When the parameters of the atmospheric expansion have to be set, the “DNV GL recommended” option chooses between isentropic and conservation of momentum. According to CO2PIPETRANS validation (Witlox, Harper, & Oke, 2012), the software recommended option is always the isentropic one, exception done for gaseous inventories, for which the default model assumes the conservation of momentum. Consequently, in order to fit the BP and Shell experimental results, the “conservation of momentum” has to be set.

During the validation, the AWD model is used to describe the entrainment of air, calculating concentration values at the center-line. Thanks to the inventory high pressure and CO₂ low sublimation temperature at 1 bar (-78°C), the model predicts the mixing with air through a homogeneous equilibrium that results in no rainout. In fact, as demonstrated through experimental results, the solid CO₂ particles sublime within the cloud. In conclusion, solid deposition and delayed sublimation of the bank are never considered by the UDM for CO₂ applications, that, using a solid-vapour equilibrium model, matches the experimental observations.

During BP and Shell experiments, the entity of the dispersion is analyzed measuring the CO₂ concentration at downstream (from 5 to 80 meters) and cross-stream (from -20 to +20 degrees) different distances, through O₂ sensors. As already said, comparing these results with the Phast predicted concentration values, a good compatibility is found, especially for near-field evaluations. In the far-field, where results are more affected by wind speed, some differences are detected. In fact, according to Phast UDM the release direction overlaps the wind direction, while in experimental conditions there could be a consistent deviation (Witlox, Harper, & Oke, 2012).

12.2.2. System modelling

In order to perform the analysis of consequences for the Allam Cycle, the plant is modelled through the characterization of some points for which thermodynamic conditions are known. Each of these interest points

corresponds to the inlet or the outlet section of plant's components described through values of temperature and pressure, as reported in the process flow diagram. Only points for which all necessary data are available have been simulated, exception done for purified CO₂ storage tanks (T100) that have been defined through known value of pressure and estimated value of temperature, compatible with common supercritical transport conditions.

The running of calculations has been performed for each scenario representative of a dangerous release of CO₂ from modelled components of the plant. Results for different weather conditions may be obtained in form of graphs or organized reports. In case of carbon dioxide modelling, the dispersion and toxic default graphs are plotted, but also the "Graph Wizard" tool may be exploited to investigate additional correlations. The same data are visible on the map of the plant, where the "shape only" and the "effect zone" plot option can be chosen to represent the cloud footprint, as consequence of the release. When the "Report" tool is used, discharge, dispersion and toxic reports may be exported for each scenario for post-processing of results.

In this Chapter the setting of "Map", "Weather", "Materials" and "Models" sections is described.

MAP AND WEATHER SECTION

The first step of the system modelling is the setting of the Map tab section. It is useful to obtain a scaled graphical representation of the plant, to define the plant boundaries and to graphically represent the consequences obtained from the simulation. Due to the absence of detailed information about terrain type of the area, the default values have not been changed. Also the definition of buildings has been ignored, since the analysis of consequences for indoor populations and toxic effects of the deposited dense cloud inside building will not be carried out. At the same tab section, the map of the plant has been loaded in ".bmp" format, without any constraint about co-ordinate of the plant. Once scaled (1':30'), the map appears in the GIS Input window. Here, equipment that will be included in the study may be visible as dots in a user-defined location.

In the weather tab section, weather conditions, atmospheric parameters and substrate data may be modified. Results are plotted for each weather folder. In order to describe the level of turbulence in atmosphere, two Pasquill stability classes have been chosen for the simulation:

- Class 5/D: neutral, with little sun and high wind or overcast-wind night. Wind speed of 5 m/s, constant during release and dispersion.
- Class 2/F: stable, with reduced turbulence intensity, moderate clouds and light-moderate wind. Wind speed of 2 m/s, constant during release and dispersion.

Some site conditions have been added to atmospheric parameters, used for each stability class. The atmospheric temperature of 22°C and the relative humidity of 64% have been set according to project data (Fernandes, Wang, Xu, Buss, & Chen, 2019).

MATERIALS SECTION

Phast database contains a list of materials and their properties that can be selected to describe the streams of the Allam cycle. The following three streams have been defined in the simulation:

- **CARBON DIOXIDE**
In "Materials" tab section, this stream has been modelled as a "Pure Component" that represents the recycle CO₂, 97.25% of the total mass amount circulating in the cycle. Exiting the water separation filters and entering the compressor, its 41% will be mixed with purified O₂, while the remainder circulates in the main heat exchanger. The stream represents the working fluid, the turbine cooling

stream, the diluent for exhaust fumes in the combustor and part of the oxide mixture. The flow has been also used to describe the CO₂ exported from the plant and deposited in storage tanks.

The actual composition of the stream has not been simulated. Simplifying the calculation for definition of oxidant and exhaust gases, the recycle stream has been considered as 100% of carbon dioxide, neglecting other non-toxic elements.

In order to define toxicity of CO₂, the toxic flag has been activated for comparisons between Phast proposed lethality and concentration-distance results, obtained from the simulation. As toxic parameters, the “Dangerous Doses”, the “Dangerous Toxic Load”, and probit coefficients “A”, “B”, “N” have been defined. Due to the absence of CO₂ in DNV Green Book description, the HSE SLOT and SLOD values are used by “Phast”. The associated probit functions are:

$$- Y_{1\% \text{ lethality}} = 2.67 = A + B * \ln(\text{HSE SLOT})$$

$$- Y_{50\% \text{ lethality}} = 5.0 = A + B * \ln(\text{HSE SLOD})$$

The “A”, “B” and “N” coefficients result to be -90.778, 1.01 and 8 respectively. According to this correlation, the 0% of probability of death is associated by the program to a user-defined “Dangerous Toxic Load”, with concentration expressed in ppm and time in minutes. In order to perform dispersion calculations, also dangerous doses may be set in the “Materials” section. In particular, a concentration of 40000 ppm has been imposed as IDLH for 30 minutes of exposure, while 15000 ppm have been chosen to STEL for a duration of 15 minutes, according to limit values reported in table 1.

- **OXIDANT**

This flow has been modelled as a “Mixture” of pure carbon dioxide and oxygen, as result of mixing the 41% of recycle CO₂ and the rich-O₂ stream that comes from the Air Separation Unit. As for pure CO₂, the 159.30 t/h of separated flow have been considered pure O₂, thanks to a high reached purity of 99.5 mol% in the ASU.

When a mixture has to be set, the mass amount or the molar amount of constituents is needed.

Considering that 106.28 or 108.68 t/h, the 5% of the dehydrated CO₂, are exported from the plant, the recycle amount is of about 2064.92 t/h. Only 846.62 t/h of them are mixed with O₂, obtaining a flow of 2907.54 t/h.

The 159.30 t/h of CO₂ and the 846.62 t/h of O₂ are the mass amounts chosen to set the relative proportions for the oxidant mixture. Once defined the composition, the mixture properties have been calculated through the “Phast MC” model.

After the mixing, this modelled stream enters a pump, increasing its temperature in the main heat exchanger, in order to participate the combustion at proper thermodynamic conditions.

- **EXHAUST**

Also the exhausted fumes produced from natural gas combustion have been described as a “Mixture” in the “Materials” tab section. In Eni’s documentation about Allam cycle, due to adopted fuel purity, this stream is defined as mixture of H₂O and CO₂, without any other impurity as combustion product. For common oxy-fuel gas fired plants, only traces of CO, NO_x, SO_x and H₂S may be found in the produced stream. In this specific case, their presence has been neglected, considering the reaction between pure CH₄, O₂, and CO₂. Through stoichiometric reaction the produced fumes result to be composed by the same molar fraction of CO₂ and H₂O. Due to the fact that the program definition of mixture proportions is not dependent on used units, it has been decided to account 0.5 to each of H₂O and CO₂ molar amounts.

The exhaust mixture has been selected to analyze the cycle from the end part of combustor, until gas condenser, passing through the heat exchanger.

In this section the scenarios, accidental releases from different equipment, have been modelled. Three levels of the study have been configured: the “Workspace”, the “Study” and the “Equipment Items”.

In the “Workspace” inputs about graphs and reports have been set. In particular, the initial view time for dispersion graphs, useful for instantaneous releases, has been imposed at zero seconds, while for continuous releases the initial view time for dispersion graphs has been set at the end of release itself. In the “Workspace” more than one “Study” may be defined. In each of these subsections, the unique weather folder and the parameter set have been selected.

Once defined the shared characteristics, the initial conditions for each simulated event need to be defined. The scenarios can be modelled as releases from a “Pressure Vessel”. In this case, each analyzed part of plant has been added in the “Study” as a separated component, considered as pressurized containment of infinite mass, setting mass inventory at 1000 kg. Storage values of temperature and pressure correspond to conditions of streams entering or exiting Allam cycle simulated components.

During the setting of these parameters, some constraints cannot be overcome. For this reason, when the exhaust gas coming from the combustor needs to be modelled, the actual temperature of 1150°C has been limited to the upper value of 926.85°C (see table 15). All default limits reported in “Dispersion parameters” section cannot be modified.

Taking into account labels of components reported in the cycle PFD (see Appendix B) and the thermodynamic properties extracted from figure 46, the representative points have been simulated as “Pressure Vessel Items”. These elements have been located on the map of the plant as dots in correspondence of indicative inlet or outlet end of components. Data reported in the following table have been added in “Material” characterization for each “Model” tab section.

Table 15 Thermo-physical characterization of modelled points of the Allam cycle

| Vessel Code | Component | Material | Pressure [bar] | Temperature [°C] | CO ₂ Phase |
|-------------------|-----------|----------------|----------------|------------------|-----------------------|
| CO2cool_turb_in | CGT100 | Carbon Dioxide | 303 | 399 | Supercritical |
| CO2cool_exch_out | E102R | Carbon Dioxide | 303 | 399 | Supercritical |
| CO2exhgascond_out | FT100 | Carbon Dioxide | 33 | 20 | Vapour |
| CO2compr_in | C200 | Carbon Dioxide | 33 | 20 | Vapour |
| OXcomb_in | CGT100 | Oxidant | 303 | 720 | Supercritical |
| OXexch_out | E101D | Oxidant | 303 | 720 | Supercritical |
| CO2comb_in | CGT100 | Carbon Dioxide | 303 | 720 | Supercritical |
| CO2exch_out | E101C | Carbon Dioxide | 303 | 720 | Supercritical |
| EXcomb_out | CGT100 | Exhaust | 303 | 1150 → 926.85 | Supercritical |
| EXturb_out | CGT100 | Exhaust | 34 | 745 | Vapour |
| EXexch_in | T102 | Exhaust | 34 | 745 | Vapour |
| EXexch_out | T103 | Exhaust | 33 | 67 | Vapour |
| CO2export | T100 | Carbon Dioxide | 110 | 32 | Supercritical |
| CO2compr_out | C200 | Carbon Dioxide | 80 | 42 | Supercritical |
| CO2aftercool_in | E201 | Carbon Dioxide | 80 | 42 | Supercritical |
| CO2pump_in | P400 | Carbon Dioxide | 80 | 26 | Liquid |
| CO2aftercool_out | E201 | Carbon Dioxide | 80 | 26 | Liquid |
| CO2recpump_out | P200A | Carbon Dioxide | 305 | 52 | Supercritical |
| CO2exch_in | E103R | Carbon Dioxide | 305 | 52 | Supercritical |

Once the material and storage characteristics have been defined, the hazardous events may be described for each “Pressure vessel”. In order to perform a QRA, the first step is the identification of accidental events able to generate a toxic dispersion. Generally, the analysis has to be focused on incidents that generate the highest

damage level. For containment of toxic substances, accidental losses of material through orifices have been modelled as leaks. The chosen “Leak” scenarios describe release of CO₂, Exhaust or Oxide streams through orifices of various diameters.

Due to the damage dependence on release duration and mass flowrate, apart from inventory initial conditions and volume, the first needed data are the hole size and release location and direction. No information about operating valves used to control and stop the discharge, limiting the damage, has been added. For each simulated point the considered leaks have been modelled to occur from orifices with diameters of:

- 7 mm
- 22 mm
- 70 mm
- 150 mm

These representative measures correspond to nominal diameters for “Small” (from 1 to 10 mm), “Medium” (from 10 to 50 mm), “Large” (from 50 to 150 mm) and “Full Bore” (>150 mm) ruptures, respectively (DNV GL, 2013).

Apart from simulation of consequences of different release scenarios, the equipment leak frequencies are needed. A proper risk analysis passes through evaluation of the initiating events evolution, for example through an Event Tree Analysis (ETA), obtaining the frequencies of all defined sequences and incident scenarios. In this case study, qualitative evaluations have been done, considering the consequences of different kinds of equipment’s loss of containment, associating to each scenario the probability of occurrence of its initiating event.

A variety of datasets for process equipment loss of containment may be used to determine leak frequencies. The DNV guidance proposes the best practice to use one of them, the Hydrocarbon Release Database (HCRD). This document, gives information about leaks for QRA of offshore and onshore installations, collecting data from events in the oil and gas field occurred in UK since 1992 (Spouge, 2006) and processed by UK HSE. These data were put together to produce a list of generic leak frequencies for 17 equipment types. Even if the dataset is based on offshore events, the DNV proposes the same approach also for onshore plants, for which a lower failure probability is expected. The leak frequencies are defined for compressors, filters, flanges, heat exchangers, pipes, pumps, instruments, valves, pressurized vessels and atmospheric storage tanks.

For each equipment type and size, different frequencies of release are considered for six subcategories of orifice dimension, included in “Small”, “Medium”, “Large” and “Full Bore” classes. For each of them “Total”, “Full Pressure” and “Zero Pressure” leak frequencies may be adopted. In the simulated case, where the leaking equipment has been modelled with initial pressure higher than 0.01 bar, the “Full Pressure” leak probability of failure has been used. This approach is confirmed by the fact that, for two-phase leaks, the 98% of events can be associated to “Full Pressure” leaks, 67% of which are limited and 31% are full leaks (DNV GL, 2013).

In correspondence of each modelled “Pressure Vessel” and orifice dimension, the failure probability has been reported, taking data about “Full Pressure” leaks from different types of equipment (IOGP, 2021). The frequency values are based on UK HSE HCRD data, collected from 1992 to 2015.

In the following table leak frequencies for simulated releases are visible. For each equipment type the corresponding Allam cycle components have been associated.

Table 16 Leak frequencies for plant components (IOGP, 2021).

| Hole diameter [mm] | Leak frequency [y^{-1}] | | | |
|--------------------|-----------------------------|---------|---------|---------|
| | 7 | 22 | 70 | 150 |
| C200 - C001 | 1.6E-03 | 7.2E-04 | 1.6E-04 | 1.1E-04 |

| | | | | |
|---|---------|---------|---------|---------|
| Centrifugal compressor | | | | |
| P400 - P200A Centrifugal pump | 1.4E-03 | 3.0E-04 | 3.0E-05 | 8.9E-06 |
| T102-T103 Heat exchanger Shell & Tube (Shell side) | 6.0E-04 | 3.0E-04 | 7.4E-05 | 6.1E-06 |
| E103R-E101C-E102R-E101D-E201 Heat exchanger Shell & Tube (Tube side) | 2.9E-04 | 1.8E-04 | 6.1E-05 | 7.7E-05 |
| CGT100 Turbine and Combustor | 2.4E-03 | 7.9E-04 | 1.3E-04 | 2.1E-04 |
| FT100-T100 Process (pressure) vessel | 2.6E-04 | 1.4E-04 | 3.8E-05 | 3.6E-05 |

Once set the orifice diameter, the “Release Location” can be imposed. The distance of leak from ground level has been fixed at a value of 2 meters, in order to consider standing people near the release point and along dispersion line.

Also “General parameters” can be defined. In particular, the default value of 3600 s for maximum release duration has not been changed, while an “Height of interest” of 2 meters has been chosen for plotting of results about concentration. This value results to be equal to the location of releases from the modelled vessels. However, in graphs view the height of interest may be modified, according to the observed shape and height of the cloud.

12.2.2.1. Variable parameters of the simulation

Changing the “Models” and “Parameters” options of the simulation, a sensitivity analysis has been conducted.

First of all, investigation about how the choose of “Outdoor release direction” affects the dispersion behavior has been done. The “Horizontal” initial direction of the plume has firstly been used, due to larger damage area expected after the cloud discharge and dispersion. For each leak scenario also the “Horizontal impingement” release option has been simulated. This kind of discharge model is expected to result in the most conservative consequences analysis. In fact, with impingement higher distances are covered by higher concentrations of toxic substance, because, losing momentum, the initial plume dilution-rate is reduced and the dispersion is slowed down. The impinging can occur because of the presence of buildings and equipment of the plant itself.

For toxic doses evaluations, constant values of CO₂ concentration, at which a person in a given position is exposed for a given period of time, are needed. Because of the entity of the release, and the variability of wind speed and direction, some turbulent flows can be generated inside the toxic plume. In order to consider fluctuations, the “Averaging time for concentration of interest” has to be set. Through this parameter, the dimension of the cloud at defined concentration of interest can be evaluated. The same value has to be selected in the “Toxic parameters” tab section, through which the dimensions of the dispersed cloud at different toxic concentrations may be graphically obtained.

The Phast default value for averaging time is 10 minutes (600 s), as usually set for QRA of toxic materials whose effects are driven by adsorbed dose. For these substances the long-term exposure at a given concentration has more severe health effects compared with peak values. When CO₂ toxic effects are evaluated, the 600s-averaging time approach is considered a not proper way to define the concentration of the cloud at a given distance. In fact, analyzing all the literature proposed probit function, the lethality of CO₂ is driven by concentration, as it is more dependent on peak values than on duration of the exposure. This could be confirmed by the “N” value of probit functions (higher than 1). According to these CO₂ characteristics an instantaneous evaluation of concentration has also been proposed, by setting the averaging time at 18.75 s in “Calculation options” (Fernandez, 2020). Changing the averaging time in “Toxic Parameters” tab section, a sensitivity analysis has been conducted. Comparisons between 15 or 30 minutes and 600 or 18.75 seconds averaged concentrations have been performed for some leak scenarios.

The “Dispersion results” section of equipment report can show concentration results also in terms of distances at which STEL and IDLH limits are reached. This is useful to investigate effects of toxic CO₂ after 15 and 30 minutes, including additional averaging times in “Dispersion” study section. The volumetric percentages referred to these exposure durations are part of “CARBON DIOXIDE” parameters.

Through these simulations, the influence of averaging time on damage distances defined by a given concentration value has been investigated.

The 8.23 version offers the possibility to obtain dispersion results before and after the Along Wind Diffusion (AWD). Comparison between these two categories of consequence results has been performed. The before AWD results consider that, during continuous releases, only entrainment of air through the lateral sides of the plume could be expected. This assumption produces too high dispersion distances and overestimated dangerous areas. Thanks to the inclusion of the AWD model, it is possible to add the contribution of entrainment also through the front and back sides of the cloud. The AWD gives a more consistent and smooth dispersion profile and it is the default method used by Phast 8.23 for time-varying or continuous release scenarios. The core dispersion calculations are based on results collected by ‘observers’, sensors released within the cloud. Simulating uniform discharge rates without rainout, the two sensors are both continuous. In this case the observers in the steady-state cloud are not able to consider the along-wind gradients of concentration and density, so the along wind diffusion and gravity spreading are included during the post-processing of dispersion results, through Gaussian integration of the concentration values obtained from the two observers. All default parameters, that refer to AWD most accurate method, have not been modified.

“Summary Report” and “Graphs” take data from post-processing results, while “Equipment Report” results are based on before AWD calculations. The differences between pre and post-AWD concentrations have been evaluated (DNV GL, 2017).

12.2.3. Vulnerability criteria applied to Phast results

The aim of the case study application is collecting consequences data useful to conduct a QRA of supercritical CO₂ capture process, the Allam cycle plant. The application of the proposed vulnerability thresholds for people and structures has been done in order to obtain safety distances from the analyzed process.

Once investigated the correlation between inputs and outputs of the simulation, useful data for vulnerability analysis have been collected, for each component, weather condition, orifice diameter and release direction. By obtaining the downwind temperature and concentration distributions, some significant impact area may be selected on the map of the plant. For each scenario distances from the leak have been associated to the following doses of CO₂ and low temperature values, for which a different probability of death is expected. The vulnerability thresholds reported in table 17 are extracted from results proposed in table 13.

Table 17 Fatality threshold for temperature and concentration

| | IDLH | 1% fatality | | 50% fatality | | | |
|-----------------|--------------------|--------------------|--------------------|---------------------|---------------------|--------|---------------------|
| Value | 4% CO ₂ | -26 °C | 8% CO ₂ | -40 °C | 11% CO ₂ | -34 °C | 10% CO ₂ |
| Duration | 30 min | 5 min | 5 min | 5 min | 5 min | 10 min | 10 min |

Through these vulnerability calculations it is possible to compare distances with the same level of harm and fatality for toxic inhalation and cold exposure. Selecting the toxic flag in “Materials” tab section, lethality calculations of toxic concentration of CO₂ have been allowed. For “Oxidant” and “Exhaust” mixtures, the toxic calculations are performed tracking pure CO₂. For this reason, for this working fluids the outputs of the simulations are pure CO₂ concentration and mixture plume temperature.

Defining some toxic parameters for the simulation, according to the HSE methodology used for the identification of threshold in table 17, some comparisons between obtained toxicological and equivalent concentration results could be done. In order to obtain toxic contours as output of the simulation, dose, probit

and lethality levels may be defined, exploiting the probit coefficients imposed in the “Materials” tab section. As a first analysis the following toxic levels have been plotted, using the UK HSE SLOT and SLOD values and probit function with concentration expressed in ppm and time in minutes.

Table 18 CO₂ toxic contours

| Dose levels [<i>ppm</i> ⁸ . s] | Probit levels | Lethality levels [fraction] |
|--|---------------|-----------------------------|
| 1.5E+40 | 2.67 | 0.01 |
| 1.5E+41 | 5.00 | 0.5 |

Due to the fact that no lethality assumption could be done without concentration values, the averaging time has been imposed to be equal to exposure time. By selecting the “Use a fixed averaging time” flag in toxic parameters section for each scenario, the program has been forced to calculate doses after a fixed duration, that corresponds to the defined averaging time for concentrations.

When the “Use probit” option is selected as calculation method, the toxic contours are visible in “Graphs” results, in function of time, distance and height. When “Prefer dangerous dose” is set, the “Report” section gives information about maximum distance and duration of exposure for which each “dangerous dose” defined for materials is reached. Outputs about dangerous doses are plotted only if the “Dangerous toxic load” is imposed as the lowest value among other required dangerous doses. In fact, the program performs calculations until the DTL limit is reached.

The Allam cycle includes a combustion process in which natural gas, modelled as pure methane, is the fuel that, before entering the combustor (CGT100) needs to be compressed from 70 bar to 303 bar, reaching a temperature of 128 °C. Due to the presence of this flammable fluid, comparisons about safety distances obtained for CH₄ and CO₂ releases have been finally done, in order to test the proposed QRA for supercritical carbon dioxide, in opposition to a well-known and shared hydrocarbon risk assessment.

The release of methane has been modelled, adding the pure component in “Materials” section without any changes in default parameters. Methane is defined as flammable substance in Phast database and for this reason no comparisons about concentrations with CO₂ may be done. The DTL concept has been substituted by the Dangerous Thermal Dose (DTD):

$$DTD = I^{4/3} * t$$

The thermal dose depends on irradiation (*I*) in kW/m² and time of exposure (*t*) expressed in seconds. The UK HSE manual suggests some fatality criteria for thermal radiation according to which a given DTD is obtained for different duration of the exposure, as reported in the following table.

Table 19 Suggested fatality criteria for thermal radiation. (OSD3.2, January 2006)

| | 1% fatality | | | 50% fatality | | |
|---|-------------|------|-------|--------------|-------|-------|
| Thermal radiation [kW/m²] | 12.5 | 6.0 | 4.0 | 12.5 | 6.0 | 4.0 |
| Duration of exposure | 32 s | 90 s | 160 s | 1 min | 3 min | 5 min |

The comparisons of lethality with carbon dioxide have been done considering an equivalent of SLOT and SLOD, as proposed in the UK HSE tables: the “1% fatality”, whose DTD is of about 1000 tdu, and “50% fatality”, for which a DTD of about 1900 tdu is perceived. This approach may be used to evaluate the consequences of a fireball or a jet fire of methane. For CH₄ lethality evaluations, the HSE method does not include the flash fire option because of the buoyancy effects. In conclusion jet fire and fireball damage areas have been compared with that obtained considering toxicological effects of CO₂.

Once the acute hazards of methane, such as ignition of flammable cloud, have been considered, the effects of CH₄ concentration on human health could be analyzed. This aspect assumes more importance in congested and poor ventilated areas. Methane and other “gaseous” alkanes show low toxicity, but at high volumetric concentration they can cause oxygen depletion, generating asphyxiation of people present in the cloud (HSE UK).

The HSE in 2009 proposed a limit value of CH₄ concentration of 476200 ppm as threshold above which asphyxiation starts to cause death (Wilday, McGillivray, Harper, & Wardman, 2009). For this reason, comparisons with other hazards may be done associating at this phenomenon a fatality of 1%. The defined threshold of 47.62% of methane corresponds to the EIGA dangerous oxygen concentration of 11%. This oxygen content falls within the conditions of the third stage of asphyxiation, during which collapse and brain damages are reported (see table 6).

Collected results about leak of CH₄ changing orifice diameter dimensions, weather conditions and directions of release, have been used to evaluate distances that match fatality criteria for thermal radiation and asphyxiation. Through these data, comparisons between CH₄ and CO₂ hazard ranges could be done.

In order to define distances at which vulnerability thresholds for metallic and structural materials are reached, more precise information about equipment is needed. In general, the -100°C MDMT has been used as limit to identify safety distances for engineered CCUS plant components.

When functionality of escape routes has to be analyzed, the limit values reported in table 14 have been followed, considering for different kinds of lighting a limit temperature of -30°C. Also the impact of the cold plume on electrical equipment may be defined in terms of critical areas inside which a temperature lower than -20°C is reached.

Considering that each scenario is characterized by a frequency of occurrence, comparisons between different areas of damage may be done also including the leak probability. Knowing that, increasing the orifice diameter the failure frequency decreases, the medium size of 22 mm has been chosen to find correlations between inventory conditions and produced damage areas, without underestimating or overestimating the component’s probability of rupture.

12.3. Results

All defined scenarios have been simulated considering different values of averaging time through which the wind-minder effects on concentrations are included. From “Averaging times” report, regardless of what are the inventory simulated conditions, at a given distance downwind, the same concentration values are obtained varying averaging time between 600 and 18.75 seconds.

In the “Consequence Summary” report for all equipment items, the “Distance downwind to STEL (900s)” and the “Distance downwind to IDLH (1800s)” have been extracted and compared with “Equipment Dispersion” default results. This has proved that, also using higher averaging times of 900 or 1800 seconds, the dispersion results do not differ from 600s-averaged default values. That validates the assumption reported in Phast guidelines according to which the accuracy of dispersion calculations with Phast is lower than the error obtained comparing outputs of different averaging times.

The discriminating factor for choosing the proper averaging method may be the time required for the calculations, that decreases when a higher averaging time is selected for the simulation. For this reason, even if 18.75 s is recommended for evaluating toxic effects driven by concentration (Fernandez, 2020), the default “Toxic” averaging time of 600 s has been preferred.

For each scenario, concentration results have been obtained from releases with and without horizontal impingement. For each of these simulated options, graphs have been generated for both 5D and 2F weather conditions. From “Max Footprint” dispersion graphs, distances downwind at which, for each conducted

simulation, the IDLH limit value of 40000 ppm is reached at the centerline, have been collected and used for sensitivity analysis. All dispersion evaluations have been done considering post-AWD results.

Firstly, only pure CO₂ inventory releases have been compared. In the radar chart reported in figure 47, the IDLH maximum distances for each different storage and release condition are represented. Generally, it can be said that, increasing the orifice diameter, the reached distances rise because of the highest peak flowrate obtained at the discharge plane. In fact, for 7 mm and 22 mm orifice, the release lasts longer and the dilution effects of air are enhanced.

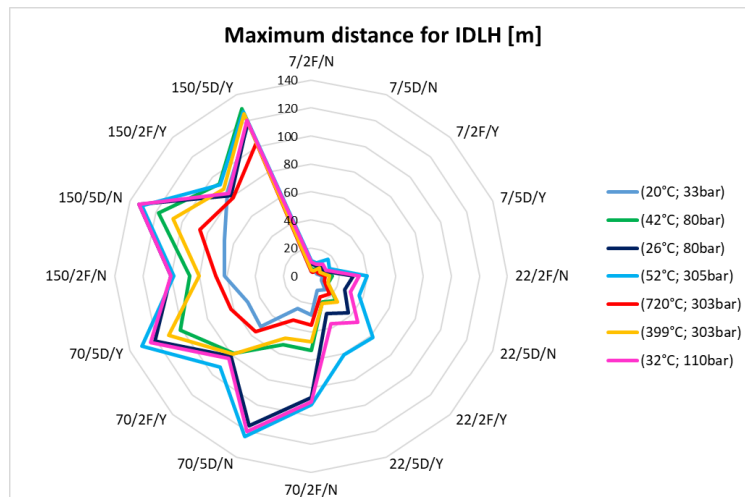


Figure 47 Radar chart obtained from pure CO₂ release outputs. Values for different orifice diameters (7, 22, 70, 150 mm), stability class (2F, 5D) and for releases with (Y) or without (N) impingement.

Analyzing results in figure 47, different considerations may be done for two ranges of hole diameter, in fact the 7 and 22 mm leaks show a shared behavior that is not complied with by all 70 and 150 mm release scenarios.

For hole diameter in between 7 and 22 mm, whatever the inventory conditions are, the longest distances are reached in case of “Horizontal impingement” release, when external conditions are represented by weather class 2F. These results are consistent with the dispersion model assumptions. In fact, with low wind speed and stable atmospheric class, the cloud dispersion is slowed down and the dense CO₂-rich cloud tends to accumulate on the ground. The same effect is given by impingement that, reducing the jet momentum, limits the plume dilution-rate, increasing the dispersion distances.

In case of 70 and 150 mm leaks, the impact of impingement is no longer so evident and in most cases the 5D weather category generates longer dispersion distances than stable 2D conditions.

For 7, 22 and 70 mm leaks, the inventories that result in the longest dispersion distances, in decreasing order of obtained length, are:

- The supercritical CO₂ stored at 52°C and 305 bar, representative of the recycle stream entering the main heat exchanger;
- The supercritical CO₂ stored at 32°C and 110 bar, representative of the exported stream;
- The liquid CO₂ stored at 26°C and 80 bar, representative of pump (P400) inlet.

For 7, 22 and 70 mm leaks, the inventories that result in the shortest dispersion areas, in increasing order of obtained distances, are:

- The vapour CO₂ stored at 20°C and 33 bar and released from the inlet of CO₂ compressor;
- The supercritical CO₂ stored at 720°C and 303 bar, representative of the stream entering the combustor.

Results obtained from a leak of 150 mm do not follow the same severity order. In fact, in case of 150 mm leak with impingement and stability class 2F, liquid CO₂ at 26°C and 80 results to be one of storage conditions that generate the longest IDLH distances. In general, the trend is preserved but some differences between “Horizontal” and “Horizontal impingement” release outputs may be detected. For non-impinging releases, the cases that generate the longest dispersion distances, in decreasing order of obtained length, are:

- The supercritical CO₂ stored at 32°C and 110 bar and the liquid CO₂ stored at 26°C and 80 bar;
- The supercritical CO₂ stored at 52°C and 305 bar.

For “Horizontal impingement” simulations, the longest distances are reached in case of leak of supercritical CO₂ stored at 42°C and 80 bar and released from the outlet of CO₂ compressor.

Correlations between IDLH maximum distances and stream conditions at the equilibrium plane have been found. Collecting data about solid fraction at ambient pressure, for each scenario, it has been observed that, the cloud dispersion is more extended if higher mass percentage of suspended solid particles is detected after the ATEX model application. For simulated inventory conditions, the solid contents at atmospheric pressure are reported hereafter.

Table 20 Solid percentage at the equilibrium plane

| Vessel code | Pressure [bar] | Temperature [°C] | Solid [%] |
|-------------------------------------|-----------------------|-------------------------|------------------|
| CO2cool_turb_in CO2cool_exch_out | 303 | 399 | 0 |
| CO2exhgascond_out CO2compr_in | 33 | 20 | 6 |
| CO2comb_in CO2exch_out | 303 | 720 | 0 |
| CO2export | 110 | 32 | 28 |
| CO2compr_out CO2aftercool_in | 80 | 42 | 12 |
| CO2pump_in CO2aftercool_out | 80 | 26 | 28 |
| CO2recpump_out CO2exch_in | 305 | 52 | 30 |

Observing results about 7, 22 and 70 mm scenarios, the differences between IDLH distances may be related to the sublimation of the solid particles during the plume dispersion, thanks to hotter air entrainment. This subsequent sublimation could be considered as a delayed expansion within the cloud during the dispersion phase. When the simulated scenario is a leak from vapour inventory or a supercritical one, characterized by high initial values of pressure and temperature, no solid fraction is expected at the orifice. This leads to a pure vapour dispersion that, compared with a two-phase one results in shorter reached distances.

These considerations are auditable also for other adopted concentration limit values. Increasing the concentration of interest, the same trend results to be shifted to lower distances.

The same sensitivity analysis has been conducted on “Oxidant” and “Exhaust” dispersion results. These streams have been simulated selecting as “Material to track” only pure CO₂. The obtained “Max Footprint” graphs have been analyzed and, when possible, compared with releases from components containing only pure CO₂. The discharge and dispersion of non-toxic oxygen and water, stored as part of the mixtures, are considered by Phast, because their presence alters cloud behavior and CO₂ concentration results.

Thanks to Phast 8.23 some considerations may be done changing simulated material, preserving inventory conditions. It can be proved that, when CO₂ and H₂O are released together (Exhaust), the temperature at the

orifice results to be reduced if compared with release of pure carbon dioxide. In these conditions, due to changings in mixture density, the mass flowrate is limited, so the time required to stop the discharge is increased. Sensible variations in jet velocity may be observed. The presence of water has also influence on the plume shape. The tracked CO₂ “Max Footprint” covers shorter distances and, during the release, the obtained STEL cloud is characterized by a thinner profile, reaching smaller height values (see Appendix C, table 23, figures a. and b.). As a consequence, a variation of atmospheric CO₂ concentration at the ground level results to occur only a longer period after the discharge.

For Oxidant mixture, in the following chapters, more detailed comparisons will be done with pure CO₂ release, in terms of lethal distances. In fact, the same initial conditions have been simulated for both CO₂ and Oxidant streams entering the combustor at 303 bar and 720°C. Analyzing the discharge conditions at the orifice plane, the oxidant temperature results to be lower than that obtained for pure CO₂. The transported oxygen acts as diluent for CO₂, resulting in reduced overall density and CO₂ concentration. The plume shape remains unaltered, but for oxidant leaks, the end of the release is delayed and the STEL CO₂ cloud obtained after the discharge has lower values of height and width. As for Exhaust mixture, the maximum distances at which the STEL concentration is reached result to be shorter than that obtained from a pure CO₂ release, stored at the same conditions. Even if less evident than for Exhaust mixture, at the end of the release the STEL concentration is not detected at the ground level. On the contrary, for pure CO₂, 15000 ppm are reached at the ground, at the end of discharge, after about 20 meters from the release point.

Through the side views of the released pure CO₂, the cloud shape may be analyzed considering the characteristics of the stored stream. The two scenarios that generate the STEL CO₂ plumes reported in graphs b. and d. of table 23 (Appendix C), show different behaviors. For both cases the inventory is characterized by pure CO₂ at vapour phase, but only for stream in figure b. the generation of 3% in mass of solid CO₂ particles at the equilibrium plane is expected. This phenomenon, increasing the plume density, forces the cloud centerline to reach the ground level few seconds after the release. In case of vapour CO₂ releases with no trace of solid particles in the plume (as in case d.), the could centerline never reaches the ground tending to disperse faster in the atmosphere.

In general, the presence of solid particles at equilibrium plane has two main effects on cloud dispersion. First of all, the two-phase plume shape is influenced by particles higher density. With high solid fraction, the cloud centerline is expected to touch the ground within the release duration. The other factor that influences cloud behavior is the solid particles ability to sublime within the cloud, acting as delayed expansion sources. This phenomenon increases the maximum distance at which a fixed concentration is reached, generating larger, longer and higher dangerous cloud.

Analyzing released mixtures behavior, it has been proved that only Oxidant, stored at supercritical temperature, is able to generate a dispersion “Max Footprint” comparable with other scenarios of pure CO₂. However, the over mentioned correlations between IDLH distances, weather stability and type of release from orifices of 7, 22 and 70 mm have been followed also by less impactful Exhaust gas releases.

In particular, in case of supercritical exhaust gases, exiting the combustor at 926.85 °C and 303 bar, or vapour exhaust stream, exiting the main heat exchanger at 67°C and 33 bar, the tracked CO₂ footprints result to be very similar. In these cases, maximum IDLH reached distances are longer only than that generated by vapour gases expelled from turbine. Solid fraction influence cannot be evaluated due to the too low percentage of 3% obtained only for fumes released after transferring heat in the exchanger.

In conclusion, it has been proved that, for each simulated inventory condition, the worst scenarios obtained from a leak of 7 or 22 mm, able to generate the longest dispersion distances, result to be those characterized by horizontal release with impingement, in 2F external conditions.

12.3.1. Definition of the damage areas

Starting from sensitivity analysis results, the most critical scenario has been simulated for each modelled “Pressure vessel”. The aim is to conduct preliminary risk evaluations, by collecting maximum distance values for some limit concentrations and associating leak frequencies to different components. In order to not underestimate or overestimate the release frequency, a 22 mm orifice diameter has been chosen to compare results.

Varying the “Concentration of Interest”, 80000 and 110000 ppm dispersion areas have been obtained. The distance values extracted from “Max Footprint” dispersion graphs have been used to evaluate concentration contours at which the 1% and 50% fatality is expected within 5 minutes. In table 24 (Appendix C), for each “Item”, maximum distances at which limit concentration values have been detected, are reported next to IOGP leak frequencies.

The most critical stagnation conditions result to be that represented by supercritical CO₂ stored at 52°C and 305 bar. According to previous evaluations, the determining factor is the solid fraction at the equilibrium plane, that in this case corresponds to the maximum value of 30%. The components from which this stream may be released are the CO₂ pump (P200A) and the shell side of the main heat exchanger (E103R). From these two dots on the Map, the 1% and 50% lethality are expected within 33 and 24 meters, respectively. Consequently, also the distance at which the IDLH threshold is exceeded is the longest among other simulated items. Generated effect zones on plant map are reported in Appendix D.

In “Summary Reports”, distances downwind for IDLH and STEL CO₂ concentrations are also shown. For “CO₂_recpump_out” simulated scenario, these values correspond to 62.13 and 115.18 meters, respectively. Even if, “Summary” and “Graphs” are both referred to post-AWD outputs, the same concentration levels extracted from “Dispersion” graphs are obtained for distances of 61.98 and 114.49 meters.

In order to determine the differences between these two components, the leak frequencies have been used. Through a preliminary risk analysis, the P200A element may be defined as the most critical component, considering that the occurrence of a 22 mm leak is higher for a CO₂ pump than for heat exchanger (E103R). If the IDLH approach is used, the worst condition is represented by the CO₂ at the entrance of turbine (CGT100). Its higher frequency value compensates the lower distance value, if compared with “CO₂recpump_out” conditions.

The same analysis may be done exploiting Phast toxic results. Through the UK HSE probit function, the software evaluates lethality of CO₂, plotting doses, lethality percentages and probit values for user defined levels. Using an averaging time that corresponds to an exposure time of 10 minutes, the obtained maximum distances at which 50% mortality is reached may be compared with dispersion “Max Footprint” results obtained for a constant concentration of 110000 ppm. In simulated case of “CO₂recpump_out”, the centerline SLOD distance, obtained from “Dispersion” graphs, is about 8 meters longer than that obtained from “Toxic” graphs. In fact, Phast toxic evaluations about received dose at a certain distance take into account a variable exposure time, that could be lower than the proposed averaging time. As a result, the maximum distance at which, according to “Toxic” graphs, the SLOD dose is expected, may be characterized by a concentration higher than 11%, but an exposure time shorter than 600s. In figure 50 (Appendix C), the 8% and 11% isopleths, obtained for a 22 mm leak from “CO₂recpump_out” conditions, are compared with the corresponding 2.67 and 5.0 “Toxic Outdoor Probit Footprints”.

Apart from the actual values of distances at which SLOD and SLOD toxic loads are obtained, by applying Phast toxic models, the relative differences between simulated scenarios result to be preserved. The proportion between generated 1% and 50% fatality areas is not altered, if compared with concentration contours that have been associated to a given dose and lethality through a post-processing of Phast dispersion outputs. The obtained effect zones plotted on plant map, for each simulated release scenario, are reported in Appendix D.

From “Dispersion Reports” and “Graph Wizard” Phast tool it is possible to obtain centerline temperature values for each scenario, in order to define dangerous areas around equipment within which registered cryogenic conditions are able to cause death. However, these data cannot be compared with concentration values extracted from “Graphs” and previously analyzed. In fact, for temperature only “before along-wind diffusion” results may be obtained. For consistent comparisons, also pre-AWD distances for fixed centerline concentration values have been extracted from “Reports”.

Through Phast simulation, it is possible to evaluate the influence of air entrainment in front of and behind the cloud, comparing post-AWD results with less consistent pre-AWD dispersion outputs. For long-distance evaluations, the pre-AWD model is not able to consider the effective dilution of the cloud. As a consequence, it results in higher values of maximum distances, at a fixed CO₂ concentration, overestimating the generated damage areas. As shown in figure 48, increasing the solid CO₂ fraction obtained at equilibrium plane, the AWD model has higher impact on downwind distribution of concentration. Differences are less evident in case of mixtures, for which the effects of water or oxygen dilution dominate the far-field cloud behavior.

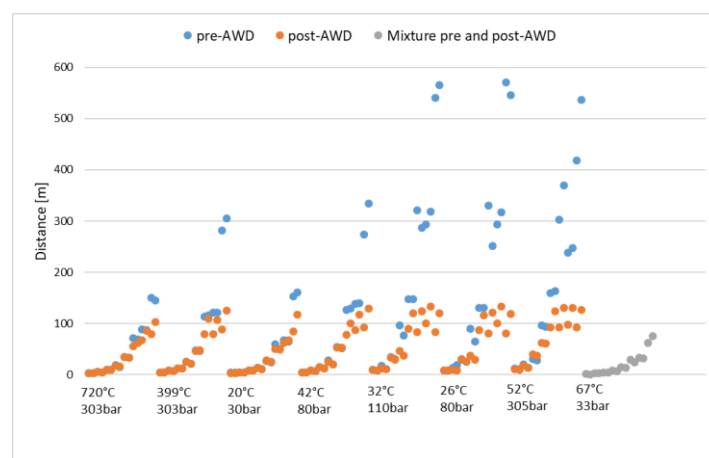


Figure 48 IDLH maximum distances obtained from different stagnation data.

Below 50 meters from the release, pre-AWD concentration results overlap post-AWD ones. At 100 meters, the differences between simulation outputs start to be more evident. Pre-AWD results that exceed 150 meters have to be discarded because too different from post-AWD ones.

Once analyzed CO₂ concentration distribution, at the same pre-AWD conditions, temperature results have been obtained from “Reports”. Vapour and solid temperatures at a given distance downwind may be used to investigate the characteristics of the cloud. Generally, two different patterns have been recognized. The first one, typical of vapour releases for which no solid fraction is expected, and the other one influenced by the presence of dry-ice particles in the plume, for which a temperature of -78°C is reached at the equilibrium plane. For hot vapour releases, the orifice temperature decreases with distance, until reaching ambient conditions. For cryogenic releases, after the discharge, temperatures rapidly increase with distance, thanks to hotter air entrainment and energy absorbed from the surrounding heat sources. For plume in which consistent solid fraction is present, not all the particles are expected to directly sublime at ambient pressure. In fact, some obtained temperature profiles show zones for which temperature falls below the sublimation limit of -78°C. This cooling behavior, representative of a delayed sublimation of solid CO₂ in the jet, has been verified for releases with a solid fraction higher than 6%. These Phast obtained outputs are consistent with analyzed experimental and simulated results reported in literature (Pursell, 2012). In the following figure, three different temperature profiles have been proposed. The first one is representative of vapour release, the second one of a jet characterized by a small solid fraction at the orifice plane, and the last one with 28% of solid CO₂, able to reach temperatures below -78°C.

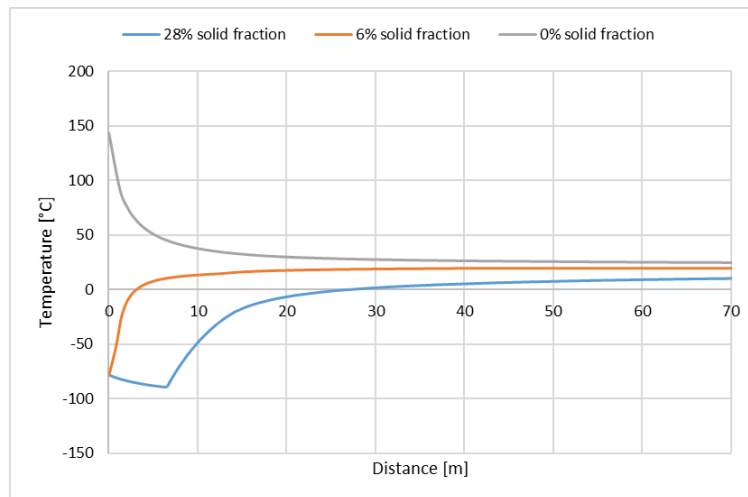


Figure 49 Typical pre-AWD temperature profiles for 22 mm leak

Temperature profiles reported in figure 49 show that pre-AWD results about cryogenic conditions may be used for reliable risk assumptions, if a 22 mm leak is considered. In fact, at this case, the cryogenic phenomenon is extinguished within less than 50 meters, distances for which pre-AWD results are still considered a good approximation of post-AWD ones.

According to predefined vulnerability criteria for exposure to low temperatures, distances at which the “continuous observers” detect temperatures of -26°C , -34°C and -40°C have been collected for each release scenario. In this way the 1% and 50% fatality contours may be determined. The Phast pre-AWD outputs make possible to consider distances at which the same fatality level is reached, due to inhalation of toxic CO_2 or exposure to cryogenic environment. After 5 minutes from the beginning of the exposure, the 1% fatality has been estimated. Observing results in figure 51 (Appendix C), it is evident that low temperature hazard is able to generate a large damage area only in presence of 28% or 30% of solid fraction. Increasing the orifice size and adopting a horizontal release with impingement, the difference between -26°C and 8% contours increases. However, this is more evident for scenarios characterized by a smaller solid fraction at equilibrium plane (3%, 6%, 12%). Even with reduced differences between concentration and temperature contours, this behavior is preserved in case of comparisons between 50% fatal limits of -40°C and 11% CO_2 . If these 50% fatality considerations are extended to a prolonged exposure time of 10 minutes, the trend and relative differences between limit temperature and concentration distances result to be preserved.

For temperature hazard, the worst case is “large” leak of liquid CO_2 stored at 26°C and 80 bar followed by supercritical CO_2 stored at 32°C and 303 bar or 52°C and 305 bar. In the following histograms, for different solid fractions, the 1% and 50% fatality distances, obtained for cryogenic exposure and toxic CO_2 inhalation, are compared. Considering that pre-AWD temperature and concentration results are reasonable only for distances below 100 m, for releases that generate an equilibrium solid fraction of 28% or 30%, the outputs of 150 mm leak simulations are not useful for comparisons.

It can be concluded that, for scenarios able to generate a higher number of deaths due to CO_2 inhalation, the risk is amplified by the effects of cryogenic environment on human health. On the contrary, for scenarios in which shorter lethal distances are obtained because of CO_2 toxicity, death may be caused by low temperatures only within few meters from the release.

The temperature profile has been used to determine the indicative maximum distances below which functionality of lighting and safety equipment may be impaired. The -20°C limit has been chosen for thermal-magnetic circuit breakers location, while -30°C has been considered as functionality threshold for common LED and cryogenic BDVs and SDVs. If a leak of 22 mm occurs, generally no limited functionality of safety systems and escape facilities is expected beyond one meter from the release point. However, when the temperature profile of jet characterized by a high solid fraction at the equilibrium plane is considered, the

following distances have to be defined as contours inside which thermal-magnetic circuit breakers, common lighting and safety valves should not be located.

Table 21 Minimum distances from the release to install typical plant equipment

| Component | Limit for valves and lighting (-30°C) [m] | Limit for circuit breakers (-20°C) [m] |
|---------------|---|--|
| C200 – E201 | 3 | 4 |
| P400 | 11 | 12 |
| T100 | 12 | 14 |
| P200A – E103R | 15 | 18 |

The -20°C and -30°C limit contours, inside which circuit breakers, lighting, BVSs and SDVs are impaired, may be also plotted on the plant map (see Appendix C, figure 52). When the presence of these components is not avoidable inside these limited areas, more expensive and advanced equipment for cryogenic applications should be exploited. Advanced thermal-magnetic circuit breakers may be located at a distance for which a temperature of -40°C is never exceeded. Finally, if advanced LED drivers are used for escape routes, lighting functionality is preserved also for shorter distances that correspond to a threshold of -55°C. These temperatures are usually exceeded beyond one meter from the release, exception done for components P400, T100 and P200A or E103R, for which also advanced LED functionality is not guaranteed within 8, 9 and 11 meters from the release point, respectively.

12.3.2. Comparison between CO₂ and CH₄ release consequences

The CO₂ contribution to risk assessment of typical plants, characterized by the presence of hydrocarbons, has also been discussed. In particular, the identified worst case of supercritical CO₂ release has been compared with release of CH₄ also processed in the Allam cycle plant. The CH₄ exiting from compressor has been modelled as pure methane stored at 128°C and 303 bar. Adopting default parameters for the simulation, results about “Intensity Radii” of generated fireball and jet fire scenarios have been extracted from “Graphs”. The 4 kW/m² limit value has been plotted to compare CH₄ with 11% CO₂ generated damage area, at which a 50% lethality may be expected after 4-5 minutes of exposure.

In case of a fireball, a maximum distance of 54 meters has been obtained for a 4 kW/m² intensity value, whatever weather conditions are considered during the simulation. A circular area surrounding the release point has been delimited by the 50% mortality. When a jet fire is considered, the maximum distance varies from 10 meters, in case of release with impingement from a 7 mm orifice, to 378 meters, when the leak occurs from a 150 mm orifice without impingement. For jet fire, the 4 kW/m² contour assumes an elliptical shape. In both cases, the simulated releases are concluded in a maximum of few seconds.

Comparison in terms of risk between CO₂ and CH₄ releases has been done, taking into account distances for CO₂ SLOD value, obtained from “CO2recpump_out” simulation, and 4 kW/m² thermal radiation contours generated by a jet fire. When scenarios produced by small, medium or large size hole leaks are observed, the damage areas obtained from a jet fire, as a consequence of CH₄ release, are always larger than that obtained accounting toxicity of carbon dioxide. In fact, apart from maximum distances, also the width of the CO₂ cloud is lower than the 4 kW/m² intensity radii, obtained from a CH₄ discharge.

This behavior is not followed if fireball is considered. In fact, the 11% CO₂ maximum distances, obtained from a 150 mm release scenario, result to be longer than the fireball 50% fatality radius. In case of release with impingement, this is also true for a 70 mm scenario.

Another hazard that could be taken into account is asphyxiation. As for CO₂, also a huge CH₄ concentration in air may cause oxygen depletion. For this reason, the SLOD CO₂ concentration of 8% has been compared with the 47.62% of CH₄, as proposed by UK HSE (Wilday, McGillivray, Harper, & Wardman, 2009). Through this analysis the CO₂ asphyxiating power has not been considered, but only its lethal concentration of 8% has been

related with asphyxiating CH₄ air content. To compare gases ability to displace O₂, a CO₂ concentration of about 50% should have been proposed.

For plant risk evaluations, the 1% lethality distances, obtained inhaling too high concentrations of CH₄ and CO₂, have been analyzed. All simulated CO₂ release scenarios have been compared with methane asphyxiating power, always obtaining higher SLOT distances. In particular, comparing the worst scenario generated by a CO₂ release with the greater distances reached by the 47.62% CH₄ threshold, results about 1% fatality limit have been collected.

Results of the over mentioned SLOD and SLOT comparison between CH₄ and CO₂ are reported in the following table.

Table 22 Comparison between 50% and 1% fatality distances generated by a CH₄ or a CO₂ release.

| | 50% fatality distance [m] | | | | 1% fatality distance [m] | | | |
|------------|--|-----------------------------|--|-----------------------------|--------------------------|----------------------------|--------------------------|----------------------------|
| | NO Impingement | | Impingement | | NO Impingement | | Impingement | |
| | Jet Fire CH ₄ [4kW/m ²] | Worst CO ₂ [11%] | Jet Fire CH ₄ [4kW/m ²] | Worst CO ₂ [11%] | CH ₄ [47.62%] | Worst CO ₂ [8%] | CH ₄ [47.62%] | Worst CO ₂ [8%] |
| 7 mm (2D) | 18 | 5 | 7 | 8 | 1 | 6 | 1 | 10 |
| 7mm (5D) | 18 | 5 | 7 | 7 | 1 | 6 | 1 | 9 |
| 22mm (2F) | 62 | 14 | 30 | 24 | 2 | 19 | 2 | 33 |
| 22 mm (5D) | 61 | 14 | 29 | 22 | 2 | 18 | 2 | 30 |
| 70mm (2F) | 189 | 46 | 106 | 59 | 2 | 59 | 2 | 69 |
| 70mm (5D) | 190 | 50 | 104 | 80 | 2 | 71 | 2 | 93 |
| 150mm (2F) | 377 | 57 | 228 | 60 | 2 | 70 | 2 | 70 |
| 150mm (5D) | 378 | 72 | 222 | 82 | 2 | 91 | 2 | 95 |

For effect zones comparisons, the 22 mm “medium” orifice scenario has been simulated. Apart from the actual shape of the generated damage areas, influenced by wind direction, also the circular areas surrounding the release points, have been extracted from Phast results. Effect zones for 2F condition are reported in table 25 (Appendix C).

For a preliminary risk analysis also differences between leak frequencies of involved equipment have to be assessed. A leak from the CH₄ compressor (C-001) results to be more frequent than a leak from heat exchanger and CO₂ pump. However, the chain of event from methane leak to fireball or jet fire needs to be considered, also investigating the timing of different scenarios. For example, even if in some cases the CH₄-50% fatality distances are not exceeded by CO₂ toxicity, the combustion requires an ignition that changes the scenario probability to occur. This may increase the time after which a given heat radiation is reached at a given distance, consequently enhancing the corresponding CO₂ received dose.

It can be concluded that, the impact of supercritical CO₂ on safety considerations about a plant, in which also vapour CH₄ is stored, cannot be neglected. In fact, in some conditions the risk zones generated by CO₂ could exceed that caused by methane release. For example, when no ignition occurs, the CO₂ toxicity generates larger SLOT areas than asphyxiation caused by high CH₄ concentration. Also in cases for which a fireball is expected, the toxicity of CO₂ may define longer SLOD distances. In general, the damage level obtained from a CO₂ release, in some conditions, is comparable with that generated by the flammable CH₄.

13. Conclusions

In order to identify vulnerability thresholds for a QRA, the first part of this thesis has been focused on the analysis of existing methodologies, already applied to identify lethality correlated to a CO₂ accidental release from a CCUS utility.

Nowadays risk assessment for this hazardous substance is based on evaluation of its toxicity and asphyxiating power, also thanks to military experience and conducted laboratory tests during the last decades. On the other hand, exposure to cryogenic conditions is not considered in CCUS QRA studies found in literature and no standard methodology, to associate mortality to a given cold exposure, may be obtained. On the contrary, to evaluate effects of a physical blast, shared UK HSE and TNO models may be used, but only the Energy Institute has developed an empirical approach able to transfer previous knowledge on CO₂ releases.

Among prohibit methods to assess CO₂ toxicity, the UK HSE functions result to be the most representative of CO₂ behavior, in line with concentration limit values extracted from prior experience, as it has been tested through Phast application to the Allam cycle. For equipment and individuals' vulnerability to cryogenic conditions, the conducted research work has led to definition of useful mortality thresholds, based on frostbite and hypothermia occurrence, and limit operating temperatures for facilities.

In order to apply proposed vulnerability thresholds on the Allam cycle plant, Phast 8.23 has been used, also investigating software limitations to describe CO₂ releases.

A complete analysis should consider all possible effects of an event. Nevertheless, Phast models CO₂ as toxic component and no results about released energy or generated overpressure peaks may be extracted. The air entrainment effect is considered through the DISC approach, but the water vapour content cannot be obtained as output of the simulation. As a result, also the reduced visibility around the release point is not evaluable. According to some experimental results, through sensors and cameras, the fog formation could be associated to a defined CO₂ concentration. However, changing the experimental setup, the correlation is not preserved. For this reason, no visibility impairment has been evaluated for the analyzed case study. Another limitation of the DNV GL software is the modelling of solid CO₂ particles. In fact, not considering the dry-ice bank deposition and consequent sublimation, the duration of the exposure to high concentration of CO₂ and the damage area result to be underestimated.

The pre-AWD outputs of the simulation result to be not able to describe the cloud dispersion in a reliable way, especially for far-field evaluation. For this reason, the proposed vulnerability thresholds are preferred to be applied to post-AWD results. These outputs have been used to compare 1% and 50% fatality contours obtained from leaks of liquid, vapour and supercritical CO₂. The scenarios able to generate the highest damage areas due to CO₂ toxicity are those for which supercritical CO₂ is released, obtaining high value of solid fraction at atmospheric pressure.

From Phast 8.23 the needed temperature profiles after the along wind diffusion calculations are not yet available, so the safety distances for people, safety systems and other equipment obtained from pre-AWD temperature values may be overestimated. In general, pre-AWD data may be considered a good approximation of the post-AWD more consistent results in the near-field. As a consequence, distances at which proposed limit temperatures are reached, are useful for a qualitative comparison with pre-AWD concentration results and for definition of minimum distances at which 1% and 50% probability of death is expected. Through these results also minimum distances between possible release points and vulnerable plant components may be determined.

Using proposed temperature thresholds to identify 50% and 1% fatality distances, the release scenarios that result to be the most critical according to SLOT and SLOD toxic evaluations, are also those for which severe cryogenic conditions are expected for larger distances from the release point.

To evaluate the applicability of traditional QRA methodologies to supercritical carbon dioxide, the Allam cycle case study has been exploited, comparing entity of effects of an accidental release of CO₂ with those of CH₄ used as fuel in the combustor. Apart from uncertainties about leak frequencies associated to items containing

CO₂, the two hazardous substances may be analyzed in terms of generated SLOT and SLOD areas for comparable physical effects. In most of cases, the SLOD areas defined for heat radiation result to be larger than those defined for toxicity of CO₂. However, the risk linked with CH₄ asphyxiating power results to be negligible if compared with toxicity of CO₂. Further considerations about reduced frequency of CO₂-induced ruptures and incidental sequences of CH₄ and CO₂ releases are needed, in order to better understand the CO₂ connected risks, comparing the two hazardous streams' behavior.

Future works may be focused on validation of proposed correlations between low temperatures, duration of exposure and effects on human health. Also metallic and non-metallic materials' behavior has to be deeply understood, obtaining reference thresholds able to foresee embrittlement and degradation, for different classes of materials. In addition, further investigations are needed to found an easily measurable parameter, different from CO₂ concentration, able to detect when loss of visibility inside the cloud could compromise the successful emergency evacuation of the release zone. In order to apply these models to a vulnerability analysis, it is also important to obtain reliable description of consequences, exploiting tools able to consider all physical effects of a CO₂ release.

Appendix A

Literature review on vulnerability models for accidental CO₂ release

| Source | Inventory conditions | | Discharge geometry | Vulnerability Model | Results |
|--|--|--------------------------------------|---------------------------------|----------------------------------|--|
| (Mocellin, Vianello, & Maschio, 2016) | 4.2 km pipeline | Q: 251.67 kg/s T: -78°C | Orifice 600 mm | Concentration (bank) | - 20% CO ₂ at max distance of 10 m - 7-10% CO ₂ at max distance of 50 m |
| (Preeti, Prem, & Qingsheng, 2016) | 6.3 m ³ vessel | P: 15.74 MPa T: 148.1°C | Orifice 11.94 mm | Concentration (jet) | - 4% CO ₂ at 12 m (10 s) (increased concentration near obstacles of 55%) |
| (Hill, Fackrell, Dubal, & Stiff, 2011) | Pipeline | P: 150 bar T: 10-20°C | Orifice 500 mm | Concentration | - 5% CO ₂ max distance 530 m (simulation) |
| (Liu, Godbole, Lu, Michal, & Venton, 2015) | 300 km pipeline | P: 15 MPa T: 20°C | FBR | Concentration (H ₂ S) | - 200ppm H ₂ S and 50000ppm CO ₂ (needed source H ₂ S<0.6%) - 500ppm H ₂ S and 80000ppm CO ₂ (needed source H ₂ S<0.4%) |
| (Ahmad, et al., 2015) | Vessel + pipeline | P: 15.08 MPa T: 14.2°C | Orifice 4 mm | Concentration | - at 50 m 10% CO ₂ 30-45° downwind, 12% CO ₂ downwind and 16% CO ₂ instant upwind |
| (Witlox, Harper, & Oke, 2012) | 5.5 m pipeline | P: 103.4-157.8 bar T: 5-149.37 °C | Orifice 25.62-11.94-6.46 mm | Concentration | 22%mol CO ₂ max concentration 5 m after 115 s 5.5%mol CO ₂ max concentration 15 m after 125 s 1.6%mol CO ₂ max concentration 40 m after 130 s |
| (Guo, et al., 2016) | 257 m pipeline | -Gas -Dense | -Orifice 15-50 mm -FBR | Concentration | - 5% CO ₂ for gas 15mm-50mm-FBR releases at 8-12-19 m - 5% CO ₂ for dense releases at more than 20 m - 10% CO ₂ for dense 50mm-FBR releases at 20-50 m |
| (Quest Consultants Inc., 2010) | Pipeline | P: 160 bar T: 37 °C | -FBR -Orifice 25.4-6.4 mm | Dose | - HSE probit : 1%mortality: 139-131-110-66-31-0 m 50%mortality: 101-114-79-54-24-0 m 100%mortality: 77-97-29-43-0-0 m -No mortality for flash fire, overpressure, radiation |
| (Lyons, Race, Hopkins, & Cleaver, 2015) | 8 km pipeline | P: 150 bar T: 30 °C | Double ended break | Dose | - HSE probit (simulation): 3% lethality for SLOT 50% for SLOD |
| (Vianello, Macchietto, & Maschio, 2013) | 4.8/29 km pipeline | P: 100 bar T: 35°C | -FBR -Hole 20% of diameter | Dose | -FBR: LC50 (11% CO ₂ 15min) at 118-335 m IDLH NIOSH (4% CO ₂) at 263-711m -Hole: LC50 (11% CO ₂ 15min) at 119-319 m IDLH NIOSH (4% CO ₂) at 249-626 m |
| (Vianello, Macchietto, & Maschio, 2012) | A: 30 km pipeline B: 15 km pipeline | Q: 250 t/h P: 35 bar T: 7°C | FBR | Dose | A: Max IDLH NIOSH distance 750 m B1: Max HSE SLOT distance 643 m B2: Max HSE SLOT distance 358 m B3: Max HSE SLOT distance 183 m |
| (Cooper & Barnett, 2014) | 96 km pipeline | P: 150 bar T: 30°C | -Rupture -Puncture | Dose | - HSE SLOT and SLOD from dispersion model -Societal risk for pipeline routing and QRA |

Appendix C

Table 23 Phast generated cloud Side Views at the end of horizontal releases with impingement, for weather condition 2F and CO₂ concentration of 15000 ppm (STEL).

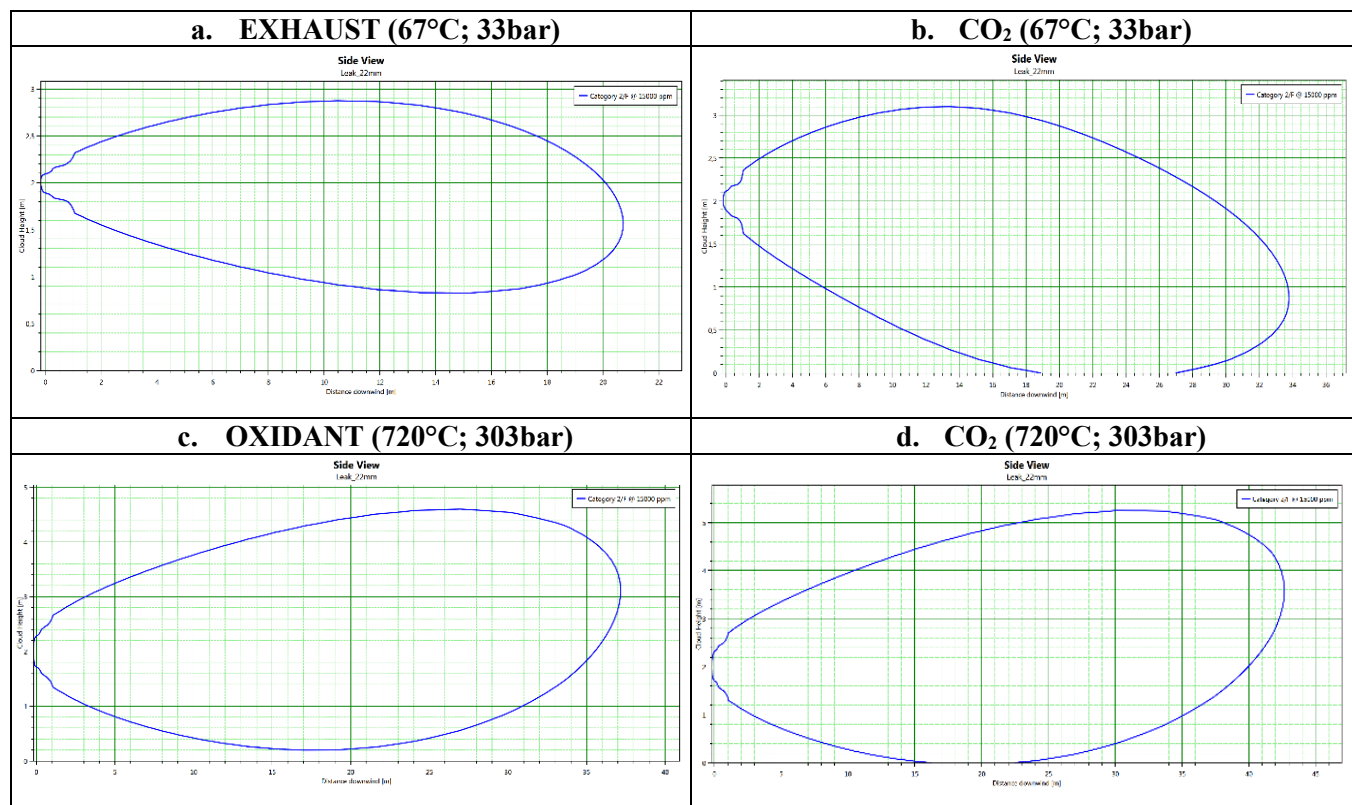


Table 24 Limit distances and leak frequencies for different release scenarios

| Vessel code | IDLH distance [m] | 1% fatality distance [m] | 50% fatality distance [m] | Leak frequency [y ⁻¹] |
|-------------------|--------------------|--------------------------|---------------------------|-----------------------------------|
| | 4% CO ₂ | 8% CO ₂ | 11% CO ₂ | |
| CO2cool turb in | 26 | 12 | 9 | 7.9E-04 |
| CO2cool exch out | 26 | 12 | 9 | 1.8E-04 |
| CO2exhgascond out | 14 | 8 | 6 | 1.4E-04 |
| CO2compr in | 14 | 8 | 6 | 7.2E-04 |
| OXcomb in | 15 | 7 | 5 | 7.9E-04 |
| OXexch out | 15 | 7 | 5 | 1.8E-04 |
| CO2comb in | 18 | 9 | 6 | 7.9E-04 |
| CO2exch out | 18 | 9 | 6 | 1.8E-04 |
| EXcomb out | 18 | 9 | 6 | 7.9E-04 |
| EXturb out | 9 | 4 | 3 | 7.9E-04 |
| EXexch in | 4 | 2 | 1 | 3.0E-04 |
| EXexch out | 4 | 2 | 1 | 3.0E-04 |
| CO2export | 8 | 4 | 3 | 1.4E-04 |
| CO2compr out | 25 | 13 | 10 | 7.2E-04 |
| CO2aftercool in | 25 | 13 | 10 | 1.8E-04 |
| CO2pump in | 37 | 18 | 15 | 3.0E-04 |
| CO2aftercool out | 37 | 18 | 15 | 1.8E-04 |
| CO2recpump out | 62 | 33 | 24 | 3.0E-04 |
| CO2exch in | 62 | 33 | 24 | 1.8E-04 |

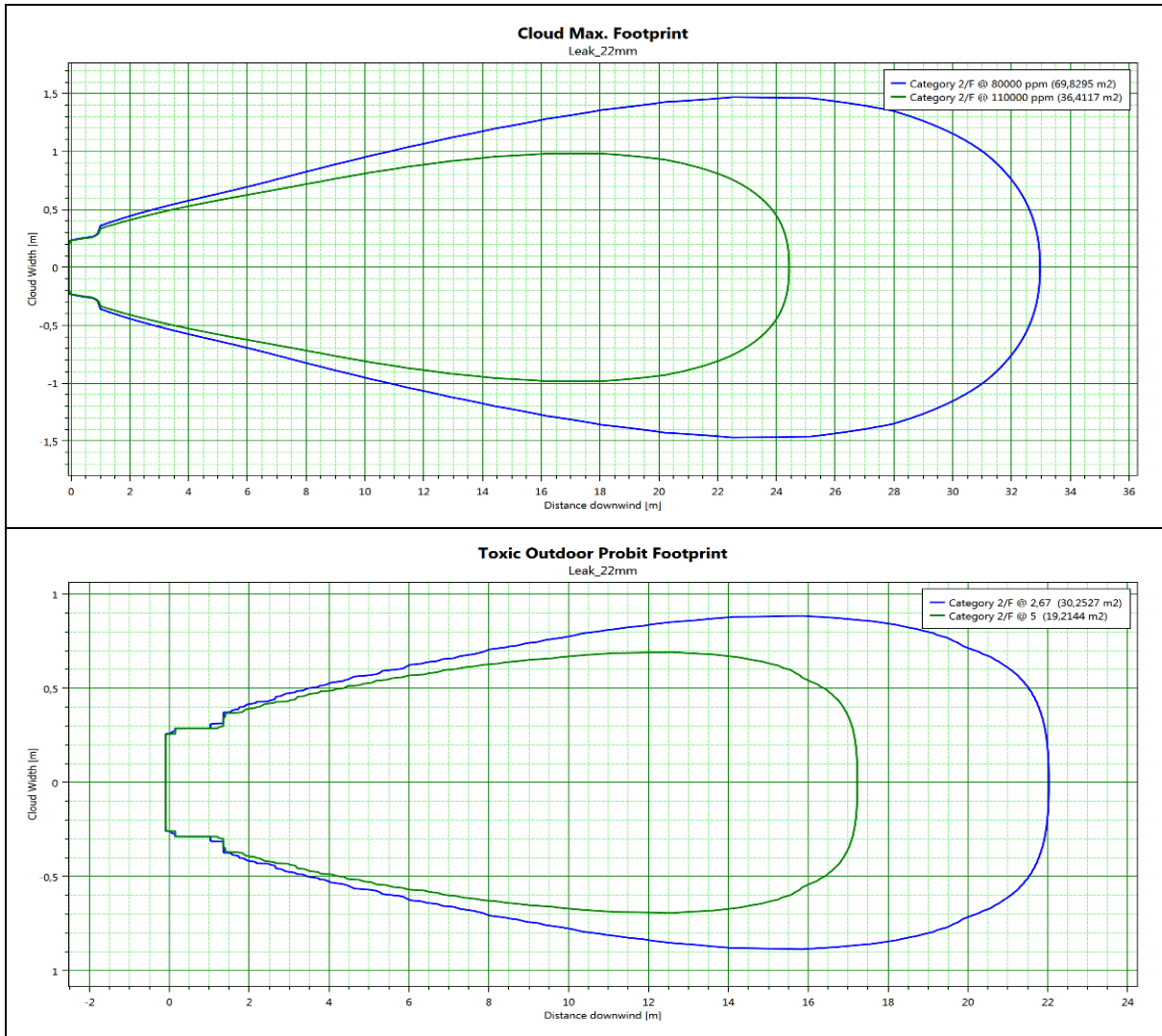


Figure 50 Maximum concentration and probit Footprints for scenario CO₂ recpump_out, weather 2F, orifice diameter 22mm and impinging release. 8% CO₂ and probit 2.67 (blue curve); 11% CO₂ and probit 5.0 (green curve).

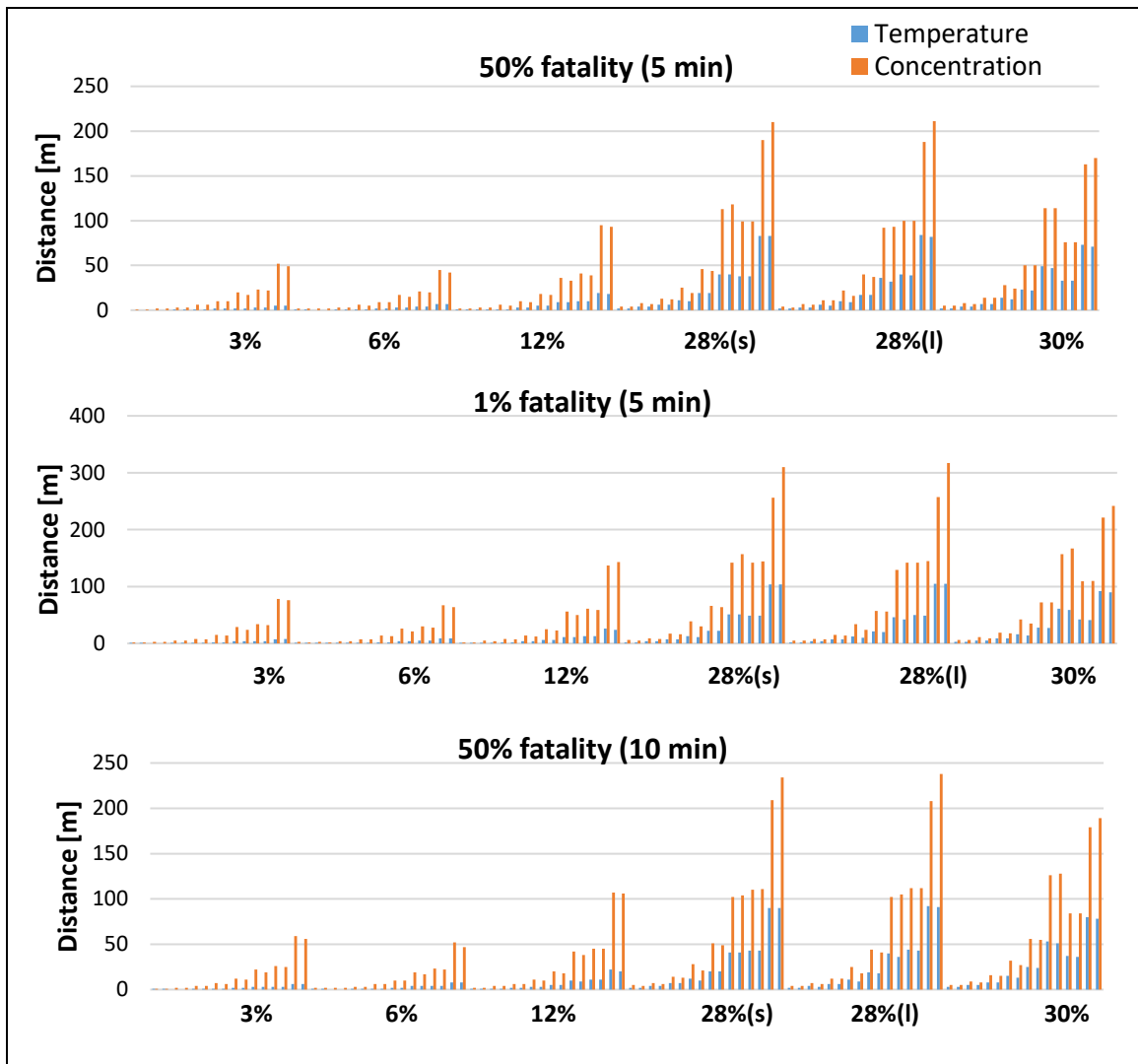


Figure 51 Maximum distances for 1% or 50% fatality due to low temperatures and high CO₂ concentrations. For solid fraction of 28%, releases of both supercritical (s) and liquid (l) CO₂ are represented.

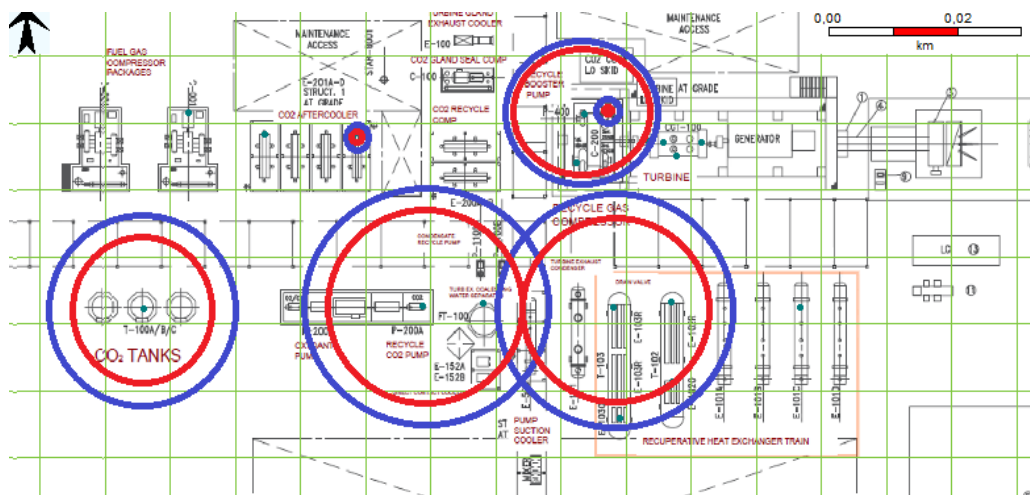
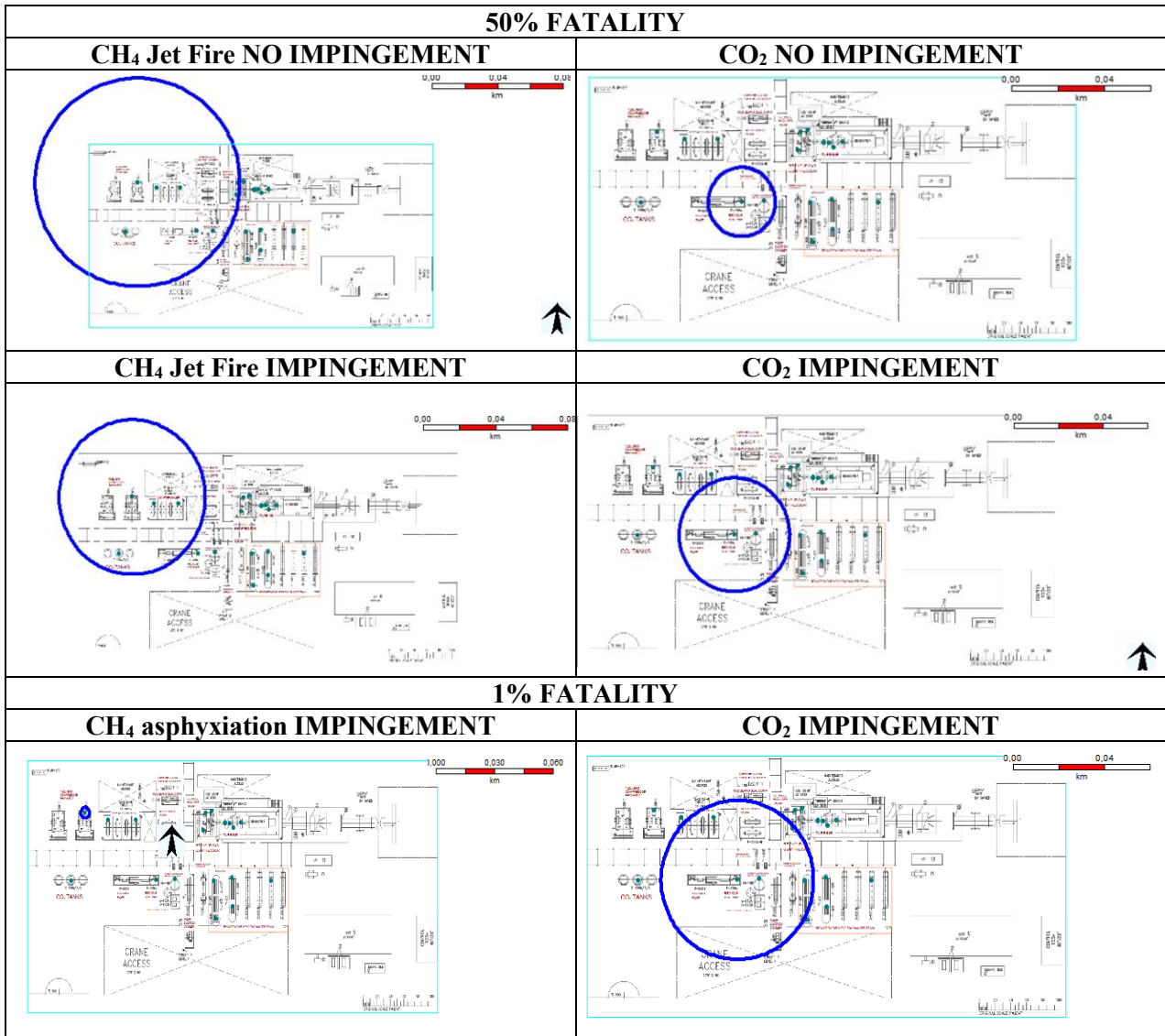


Figure 52 Minimum distances from release points to install valves and lighting (red curves) or circuit breakers (blue curves).

Table 25 Phast generated Effect Zones for CH₄ and CO₂ different hazards



Appendix D

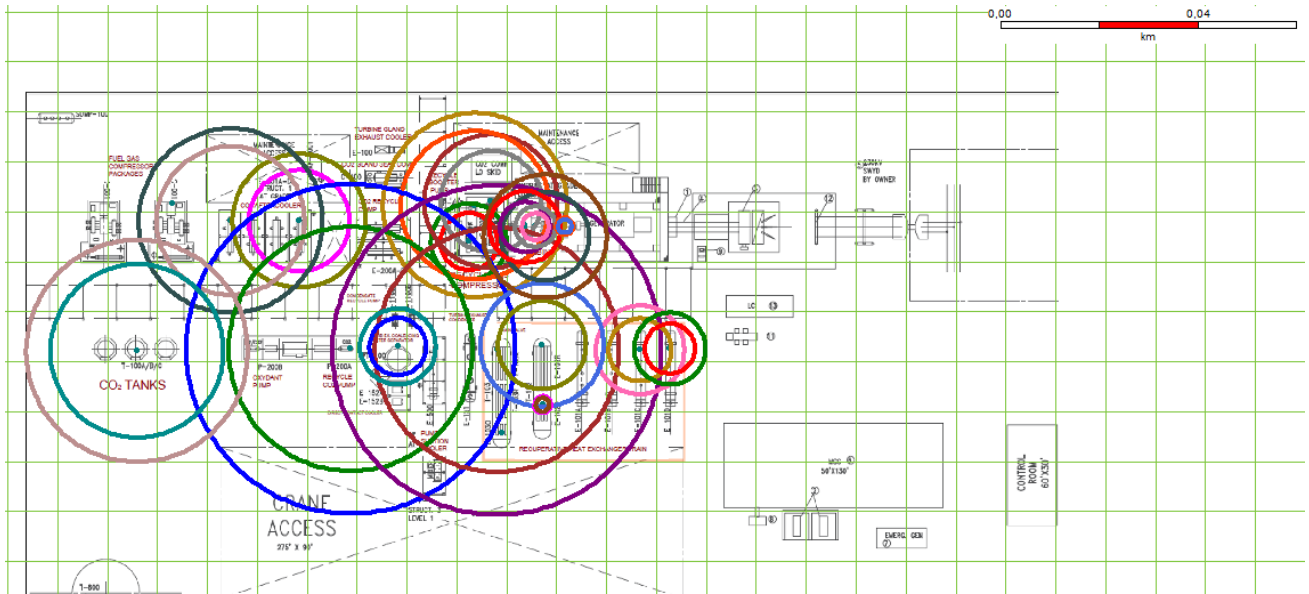


Figure 53 Effect Zones for 8% CO₂ (outer Footprint) and 11% CO₂ (inner Footprint). Grid squares of 10 meters.

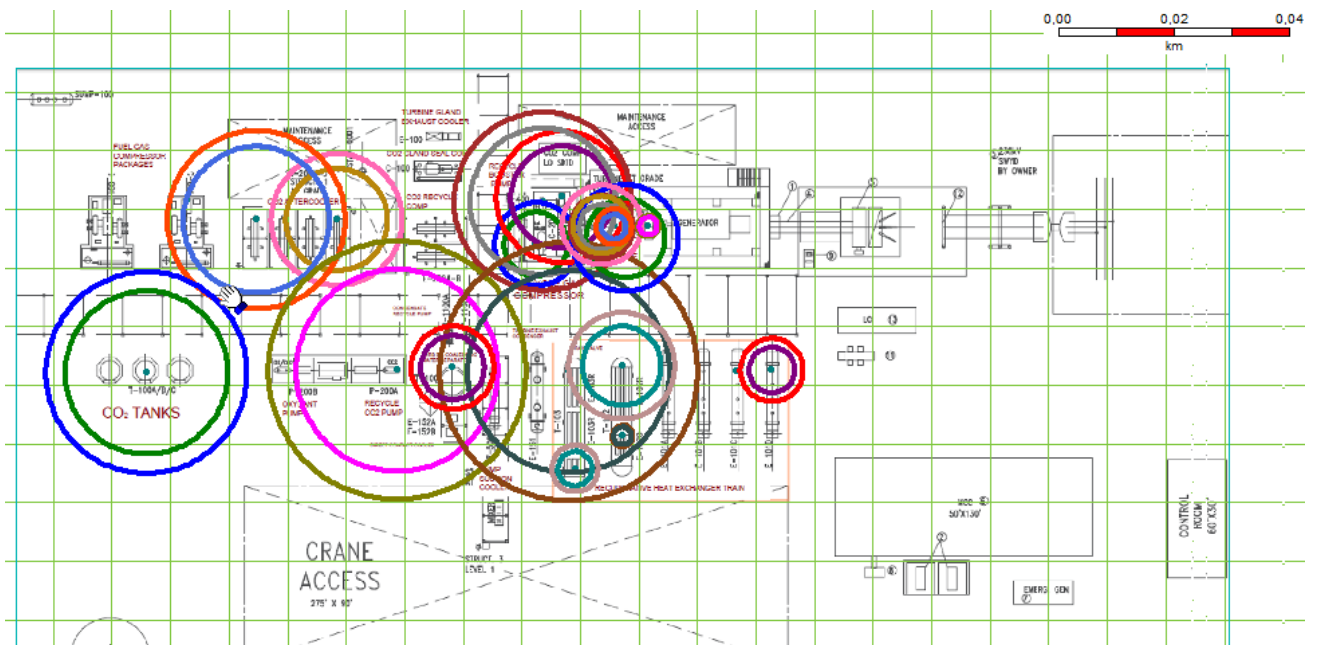


Figure 54 Effect Zones for a probit value of 2.67 (outer Footprint) and of 5.0 (inner Footprint). Grid squares of 10 meters.

14. References

- Ahmad, M., Lowesmith, B., De Koeijer, G., Nilsen, S., Tonda, H., Spinelli, C., . . . Florisson, O. (2015, April 8). COSHER joint industry project: Large scale pipeline rupture tests to study CO₂ release and dispersion. ELSEVIER International Journal of Greenhouse Gas Control.
- Amiza, S. (2019, March 22). Modeling and experiments for CO₂ blowdown from the cryogenic pilot plant and the mitigations measure. March, China, China, Beijing: International Petroleum Technology Conference.
- Annesini, M., Augelletti, R., De Filippis, P., Santarelli, M., & Verdone, N. (2013, September). Analisi tecnico scientifica di processi innovativi di upgrading dei biogas a biometano: processi di separazione della CO₂ basati sulla formazione di idrati o sull'assorbimento con ammine in ambiente non acquoso. Italy: ENEA Agenzia nazionale per le nuove tecnologie, l'energia e lo sviluppo economico sostenibile.
- Apple Rubber. (2015, September 24). *How to avoid seal failure in low-temperature environment*. Tratto da applerubber.com.
- Billingham, J., Sharp, J., Spurrier, J., & Kilgallon, P. (2003). *Review of the performance of high strength steels used offshore*. Cranfield University: Health and Safety Executive HSE.
- Buit, L. (2009). *Existing infrastructure for the transport of CO₂ - D2.1.1*. CO₂Europe.
- Cabrini, M., Lorenzi, S., Marcassoli, P., Pastore, T., & Radaelli, M. (2012). Valutazione della velocità di corrosione di acciai al carbonio per il trasporto e lo stoccaggio di CO₂ ad alta pressione (CCTS). *AIMAT 2012: XI convegno nazionale Aimat, Gaeta, 16-19 settembre 2012*. Gaeta.
- Chaturvedi, R., Kennedy, E., & Metew, S. (2021, 4 20). CO₂ sequestration by Allam Cycle. University of pennsylvania: Department of Chemical & Biomolecular Engineering.
- Cooper, R., & Barnett, J. (2014). Pipelines for transporting CO₂ in UK. Elsevier ScienceDirect Energy Procedia.
- Crivellari, A., Pelucchi, M., Ramus, M., Rossi, E., & Hantig, E. (s.d.). Safety and Environment for Carbon Caprute and Storage (SE-CCS) Initiatives.
- Del Ferraro, S., Molinari, V., Moschetto, A., & Pinto, I. (2019, June 5). Criteri e metodi per la valutazione del rischio microclima ambienti moderati e ambienti severi. P.A.F. Portale Agenti Fisici.
- Demofonti, G., & Spinelli, C. (2011). Technical challenges facing the transport of anthropogenic CO₂ by pipeline for carbon capture and storage purposes.
- DNV GL. (2013, April). Failure frequency guidance: Process equipment leak frequency data for use in QRA.
- DNV GL. (2017, October). Release notes Phast 8.0: Taking hazard and risk analysis one step further.
- DNV-RP-J202, R. p. (April 2010). *Design and operation of CO₂ pipelines*.
- Dugstad, A. (2006). Fundamental aspects of CO₂ metal loss corrosion. Part I: Mechanism. Norway: Corrosion Nacexpo.
- ELAND . (2020). *What is the operating temperature for electrical cable*. Tratto da <https://www.elandcables.com>
- Energy Institute. (2010, September). Technical guidance oh hazard analysis for onshore carbon capture installations and onshore pipelines.

- European Committee for Standardization. (2005, November). Ergonomics of the Thermal environment - Analytical determination and interpretation of thermal comfort using calculation of the PMV and PPD indices and local thermal comfort criteria . *EN ISO 7730*. Tratto da Portale di Bioclimatologia applicata della Riviera delle Palme (AP) Italia:
http://www.meteorivierapicena.net/resistenza_termica_vestiario.htm
- Fernandes, D., Wang, S., Xu, Q., Buss, R., & Chen, D. (2019, October 12). Process and carbon footprint analysis of the allam cycle power plant integrated with an air separation unit. *Clean technologies MDPI*.
- Fernandez, M. (2020, March). THEORY: Toxic calculations. DNV GL.
- Ferrari, N., Mancuso, L., Davison, J., Chiesa, P., Martelli, E., & Romano, M. (2016). Oxy-turbine for Power Plant with CO2 capture. *13th International Conference on Greenhouse Gas Control Technologies*. Lausanne.
- Gant, S., & Kelsey, A. (2011, June 20). Accounting for the effect of concentration fluctuations on toxic load for gaseous releases of carbon dioxide. *Journal of Loss Prevention in the Process Industries*.
- Gasparini. (2019, January 14). *Metals and materials for low temperatures and cryogenic applications*. Tratto da <https://www.gasparini.com/en/blog/metals-and-materials-for-low-temperatures/#:~:text=Metals%20such%20as%20copper%2C%20silver,be%20added%20to%20the%20list>.
- Gelderen, L. v. (2013). Improving a risk assessment method for CCS. Vrije Universiteit Amsterdam: National Institute for Public Health and the Environment.
- Gillivray, A., & Wilday, J. (2009). Comparison of risks from carbon dioxide and natural gas pipeline. *Health and Safety Laboratory*.
- Guo, X., Chen, S., Yan, X., Zhang, X., Yu, J., Zhang, Y., . . . Brown, S. (2017, September). Flow characteristics and dispersion during the leakage of high pressure CO2 from an industrial scale pipeline.
- Guo, X., Yan, X., Yu, J., Zhang, Y., Chen, S., Mahgerefteh, H., . . . Proust, C. (2016). Under-expanded jets and dispersion in supercritical CO2 releases from large-scale pipeline. *Applied Energy*.
- Harper, M., & Witlox, H. (2017, September). Multi-Components in Phast and Safeti. DNV-GL.
- Hechtel, K. (2014, October). Design considerations for the use of plastic materials in cryogenic environments. Curbell Plastics.
- Heijne, M., & Kaman, F. (2008). Veiligheidsanalyse Ondergrondse Opslag van CO2 in Barendrecht. Tebodin B.V.
- Herrom, S., & Myles, P. (2013, August). Quality guidelines for energy system studies: CO2 Impurity Design Parameters. NETL (National Energy Technology Laboratory).
- Hill, T., Fackrell, J., Dubal, M., & Stiff, S. (2011, February). Understanding the Consequences of CO2 Leakage Downstream of the Capture Plant. Elsevier ScienceDirect.
- Holt, H. (2020). *CO2RISKMAN Guidance on CCS CO2 Safety and Environment Major Accident Hazard Risk Management - Level 3- Generic Guidance*. DNV GL. DNV GL.
- Holt, H. (2020, January 30). *CO2RISKMAN Guidance on CCS CO2 Safety and Environment Major Accident Hazard Risk Management - Level 4- Specific CCS Chain Guidance*. DNV GL.

- Holt, H. (2020). *CO2RISKMAN Guidance on CCS CO2 safety and environment major accident hazard risk management - Level2 - Overview*. DNV GL.
- Holt, H. (2021, February 24). CCS CO2- Aspects of CO2 that could cause or contribute to a major accident. *Fire and blast information group*.
- HSE UK. (2020, June 10). Offshore Emergency Response Inspection Guide. Offshore safety Directive Regulator.
- HSE UK. (2020, December 11). *Toxicity levels of chemicals: Assessment of the Dangerous Toxic Load (DTL) for Specified Level of Toxicity (SLOT) and Significant Likelihood of Death (SLOD)*. Tratto da Health and Safety Executive: <https://www.hse.gov.uk/chemicals/haztox.htm>
- HSE UK. (s.d.). *Methods of approximation and determination of human vulnerability for offshore major accident hazard assessment*. Tratto da https://www.hse.gov.uk/foi/internalops/hid_circs/technical_osd/spc_tech_osd_30/spctecosd30.pdf
- Hurlich, A. (s.d.). Low temperature metals. San Diego, California: General Dynamics/Astronautics.
- International Energy Agency. (2021, October). Net Zero by 2050: A roadmap for the global energy sector.
- IOGP. (2021, May). Process Release Frequencies. *Risk assessment data directory*.
- IOGP Risk Assessment Data Directory. (March 2010). *Report No. 434-14.1 - Vulnerability of humans*. Internal Association of Oil & Gas Producers.
- IOGP Risk Assessment Data Directory. (March 2010). *Report No. 434-14.1 - Vulnerability of humans*. Internal Association of Oil & Gas Producers.
- Istituto Superiore di Sanità. (2020, February 7). *Congelamento e ipotermia*. Tratto da ISSalute Informarsi Conoscere Scegliere.
- Jacob Leachman. (2019, 02 18). *Cryogenic Hydrogen Embrittlement*. Tratto da Washington State University: <https://hydrogen.wsu.edu/>
- Jensen, M. D., Schlasner, S. M., Sorensen, J. A., & Hamling, J. A. (2014). *Subtask 2.19 - Operational flexibility of CO2 transport and storage*. Energy & Environmental Research Center - University of North Dakota.
- Johnsen, K., Holt, H., Helle, K., & Sollie, O. K. (2009, 01 21). Mapping of potential HSE issues related to large-scale capture, transport and storage of CO2. Norway: Det Norske Veritas (DNV).
- Joris Koornneef, M. S. (2009). Quantitative risk assessment of CO2 transport by pipelines- A review of uncertainties and their impacts. *Journal of Hazardous Materials*.
- Juhani Hassi, K. K. (December 1999 - May 2001). *Risk assessment and management of cold related hazards in arctic workplaces: network of scientific institutes improving practical working activities*. Barents Interreg IIA- Programme - ERDF.
- Keane, B., Schwarz, G., & Thernherr, P. (2013, October). Electrical equipment in cold weather applications. *White Paper WP083007EN*. IEEE.
- Kermani, B., Martin, J., & Esaklul, K. (s.d.). Materials design strategy: effects of H2S/CO2 corrosion on materials selection.
- Koornneef, J. M., Spruijt, M., Ramirez, A., & Faaij, A. (2009, February). Uncertainties in risk assessment of CO2 pipelines. *Energy Procedia*.

- L. Buit, A. v. (May 2011). *Existing infrastructure for transport of CO2 D2.1.1*. CO2Europipe-Towards a transportation infrastructure for large-scale CCS in Europe.
- Le Cronache. (2017, October 4). *La morte per assideramento: un'intervista alla dottoressa Ursula Franco*. Tratto da <https://www.lecronachelucane.it/2017/10/04/dott-ssa-ursula-franco-la-morte-per-assideramento/>
- Li, K., Tu, R., Zhou, X., Xie, Q., Yi, J., & Jiang, X. (s.d.). An experimental investigation of supercritical CO2 accidental release from a pressurised pipeline.
- Li, K., Zhou, X., Tu, R., Xie, Q., Yi, J., & Jiang, X. (2017). A study of small-scale CO2 accidental release in near-field from a pressurized pipeline. *9th International Conference on Applied energy, ICAE2017*. Cardiff.
- Liu, X., Godbole, A., Lu, C., Michal, G., & Venton, P. (2015). Study of the consequences of CO2 released from high-pressure pipelines. University of Wollongong Research Online.
- Lujan, I. (2016, January 15). *Physiological effects of cold*. Tratto da Universitat de València: <https://www.uv.es/uvweb/master-fisiologia/ca/master-universitari-fisiologia/efectes-fisiologics-fred-1285881308000/GasetaRecerca.html?id=1285954729640>
- Lyons, C., Race, J., Hopkins, H., & Cleaver, P. (2015). Prediction of the consequences of a CO2 pipeline release on building occupants.
- M. M.j. Knoope, I. M. (1 January 2014). The influence of risk mitigation measures on the risks, cost and routing of CO2 pipelines. *International Journal of Greenhouse Gas Control*, 21.
- Mazzoldi, A., & Oldenburg, C. (2011). *Leakage Risk Assessment of CO2 transportation by pipeline at the Illinois Basin Decatur Project*. Decatur, Illinois.
- Mike Bilio, S. B. (2009). *CO2 pipelines material and safety considerations*. Symposium serie no. 155.
- Mocellin, P., Vianello, C., & Maschio, G. (2016, November 18). Hazard investigation of dry-ice bank induced risks related to rapid depressurization of CCS pipelines. Analysis of different numerical modelling approaches. *International Journal of Greenhouse Gas Control*.
- Mofrad, S. R. (2018, January 22). Is 600mm sufficient to keep a blowdown valve functional? Qatar.
- Nizamoglu, M., Tan, A., Vickers, T., Segaren, N., Barnes, D., & Dziewulski, P. (2016). Cold burn injuries in the UK: the 11-year experience of tertiary burns center. *Burns&Trauma*.
- Oosterkamp, A., & Ramsen, J. (2008, January 8). State-of-the-Art Overview of CO2 Pipeline Transport with Relevance to Offshore Pipelines. *Polytec*, 87.
- OSD3.2. (January 2006). *Indicative human vulnerability to the hazardous agents present offshore for application in risk assessment of major accidents*. SPC/Tech/OSD/30.
- Paschke, B., & Kather, A. (2012). Corrosion of Pipeline and Compressor Materials due to Impurities in separated CO2 from fossil-fuelled Power Plants. *Energy Procedia*.
- Podger, G. (2006, June 28). The health and safety risks and regulatory strategy related to energy developments.
- Preeti, J., Prem, B., & Qingsheng, W. (2016, October 28). Consequence analysis of accidental release of supercritical carbon dioxide from high pressure pipelines. Elsevier International Journal of Greenhouse Gas Control.

- Pursell, M. (2012). Experimental investigation of high pressure liquid CO₂ release behaviour. Buxton: Health and Safety Laboratory.
- Qiyuan, X., Ran, T., Xi, J., Kang, L., & Xuejin, Z. (2014, February 22). The leakage behavior of supercritical CO₂ flow in an experimental pipeline system. Elsevier Applied Energy.
- Quest Consultants Inc. (2010, November 15). Preliminary quantitative risk analysis (QRA) of the Texas clean energy project.
- Rettner, R. (2019, January 31). *How does a person freeze to death?* Tratto da Live Science: <https://www.livescience.com/6008-person-freeze-death.html>
- Rice, S. A. (2004). Human health risk assessment of CO₂: survivors of acute high-level exposure and populations sensitive to prolonged low-level exposure.
- Roos, i. A. (December 1989). *Methods for the determination of possible damage to people and objects resulting from release of hazardous materials CPR 16E*. Voorburg.
- Ruszczynski, R. (2011, September). Environmental impact and risk of CO₂ storage facilities in Poland - D4.4.1. *CO₂ Europipe-Towards a transportation infrastructure for large-scale CCS in Europe*.
- Schubert&Salzer. (2020). *Seat Valves: The extremely durable all-rounder of the valve technology*. Tratto da <https://controlsystems.schubert-salzer.com/en/products/seat-valves>
- Spouge, J. (2006). Leak frequencies from the hydrocarbon release database. DNV Consulting.
- Stene, J. (2017, October). Discharge Scenarios THEORY. DNV GL.
- Stene, J. (2020, April). Property System THEORY. DNV GL.
- T. Mikunda, L. Buit. (April 2011). *Report Standards for CO₂ (Rev 2)- D3.1.2*. CO₂Europipe-Towards a transport infrastructure for large-scale CCS in Europe.
- Teng, L., Li, Y., Hu, Q., Zhang, D., Ye, X., Gu, S., & Wang, C. (2018, May 11). Experimental study of near-field structure and thermo-hydraulics of supercritical CO₂ releases. ELSEVIER Energy.
- U.S. Department of Energy - National Energy Technology Laboratory. (November 2007). *Futurgen project final environmental impact statement - DOE/EIS-0394 - (Vol. II Chapter 4-7)*.
- Vianello, C., Macchietto, S., & Maschio, G. (2012). Conceptual models for CO₂ release and risk assessment: a review. Chemical Engineering Transaction.
- Vianello, C., Macchietto, S., & Maschio, G. (2013). Risk Assessment of CO₂ pipeline network for CCS - A UK case study. Chemical Engineering Transaction.
- Vianello, C., Mocellin, P., & Maschio, G. (2014). Study of Formation, Sublimation and Deposition of Dry Ice from Carbon Capture and Storage Pipelines. *Chemical engineering transactions*.
- Vitali, M., Zuliani, C., Corvaro, F., Marchetti, B., Terenzi, A., & Tallone, F. (2021, July 29). Risk and safety of CO₂ transport via pipeline: A review of risk analysis and modeling approaches for accidental releases. Gustavo Fimbres Weihs.
- W ter Burg, M. R. (2021, April 1). 20210401 -Carbon dioxide-Proposed (Technical support document carbon dioxide). National Institute for Public Health and the Environment.

- Wang, X., Song, Z., Pan, X., Zhang, L., Zhu, X., Mei, Y., & Jiang, J. (2021). Simulation study on near-field structure and flow characteristics of high-pressure CO₂ released from the pipeline. *ELSEVIER Journal of Loss Prevention in the Process Industries*.
- WEG. (2018, July). WEG Manuale generale di installazione, funzionamento e manutenzione di motori elettrici. 1.
- Weitzel, D., Robbins, R., & Herring, R. (2015). *Elastomeris ceals and materials at cryogenic temperatures*. Colorado: U.S. Department of commerce .
- Wilday, J., McGillivray, A., Harper, P., & Wardman, M. (2009). A comparison of hazard and risks for carbon dioxide and natural gas pipelines.
- Witlox, H., & Stene, J. (2015, December 21). Atmospheric expansion modelling - Literature review, model refinement and validation. *SAFETI-NL Innovative Maintenance*. DNV GL.
- Witlox, H., Harper, M., & Oke, A. (2012). Phast validation of discharge and atmospheric dispersion for pressurised carbon dioxide releases. London, UK: DNV.
- Witlox, H., Harper, M., Topalis, P., & Wilkinson, S. (2005, March). *Modelling the consequence of hazardous multi-component two-phase releases to the atmosphere*. (A. S. Engineers, A cura di) Tratto da www.dnvsoftware.com
- Wong King Lit. (1996). B3 Carbon Dioxide. In N. R. Council, *Spacecraft Maximum Allowable Concentrations for Selected Airbone Contaminants: Vol. 2*. Houston, Texas: Johnson Space Center Toxicology Group.

Ringraziamenti

Ringrazio il Prof. Andrea Carpignano per la continua disponibilità e fiducia riposta nel mio lavoro. Un sentito grazie a Stefano Pellino (Process Safety Technical Authority – Eni SpA) per avermi guidata in ogni fase di questo percorso, da un primo approccio allo studio fino alla stesura dell’elaborato finale.